X-552-69-317
PREPRINT

2

LUNAR GRAVITY FIELDS DETERMINED FROM APOLLO 8 TRACKING DATA

T. L. FELSENTREGER
J. P. MURPHY
J. W. RYAN
L. M. SALTER

JULY 1969

GSFC
GODDARD SPACE FLIGHT CENTER
GREENBELT, MARYLAND

X-552-69-317
PREPRINT

LUNAR GRAVITY FIELDS DETERMINED FROM APOLLO 8 TRACKING DATA

T. L. Felsentreger
J. P. Murphy
Mission Trajectory Determination Branch
Mission & Trajectory Analysis Division

J. W. Ryan
L. M. Salter
Data Evaluation Branch
Manned Flight Planning and Analysis Division

July 1969

GODDARD SPACE FLIGHT CENTER
Greenbelt, Maryland

LUNAR GRAVITY FIELDS DETERMINED FROM APOLLO 8 TRACKING DATA

T. L. Felsentreger, J. P. Murphy,
J. W. Ryan, and L. M. Salter

ABSTRACT

Tracking data from the eight near-circular lunar orbits made by the Apollo 8 spacecraft was analyzed in an attempt to determine spherical harmonic lunar gravity models suitable for use in future Apollo missions. Thirty-one determinations through degree and order six are presented, in addition to test and evaluation results of many of the models.

TABLE OF CONTENTS

LUNAR GRAVITY FIELDS DETERMINED FROM APOLLO 8 TRACKING DATA

INTRODUCTION

Intense interest became focused on the lunar gravity field upon the discovery of an unexpected anomaly in the tracking data of early lunar orbiting spacecrafts (the Lunar Orbiters). This anomaly manifested itself as unusually large Doppler residuals occurring mainly during periods of perilune passage, suggesting lunar gravitational inconsistencies not reflected in the accepted potential models. It was recognized that this problem, unless solved, could lead to miscalculation for lunar landing missions such as Apollo, since a good knowledge of the moon's gravitational field is imperative for orbit determination and prediction in such missions.

Since the initial cognizance of the problem, many spherical harmonic lunar gravity models have been derived from Lunar Orbiter data, some from the Doppler tracking data itself over relatively short periods of time and others from averaged orbital elements over longer time spans. Determinations were made from 1, 2, 3, 4, and all 5 of the Lunar Orbiters. All of the models suffered from the same shortcoming, i.e., they didn't very well fit data other than that used in the determinations. As a consequence, the orbit prediction capabilities of the models were rather poor.

The flight of Apollo 8 afforded an opportunity to study the effect of lunar gravity on the type of orbit which will be used for the landing missions, i.e., a low altitude, near circular, near equatorial orbit. The Apollo 8 spacecraft made 10 revolutions of the moon, the last 8 of which were near circular. A tri-axial lunar gravity model was used throughout the mission for orbit determination and, as in the case of the Lunar Orbiters, the orbit prediction capability of this model was quite poor.

The Mission Trajectory Determination Branch (MTDB), Mission and Trajectory Analysis Division (MTAD), and the Data Evaluation Branch (DEB), Manned Flight Planning and Analysis Division (MFPAD) therefore decided to embark on a joint effort to derive, from Apollo 8 tracking data, lunar gravity models suitable for adequately predicting the spacecraft's orbit outside of the data spans used in the model determinations. The best of such models could then possibly be used for the lunar landing missions under the assumption that the prediction capability of the model would remain adequate for a mission flying an Apollo 8 type orbit.

APOLLO 8 MISSION OPERATION RESULTS

General

The Apollo 8 mission was the first manned lunar flight and the manned mission utilizing the Saturn V vehicle. Launch occurred at 0751 EST on 21 December 1968. The Command Service Module (CSM) was inserted into 310 km by 109 km lunar orbit at 69:08:20 GET. After completing two lunar revolutions, a circularization maneuver was performed placing the spacecraft in a 112 km near-circular orbit. At 89:19:16 GET, after completing ten revolutions in lunar orbit, the spacecraft maneuvered into the trans-earth trajectory. Reentry occurred at 146:19 GET in the prime recovery area in the mid-Pacific Ocean.

Operational Orbit Determination Philosophy

At the time of the Apollo 8 mission, the best generally accepted lunar potential model and the field used for mission control at Mission Control Center, MCC/ Houston was the tri-axial gravity field. As such, this field was used operationally at GSFC for Apollo 8 support. The particular values of the parameters describing this field are given in Table 1 (see also Ref. 1). A point mass sun and a point mass earth completed the force model used to predict the motion of Apollo 8 in lunar orbit.

Based on the results of analysis of Manned Space Flight Network (MSFN) Lunar Orbiter data, it was decided that the optimal basic data set for orbit determination would consist of all range and range rate data from a single front side lunar pass. If data from more than a single pass had been used, it was felt there would have been a significant degradation in the fit of the range rate data. Also, the quantity of the range data and the weight assigned to the range data relative to the weight assigned to the range rate data were such that the orbit determinations were essentially range rate only.

Operational Results

The data from each of the ten front side passes was used to determine a best-estimate-trajectory (BET). The mean range rate residuals for revolutions 1 and 2, for 3, 4, 5 and 6, and for 7, 8, 9 and 10 are presented in Figures 1, 2 and 3, respectively. The mean residual is the instantaneous average of the range rate residuals of all sites tracking. In general, the dispersion about this mean was less than 10 mm/s. Table 2 is a summary of the classical elements which resulted for the orbit determinations of the ten lunar revolutions. The mean residuals have been plotted as a function of time since perilune passage, and as such, Figures 2 and 3 are plotted as a function of the same values of mean anomaly. All plots exhibit similar general characteristics at the same values of

mean anomaly, and there is even a strong correlation among the second order features. The most striking feature is a four cycle per revolution sine wave with an amplitude of approximately 35 mm/s in revolutions 1 and 2 and 60 mm/s in the remaining revolutions. The smaller amplitude in revolutions 1 and 2 is evidently due to the larger apilune height.

Operational Trajectory Propagation Results

The prime mission control requirement for precise lunar orbit determination is the requirement to predict the spacecraft position and velocity two revolutions in advance for accurate spacecraft maneuver computation. As such, an analysis was made of orbit prediction capability of the Goddard Apollo 8 orbit determination system. The solution vectors from revolutions 5 through 9 were integrated with the force model described above to the times of the solutions on revolutions 6 through 10, respectively. Table 3 presents the results of the comparisons of the propagated orbits and the solution orbits. The position error is first presented in terms of down range error, cross range error, and height error. In the lunar landing mission the de-orbit position specification is approximately .3 km in height, and 1 km in each of cross range and down range. Note that the results presented in the table are for a prediction of one revolution, not two, as in the de-orbit problem. However, the down range error is in every case larger than specification. The cross range error is in two cases larger than specification; the height error is in each case within specification, but this is in large measure due to a fortuitous choice of the anchor times.

Next the propagation error is presented in terms of the errors in three critical classical elements; namely, a, e, and I. The error in a, semi-major axis, is small and shows no trend. The largest error is .118 km, and this alone could not cause an instantaneous position error of more than .118 km. An examination of the semi-major axis itself indicates that it decreased by .5 km in the seven low orbits. No definitive explanation of this decrease has been found; however, the spacecraft venting is a likely cause. The inclination error is small and shows no clear pattern. The maximum error is .035 degrees, and this could cause a maximum cross range error of 1.1 km. An examination of the inclination itself shows that it may be changing from approximately 146.4 degrees on revolution 4 to 146.5 on revolution 10. However, this pattern is not very clearly defined. The eccentricity error pattern is the most striking result of this analysis. In every case the eccentricity prediction error is approximately 280×10^{-6} and the dispersion about this is no more than 10×10^{-6}. One effect of this error can be seen by examining the apilune and perilune prediction errors. The apilune prediction error is consistently .5 km low, while the perilune prediction is consistently .5 km high. As was stated previously, the small errors shown in the height column are misleading. The solutions were anchored near 90 degrees

mean anomaly. Had the vectors been anchored at apilune or perilune, the height error would have been consistently .5 km. However, this is not the most serious result of the eccentricity error. If two orbits are identical, except that one is more eccentric than the other, then at 90 degrees mean anomaly the more eccentric will lead the less eccentric along the down range component of position. The effect of this type of error is clearly seen in the down range position error. The solutions were all anchored near 90 degrees mean anomaly and in each case there was a +4 to +6 km prediction error in the down range component. Also, the prediction was short of the actual position, which is consistent with the fact that prediction was based on an orbit which had a too small eccentricity. An examination of the eccentricity parameter itself lends some insight into the problem. In each case the tri-axial moon force model predicted that the eccentricity should decrease by approximately 10×10^{-6}. The eccentricity actually increased by approximately 280×10^{-6}.

In summary, the Apollo 8 eccentricity increased in a very consistent and significant manner in the seven low lunar orbits. The tri-axial moon force model completely failed to predict this change. If a force model can be found which adequately predicts this change, it would most likely eliminate most of the prediction error seen in down range and height.

DERIVATION OF LUNAR GRAVITY FIELDS

The computer program used in the determination of the lunar gravity models is the Lunar Gravity Field In Spherical Harmonics (LUNGFISH) program, as modified by the Computer Usage Development Corporation (CUDC) for Goddard. The original version of LUNGFISH was developed by CUDC for the Langley Research Center to operate on the IBM 7090 computer; this version was a single precision program, could process only Deep Space Network (DSN) tracking data, and was able to solve for up to 58 parameters, including position and velocity. The new Goddard version has been designed to operate on the IBM 360/75, 91, and 95 computers, is a double precision program, is able to process DSN, MSFN, and Satellite Tracking and Data Acquisition Network (STADAN) tracking data, and can solve for up to 200 parameters on the 360/75, 91 and 500 parameters on the 360/95. Also, the program can handle gravity harmonic coefficients of higher degree and order than the 7090 version (up to degree and order 20 in the basic field, plus 25 "spot" harmonics of even higher degree and order).

Tracking data from the 8 near-circular Apollo 8 lunar orbits was processed using the LUNGFISH program to derive representations of the lunar gravity field for the area of the moon traversed by the Apollo 8 spacecraft. The data used was MSFN 60 seconds, 2- and 3-way Doppler involving multiple receiving stations per view period, and is summarized in Table 4. Each station pass is identified by

a number along with the initial and final times and number of observations. The geocentric station coordinates are given in Table 5. Following is a list of the pertinent constants used:

Moon gravity = 4902.778 km^3/sec^2

Earth gravity = 398604.6 km^3/sec^2

Sun gravity = 1.3271482×10^{11} km^3/sec^2

Moon radius = 1738.09 km

Speed of light = 299792.5 km/sec

Light travel time (for mean earth-moon distance) = 1.282219 sec

Transmitting frequency for all stations = 2106.4063 MHz

In processing the data, all 3-way Doppler biases were assumed to be zero, and observations taken below an elevation angle of about 10 degrees were omitted. Additional bad observations were deleted by time. For some of the determinations, observations were deleted if the residuals exceeded a preassigned "rejection sigma".

In all, thirty-one lunar gravity determinations were made, and are presented in Tables 6 and 7 in unnormalized form. The indices m and n are the order and degree, respectively, for the coefficients C_{nm} and S_{nm}. All the fields, with the exception of nos. 23 and 31, were obtained from single arcs, each arc consisting of two or more revolutions of data. A state (i.e., position and velocity) was determined for each arc along with the gravity field. Fields 23 and 31 were derived as multi-arc solutions by considering revolutions 6, 7, and 8 as separate and distinct arcs, each arc an independent trajectory. For each gravity field, the data sets, epoch times, and root mean squares (rms) of the residuals are given in Table 8.

Many of the fields represent attempts to improve and/or build onto the most recent model adopted for the Apollo real-time system. This model (the R2 model) was determined from long-period variations in Lunar Orbiter elements (see Ref. 2), and is as follows:

$C_{20} = -.207108 \times 10^{-3}$

$C_{30} = .210 \times 10^{-4}$

$C_{31} = .34 \times 10^{-4}$

$C_{22} = .20716 \times 10^{-4}$

For all of the determinations, C_{21} and S_{21} were set equal to zero under the assumption that the z-axis coincides with one of the moon's principal axes of inertia. Fields 1-6 are solutions for the four R2 coefficients only, while fields 7-22 represent determinations of these coefficients plus various additional ones. Model 23 is a multi-arc full (4,4) solution, while no. 24 is a single arc full (3,3) derivation. In fields 25-27, the R2 model was held fixed and additional coefficients were solved for. Fields 28-31 are higher degree and order solutions [through (6,6)].

TESTING AND EVALUATION OF GRAVITY FIELDS

General

The reason for the implementation of the following tests was to evaluate existing lunar potential fields, and the new lunar potential fields tabulated in Tables 6 and 7, for use in Apollo type lunar orbits. The first part of the Apollo problem is to predict the position of the Apollo spacecraft with sufficient precision to allow a successful LM landing at a predetermined landing site. The second and most critical part of the problem is to achieve a successful rendezvous after ascent with a minimum of maneuvers required to accomplish docking. With this in mind, the tests were chosen to determine the prediction capability of each lunar potential field.

An indicator of the quality of a potential model is the extent to which it fits the observations. Since the residuals and standard deviations are good indicators of the way the BET fit the data, they give an indication of the quality of the potential model. It was hoped that a model could be found that would provide prediction capability with small position errors and good classical element agreement. Predicted position errors or track errors are derived by converging with a given field using two data sets, and comparing the two resulting trajectories during the interval covered by the second data set.

One course of approach was to derive a potential field consisting of a fixed set of coefficients from several different data sets. Another course was to derive different lunar potential fields from the same data set. The first course was taken in order to determine the amount of change in the coefficients resulting when different data sets are used, and it was hoped that the second approach might yield the optimal lunar potential field size for this type of orbit.

Analysis Technique

As a result of the above considerations, four basic criteria were used in the evaluation of the lunar potential fields. These are as follows:

1. Plotting and analysis of residuals and analysis of standard deviations obtained using each field.

2. Plotting and analysis of track errors obtained using each field.

3. Plotting and analysis of local and predicted eccentricity and eccentricity changes introduced by different fields, and other local and predicted classical elements and changes in those elements.

4. Tabulation and analysis of coefficients obtained from different data sets.

Fields Discussed

Test runs were made on the following lunar potential fields:

Triax - Discussed in section "Apollo 8 Mission Operation Results"

R2 - Four term model, C_{20}, C_{22}, C_{30}, and C_{31}. (Ref. 2)

B - JPL Model 106, full (4,4) field with the additional zonals C_{50}, C_{60}, C_{70}, and C_{80}

3 - Four term model, C_{20}, C_{22}, C_{30}, and C_{31}, derived using data from the 6th, 7th, and 8th revolutions.

4 - Four term model, C_{20}, C_{22}, C_{30}, and C_{31}, derived using data from the 6th, 7th, 8th, 9th and 10th revolutions.

15 - Eight term model, C_{20}, C_{22}, S_{22}, C_{30}, C_{31}, S_{31}, C_{44}, and S_{44}, derived using data from the 7th and 8th revolutions.

27 - This is a full (4,4) field, with the exception of the C_{21} and S_{21} terms, derived using data from the 6th, 7th, and 8th revolutions.

30 - This is a full (6,6) field, with the exception of the C_{21} and S_{21} terms, derived using data from the 6th and 7th revolutions.

The first three fields (triax, R2, and B) were obtained from external sources. The coefficients in these fields are listed in Table 9. For the other field designations, refer to Tables 6 and 7.

Description of Graphs

Figures 4 through 19 present range rate residuals in cm/sec. plotted against time as obtained from one revolution, range rate only solutions. The curves represent the average of all stations for the triax field and an average of the two indicated stations for the other fields over one revolution data arcs.

Figures 20 through 27 present range rate residuals in doppler cycles (1 doppler cycle $\simeq$ 6.5 cm/sec.) against time as obtained from multi-revolution range rate only solutions. The curves represent the indicated stations over multi-revolution data arcs.

Figures 28 and 29 present local eccentricity for the indicated fields, obtained by converging in each revolution. Figures 30 through 32 present predicted eccentricity for the indicated fields obtained by propagating a given vector forward fourteen hours at two hour intervals. Figures 33 and 34 present predicted eccentricity for the field indicated obtained by propagating a one revolution solution ahead for one revolution. Tables 13 through 17 present local classical elements and were obtained by converging in each revolution and tabulating the orbital elements. Differences were taken between successive revolutions. Tables 18 through 24 present predicted classical elements obtained by propagating a vector forward fourteen hours at two hour intervals. Tables 25 through 29 present predicted orbital elements obtained by propagating a one revolution solution ahead for one revolution. Differences were taken between successive revolutions. Table 30 presents track error prediction bounds obtained by converging in one data arc, predicting ahead to the next data arc and comparing the resulting trajectories during the second data arc.

Figures 35 through 39 present track error predictions for the indicated revolution and field. The values which these curves represent were obtained by converging in revolution 4 and then in revolution 5, and differencing the resultant trajectories during revolution 5.

Description of Tests and Results

The purpose of the residual graphs and statistical tables is to indicate how well the data is fit by the BET using any given lunar potential field. The results from this list were used to determine when the fields had converged and which fields would receive additional testing.

Table 10 summarizes the maximum positive and negative residual excursion and maximum standard deviation for one revolution data arcs tested.

The residuals from Graphs 20 through 27 represent multi-revolution data arcs and therefore are not included in the above tabulation.

The purpose of the track error tables and graphs is to indicate how well a given lunar potential field predicts spacecraft position and the way these errors vary throughout a given period. The tables present the negative and positive extremes of the down track, cross track and perpendicular errors. These errors were derived by converging with a given field using two data sets and comparing the two resulting trajectories during the interval covered by the second data set. Each prediction was across one occultation.

Table 11 summarizes the track error bounds for the one revolution to one revolution runs tested.

The purpose of eccentricity graphs is to show the way in which eccentricity changes are predicted by different lunar potential fields. Eccentricity prediction capability gives an indication of the lunar potential fields ability to predict spacecraft position. In these tests, a vector is propagated for 7 revolutions with a given lunar potential field. The eccentricity and other classical elements were computed at 2-hour intervals. Table 12 summarizes the normalized slope of the eccentricity against time curves for the indicated lunar potential fields with the slope of the reference field curve (R2 field coverged in each revolution) as 1.

Summary

The purpose of computation and tabulation of the same coefficient sets for several data sets is to determine the effects of different sets of data on the coefficients. The purpose of computation and tabulation of different coefficients for the same data set is to determine the optimum size of and values of coefficients for a lunar potential field which fulfills the Apollo needs. Note that with the R2 type fields (C_{20}, C_{22}, C_{30}, and C_{31}) included in this report, the values of the coefficients agree fairly well with the values of the R2 and Triax field (see fields R2, 1, 2, 3, 4, 5 and 6). However, when S_{22} and S_{31} terms are added, the size of the coefficients show marked changes although the standard deviation is smaller than for an R2 type field using the same data set. The most significant change involves the C_{30} term, which is almost two orders of magnitude larger.

When the same fields are computed with different data sets (fields -1 through -20), with one exception (the C_{30} term in field -15), the coefficients agree to within an orbit of magnitude.

Conclusions

Considering the residuals and standard deviation, field 15 fits the data best. The track error results indicate that field 4 gives better position predictions; however, this result is only for one prediction (from revolution 4 to revolution 5). Among the fields where more than one position prediction was available, field 15 gives better results. The eccentricity graphs indicate that field 15 gives the worse eccentricity slope predictions of all the fields tested and field 4 gives the best slope prediction – that is, the slope of the eccentricity curves as compared to the R2 converged curve. From these results, it appears that field -15 gives the best one-revolution-to-one-revolution position prediction, and long term eccentricity prediction capability is not highly correlated to a one-revolution-to-one-revolution position prediction capability.

These results suggest that an eight term field is near the optimum size and, in particular, a field that includes one or two pairs of fourth degree terms.

COMMENTS

It was not the purpose of this investigation to produce a good, overall model describing the totality of the lunar gravitational field, but rather to derive a model giving good prediction capability for Apollo-type orbits in the equatorial region of the moon. The fact that none of the derived fields was outstanding with respect to all of the evaluation criteria points out the difficulty of the problem and the inconsistencies of the moon's gravitational field over even a narrow band around the moon. In general the use of different data sets reflecting varying ground track patterns gave markedly different results even when deriving the same set of spherical harmonic coefficients. In deriving different gravity models using the same data set, different values were obtained for harmonic coefficients common to the various models. The multi-arc solutions gave generally poorer results than the single arc, multi-revolution solutions, showing that lack of tracking data on the back side of the moon makes necessary the inclusion of two or more revolutions of data in each arc to reflect the influence of the moon's back side.

None of the above results was surprising or unexpected, however. The use of data from only one satellite should produce ground track dependent models, with the lack of consistency between models providing a rough qualitative measure of the local gravitational anomalies.

It should be mentioned that a number of the more promising fields derived in this investigation were forwarded to the appropriate personnel at the Manned Spacecraft Center for further testing and evaluation several months prior to publication of this report.

ACKNOWLEDGEMENTS

The authors wish to thank Messrs. Victor Laczo (MTDB)/(MTAD) and Stephen Zufall (DEB)/(MFPAD) for their help in processing the data and making many of the computer runs necessary for the investigation.

REFERENCES

1. Jeffreys, H., Monthly Notices of the Royal Astronomical Society, 122(5), pp. 431-432, 1961.

2. Risdal, R. E., "Development of a Simple Lunar Model for Apollo", Contract Report D2-100819-1, The Boeing Co., Seattle, Wash., 1968.

Table 1

GSFC/Apollo 8 Operational
Lunar Gravity Field*

$\mu_{\mathbb{C}}$	= 4902.778 km^3/sec^2
C_{20}	= $-.20718677 \times 10^{-3}$
C_{22}	= $+.20239141 \times 10^{-4}$
Mean Lunar Radius	= 1738.09 KM

*Unnormalized Coefficients

Table 2

Apollo 8 Trajectory Summary
Classical Elements*

Revolution #	a (km)	e	I (Deg)	ω (Deg)	Ω (Deg)	M (Deg)
1	1949.61	.050914	146.523	-123.584	-171.889	143.02
2	1949.40	.051033	146.336	-123.484	-172.014	174.62
3	1850.47	.000607	146.030	- 42.015	-172.314	81.03
4	1850.43	.000905	146.364	- 38.050	-171.996	80.63
5	1850.34	.001170	146.405	- 44.730	-171.885	90.67
6	1850.32	.001445	146.385	- 45.158	-171.892	94.37
7	1850.13	.001706	146.398	- 47.089	-171.806	99.68
8	1850.07	.001971	146.443	- 47.202	-171.736	103.17
9	1849.99	.002231	146.567	- 48.108	-171.639	107.50
10	1850.02	.002516	146.459	- 47.634	-171.712	110.42

*Based on selenocentric coordinate system, true equinox and earth equator of date.

Table 3

Apollo 8 Lunar Orbit Prediction Results

Situation	Error* Down Range (km)	Cross Range (km)	Height (km)	a (km)	e x 10^3	I (deg)	Apilune (km)	Perilune (km)
Lunar Orbit 5 to Lunar Orbit 6	+5.39	- .29	+.04	-.003	+.295	-.029	+.54	-.55
Lunar Orbit 6 to Lunar Orbit 7	+6.04	+ .45	+.00	-.118	+.279	+.003	+.35	-.54
Lunar Orbit 7 to Lunar Orbit 8	+4.87	- .61	+.09	-.006	+.281	+.035	+.49	-.68
Lunar Orbit 8 to Lunar Orbit 9	+5.28	-2.61	+.13	-.065	+.274	+.014	+.44	-.57
Lunar Orbit 9 to Lunar Orbit 10	+4.22	+2.86	+.20	+.070	+.295	-.018	+.59	-.47

*For all errors the sense is solution parameter minus propagated parameter.

Table 4

Summary of Apollo 8 Tracking Data (Lunar Revs 3-10)

Pass No.	Receiving Station No.	Start Time				Final Time				No. Obs.
		Day	Hr.	Min.	Sec.	Day	Hr.	Min.	Sec.	
301	94	359	14	41	30	359	15	51	30	71
302	23	359	14	41	30	359	15	51	30	57
303	75	359	14	41	30	359	15	51	30	71
304	04	359	14	42	30	359	15	51	30	47
305	08	359	14	41	30	359	15	29	30	49
306	91	359	14	59	30	359	15	51	30	47
401	23	359	16	42	30	359	17	50	00	45
402	02	359	16	39	30	359	17	49	30	71
403	71	359	16	39	30	359	17	49	30	69
404	91	359	16	39	30	359	17	49	30	71
405	75	359	16	39	30	359	17	49	30	71
406	04	359	16	39	30	359	17	50	30	70
407	16	359	17	29	30	359	17	49	30	20
501	04	359	18	41	30	359	19	48	30	48
502	75	359	18	41	30	359	19	48	30	52
503	02	359	18	42	00	359	19	47	30	52
504	71	359	18	41	30	359	19	46	30	35
505	16	359	18	42	30	359	19	48	30	48
506	14	359	18	42	30	359	19	47	30	49
507	23	359	18	43	30	359	19	48	30	44
508	28	359	19	12	00	359	19	47	30	27
509	92	359	19	28	30	359	19	48	30	13

Table 4 (Continued)

Pass No.	Receiving Station No.	Start Time				Final Time				No. Obs.
		Day	Hr.	Min.	Sec.	Day	Hr.	Min.	Sec.	
601	23	359	20	38	00	359	21	47	00	44
602	28	359	20	36	30	359	21	47	30	69
603	92	359	20	36	30	359	21	47	30	72
604	16	359	20	40	30	359	21	47	30	68
605	02	359	20	38	30	359	21	47	30	70
606	14	359	20	39	30	359	21	47	30	66
607	75	359	20	38	30	359	21	47	30	66
608	91	359	20	39	30	359	21	47	30	68
609	71	359	20	41	30	359	21	47	30	66
610	4	359	20	45	30	359	21	47	30	63
611	94	359	21	12	30	359	21	46	30	35
701	12	359	22	35	30	359	23	45	00	60
702	16	359	22	35	30	359	23	45	30	71
703	14	359	22	36	30	359	23	45	30	70
704	28	359	22	35	30	359	23	44	30	70
705	92	359	22	35	30	359	23	44	30	70
706	71	359	22	36	30	359	23	45	30	70
707	02	359	22	35	30	359	23	45	30	71
708	04	359	22	35	30	359	23	40	30	66
709	75	359	22	35	30	359	23	44	30	70
710	91	359	22	36	30	359	23	45	30	70
801	16	360	00	34	30	360	01	44	30	71
802	14	360	00	35	30	360	01	44	30	67
803	91	360	00	34	30	360	01	44	30	71

Table 4 (Continued)

Pass No.	Receiving Station No.	Start Time				Final Time				No. Obs.
		Day	Hr.	Min.	Sec.	Day	Hr.	Min.	Sec.	
804	12	360	00	34	30	360	01	44	30	57
805	02	360	00	34	30	360	01	44	30	71
806	71	360	00	35	30	360	01	44	30	70
807	92	360	00	34	30	360	01	44	30	68
808	28	360	00	34	30	360	01	44	30	70
809	93	360	01	22	30	360	01	43	30	22
810	24	360	01	26	30	360	01	43	30	15
901	93	360	02	32	30	360	03	42	30	71
902	16	360	02	35	30	360	03	42	30	68
903	24	360	02	34	30	360	03	42	30	68
904	25	360	02	32	30	360	03	42	30	71
905	12	360	02	32	30	360	03	41	30	54
906	92	360	02	32	30	360	03	43	30	71
907	71	360	02	33	30	360	03	43	30	69
908	02	360	02	32	30	360	02	54	30	23
909	14	360	02	33	30	360	03	42	30	70
910	28	360	02	37	30	360	03	42	30	66
911	08	360	03	10	30	360	03	42	30	32
1001	93	360	04	30	30	360	05	41	30	72
1002	08	360	04	30	30	360	05	41	30	72
1003	16	360	04	31	30	360	05	12	30	42
1004	24	360	04	31	30	360	05	41	30	71
1005	14	360	04	31	30	360	05	41	30	71

Table 4 (Continued)

Pass No.	Receiving Station No.	Start Time				Final Time				No. Obs.
		Day	Hr.	Min.	Sec.	Day	Hr.	Min.	Sec.	
1006	25	360	04	30	30	360	05	41	30	72
1007	12	360	04	31	30	360	05	41	30	69
1008	92	360	04	31	30	360	05	41	30	71
1009	28	360	04	32	30	360	05	41	30	71

Note: Pass numbers beginning with "n" correspond to the nth lunar revolution. Station number 23 (Madrid) was the sending station for revs 3, 4, 5, station number 28 (Goldstone) for revs 6, 7, 8, and station number 93 (Tidbinbilla) for revs 9, 10

Table 5

Geocentric Station Coordinates

Station Number	Station	Radius (Km)	Co-Latitude (rad.)	Longitude (rad.)
02	Bermuda	6372.101	1.0091915	5.1546872
04	Grand Canary Island	6373.604	1.0894054	6.0108605
08	Carnarvon	6374.458	2.0029560	1.9848626
12	Hawaii	6376.305	1.1869812	3.4965055
14	Guaymas	6373.515	1.0855226	4.3507419
16	Corpus Christi	6373.600	1.0909030	4.5836104
23	Madrid	6370.033	0.86803078	6.2104506
24	Guam	6377.169	1.3400062	2.5260920
25	Canberra	6372.114	2.1886929	2.6001318
28	Goldstone	6372.017	0.95713235	4.2433616
41	Grand Bahama Island	6373.916	1.1086510	4.9176805
71	Merritt Island	6373.336	1.0760447	4.8748194
75	Ascension Island	6378.322	1.7087208	6.0331219
91	Antigua Island	6376.376	1.2756078	5.2054543
92	Goldstone Wing	6372.064	0.95629688	4.2437845
93	Tidbinbilla	6371.703	2.1855144	2.6001926
94	Madrid Wing	6370.087	0.86851074	6.2090175

Table 6

Lunar Gravity Fields (m, n ≤ 4)

		Field 1		Field 2		Field 3	
n	m	C	S	C	S	C	S
2	0	-.47748300E-04	0	-.19208415E-03	0	-.18555678E-03	0
3	0	.89981492E-04	0	.85351419E-04	0	.87348083E-04	0
4	0	0	0	0	0	0	0
2	1	0	0	0	0	0	0
3	1	.28399115E-04	0	.25875283E-04	0	.27472943E-04	0
4	1	0	0	0	0	0	0
2	2	.48980846E-04	0	.48801068E-04	0	.49697892E-04	0
3	2	0	0	0	0	0	0
4	2	0	0	0	0	0	0
3	3	0	0	0	0	0	0
4	3	0	0	0	0	0	0
4	4	0	0	0	0	0	0

Table 6 (Continued)

n	m	Field 4		Field 5		Field 6	
		C	S	C	S	C	S
2	0	-.32167052E-03	0	-.19929678E-03	0	-.16141156E-03	0
3	0	.78946811E-04	0	.83279141E-04	0	.88671470E-04	0
4	0	0	0	0	0	0	0
2	1	0	0	0	0	0	0
3	1	.27076212E-04	0	.25499076E-04	0	.27194182E-04	0
4	1	0	0	0	0	0	0
2	2	.62178888E-04	0	.49596167E-04	0	.49000726E-04	0
3	2	0	0	0	0	0	0
4	2	0	0	0	0	0	0
3	3	0	0	0	0	0	0
4	3	0	0	0	0	0	0
4	4	0	0	0	0	0	0

Table 6 (Continued)

n	m	Field 7		Field 8	
		C	S	C	S
2	0	-.94542720E-04	0	-.14261924E-03	0
3	0	-.18633367E-02	0	-.21703288E-02	0
4	0	0	0	0	0
2	1	0	0	0	0
3	1	.36892664E-03	-.34553137E-03	.41365243E-03	-.40287127E-03
4	1	0	0	0	0
2	2	.67760812E-04	-.79597060E-05	.69687104E-04	-.69015562E-05
3	2	0	0	0	0
4	2	0	0	0	0
3	3	0	0	0	0
4	3	0	0	0	0
4	4	0	0	0	0

Table 6 (Continued)

		Field 9		Field 10	
n	m	C	S	C	S
2	0	-.10184620E-03	0	-.27240095E-03	0
3	0	-.21934790E-02	0	-.23277949E-02	0
4	0	0	0	0	0
2	1	0	0	0	0
3	1	.42379158E-03	-.41274877E-03	.44517440E-03	-.46592297E-03
4	1	0	0	0	0
2	2	.72762835E-04	-.68903567E-05	.89041646E-04	-.68973685E-05
3	2	0	0	0	0
4	2	0	0	0	0
3	3	0	0	0	0
4	3	0	0	0	0
4	4	0	0	0	0

Table 6 (Continued)

		Field 11		Field 12	
n	m	C	S	C	S
2	0	-.12658118E-03	0	-.20933326E-03	0
3	0	-.23902164E-02	0	.10710763E-02	0
4	0	0	0	0	0
2	1	0	0	0	0
3	1	.44955046E-03	-.45774616E-03	-.14432622E-03	.17045422E-03
4	1	0	0	0	0
2	2	.75534532E-04	-.66372290E-05	.32180256E-04	-.19853218E-04
3	2	0	0	0	0
4	2	0	0	0	0
3	3	0	0	0	0
4	3	0	0	.22620488E-05	-.11892957E-05
4	4	0	0	0	0

Table 6 (Continued)

n	m	Field 13		Field 14	
		C	S	C	S
2	0	-.94958618E-04	0	-.20941756E-03	0
3	0	-.21378518E-02	0	.13906189E-02	0
4	0	0	0	0	0
2	1	0	0	0	0
3	1	.41533104E-03	-.40294755E-03	-.20034018E-03	.22640486E-03
4	1	0	0	0	0
2	2	.59219663E-04	-.11840475E-04	.40635527E-04	-.20184747E-04
3	2	0	0	0	0
4	2	0	0	0	0
3	3	0	0	0	0
4	3	.18080847E-05	.66284901E-06	0	0
4	4	0	0	.71181038E-07	-.27750301E-06

Table 6 (Continued)

		Field 15		Field 16	
n	m	C	S	C	S
2	0	-.19876512E-03	0	-.67739005E-04	0
3	0	-.75669817E-04	0	-.22219648E-02	0
4	0	0	0	0	0
2	1	0	0	0	0
3	1	.53861330E-04	-.29084566E-04	.42782603E-03	-.41206419E-03
4	1	0	0	0	0
2	2	.49090605E-04	-.14053121E-04	.63306068E-04	-.42646783E-05
3	2	0	0	0	0
4	2	0	0	0	0
3	3	0	0	0	0
4	3	0	0	0	0
4	4	.11395952E-06	-.20088239E-06	.19694005E-06	-.81991497E-07

Table 6 (Continued)

		Field 17		Field 18	
n	m	C	S	C	S
2	0	-.12787077E-03	0	-.43974527E-03	0
3	0	-.21245931E-02	0	-.20260556E-02	0
4	0	0	0	0	0
2	1	0	0	0	0
3	1	.40459825E-03	-.40885897E-03	.40524367E-03	-.41745825E-03
4	1	0	0	0	0
2	2	.68156080E-04	-.65195078E-05	.11847936E-03	-.37998086E-05
3	2	0	0	0	0
4	2	0	0	0	0
3	3	0	0	0	0
4	3	0	0	0	0
4	4	.15192744E-06	-.15028712E-06	-.35583408E-07	-.11760250E-06

Table 6 (Continued)

		Field 19		Field 20	
n	m	C	S	C	S
2	0	-.25788695E-03	0	.20382955E-03	0
3	0	.46297039E-03	0	.37215738E-03	0
4	0	0	0	0	0
2	1	0	0	0	0
3	1	-.37482068E-04	.64128663E-04	-.22523372E-04	.48712217E-04
4	1	0	0	0	0
2	2	.30657306E-04	-.18132104E-04	-.27736834E-03	.29812258E-03
3	2	0	0	0	0
4	2	-.89763314E-05	.16955223E-06	-.17059748E-03	.18316744E-03
3	3	0	0	0	0
4	3	0	0	0	0
4	4	.98567327E-07	-.28225688E-06	-.96958517E-06	-.12320029E-05

Table 6 (Continued)

n	m	Field 21		Field 22	
		C	S	C	S
2	0	.44475390E-03	0	.36507256E-03	0
3	0	.43400536E-03	0	-.22511984E-02	0
4	0	0	0	.22807324E-03	0
2	1	0	0	0	0
3	1	-.33042705E-04	.54648735E-04	.42921915E-03	-.41758293E-03
4	1	0	0	0	0
2	2	-.35037931E-03	.32732277E-03	.63680027E-04	-.47118780E-05
3	2	0	0	0	0
4	2	-.16936881E-03	.18989687E-03	0	0
3	3	.83736097E-05	-.21566149E-05	0	0
4	3	0	0	0	0
4	4	-.14050795E-05	-.10888245E-05	.20204848E-06	-.83599954E-07

Table 6 (Continued)

		Field 23		Field 24	
n	m	C	S	C	S
2	0	-.24865223E-03	0	-.30060554E-04	0
3	0	-.44490799E-04	0	-.21150684E-02	0
4	0	-.87636401E-04	0	0	0
2	1	0	0	0	0
3	1	.13775011E-04	-.13156970E-04	.49965230E-03	-.32950596E-03
4	1	-.21568748E-05	-.15709608E-04	0	0
2	2	.18795934E-04	-.15507292E-04	.33410649E-04	.40946865E-05
3	2	.61294116E-05	-.36445992E-05	.95597587E-04	-.14867026E-04
4	2	.33440396E-05	-.74018892E-05	.0	0
3	3	.19280905E-05	-.14855343E-05	-.31424984E-05	.77048675E-05
4	3	-.15854769E-05	-.57511414E-06	0	0
4	4	.26244058E-06	-.13198670E-06	0	0

Table 6 (Continued)

		Field 25		Field 26	
n	m	C	S	C	S
2	0	-.20710800E-03	0	-.20710800E-03	0
3	0	.21000000E-04	0	.21000000E-04	0
4	0	0	0	-.36816406E-04	0
2	1	0	0	0	0
3	1	.34000000E-04	-.16389655E-05	.34000000E-04	-.16389655E-05
4	1	0	0	0	0
2	2	.20716000E-04	-.45004373E-06	.20716000E-04	-.45004373E-06
3	2	0	0	.48596936E-05	.91942924E-05
4	2	0	0	0	0
3	3	0	0	.18493695E-05	-.23402056E-05
4	3	0	0	0	0
4	4	0	0	-.18825909E-07	-.69582831E-07

Table 6 (Continued)

Field 27			
n	m	C	S
2	0	-.20710800E-03	0
3	0	.21000000E-04	0
4	0	.42336597E-03	0
2	1	0	0
3	1	.34000000E-04	-.16389655E-05
4	1	.35453029E-03	.89664366E-04
2	2	.20716000E-04	-.45004373E-06
3	2	.39637483E-05	.79527308E-05
4	2	-.16338678E-04	.28037592E-04
3	3	.59351288E-05	-.25582701E-05
4	3	.15451959E-05	-.40493034E-06
4	4	-.43031187E-06	.45239845E-07

Table 7

Higher Degree and Order Lunar Gravity Fields

		Field 28		Field 29	
n	m	C	S	C	S
2	0	-.75852895E-04	0	-.10074452E-03	0
3	0	-.22376541E-02	0	-.22130932E-02	0
4	0	0	0	0	0
5	0	0	0	0	0
6	0	0	0	0	0
2	1	0	0	0	0
3	1	.43077307E-03	-.41493560E-03	.42721699E-03	.41625410E-03
4	1	0	0	0	0
5	1	0	0	0	0
6	1	0	0	0	0
2	2	.62767467E-04	-.43834339E-05	.72625678E-04	-.66983026E-05
3	2	0	0	0	0

Table 7 (Continued)

		Field 28		Field 29	
n	m	C	S	C	S
4	2	0	0	0	0
5	2	0	0	0	0
6	2	0	0	0	0
3	3	0	0	0	0
4	3	0	0	0	0
5	3	0	0	0	0
6	3	0	0	0	0
4	4	.22704588E-06	-.59324818E-07	0	0
5	4	0	0	0	0
6	4	0	0	0	0
5	5	-.33250741E-08	-.37096675E-08	0	0
6	5	0	0	0	0
6	6	0	0	-.25353246E-09	-.24373341E-09

Table 7 (Continued)

		Field 30		Field 31	
n	m	C	S	C	S
2	0	-.61893629E-03	0	-.25275400E-03	0
3	0	-.55326755E-03	0	-.26702238E-04	0
4	0	-.58092734E-03	0	-.88942923E-04	0
5	0	-.31288510E-04	0	.56623103E-06	0
6	0	-.19636212E-04	0	-.11947185E-03	0
2	1	0	0	0	0
3	1	.12761252E-03	-.98702551E-04	.10406957E-04	-.99269870E-05
4	1	-.23104327E-04	.21811575E-04	-.14488460E-05	-.11155475E-04
5	1	.33550657E-03	-.30586567E-03	.26624421E-04	-.11398542E-04
6	1	-.12898153E-03	.76405779E-04	-.22250793E-04	.94986783E-05
2	2	.43864658E-04	-.20227167E-04	.18488716E-04	-.14649800E-04
3	2	-.27877112E-05	.12355627E-04	.53966939E-05	-.20280977E-05

Table 7 (Continued)

n	m	Field 30		Field 31	
		C	S	C	S
4	2	.14245040E-04	.85459170E-05	.38037297E-05	-.65879665E-05
5	2	-.79216140E-05	-.78930532E-04	.56394196E-06	-.39826183E-05
6	2	-.57222530E-04	.53406470E-04	-.44982497E-05	.75585989E-05
3	3	.43754171E-04	.46558827E-04	.18936775E-05	-.10277188E-05
4	3	.27364618E-05	-.11648657E-05	-.13951476E-05	-.76693417E-06
5	3	-.20158494E-05	.27179221E-04	.20008867E-06	.23939648E-05
6	3	-.16661486E-05	.18923284E-04	.61228862E-06	.16240935E-05
4	4	.65583499E-05	-.46465598E-05	.25311802E-06	-.12654819E-06
5	4	-.65854604E-05	.86220306E-05	.61671983E-06	.93725287E-06
6	4	.11859425E-05	-.27846489E-05	-.31439871E-06	-.87526765E-07
5	5	-.30899375E-06	-.10358430E-05	-.14775117E-06	.14730641E-07
6	5	.37140491E-06	-.16850191E-06	-.21183742E-07	-.27011205E-07
6	6	-.33195267E-08	.45820030E-07	.39436318E-08	-.28122807E-08

Table 8

Data Sets Used in Lunar Gravity Determinations

Field No.	Data Set	Epoch			rms (Hz)
		Day	Hr.	Min.	
1	6a, 7a	359	19	20	.52
2	7a, 8a	359	21	20	.53
3	6a, 7a, 8a	359	19	20	.96
4	6a, 7a, 8a, 9, 10	359	19	20	2.79
5	7a, 8a, 9	359	21	20	1.01
6	6b, 7b, 8b	359	19	20	.98
7	6a, 7a	359	19	20	.31
8	7a, 8a	359	21	20	.31
9	6a, 7a, 8a	359	19	20	.81
10	6a, 7a, 8a, 9, 10	359	19	20	2.53
11	7a, 8a, 9	359	21	20	.85
12	6a, 7a	359	19	20	.21
13	6a, 7a, 8a	359	19	20	.78
14	6a, 7a	359	19	20	.21
15	7a, 8a	359	21	20	.22
16	6a, 7a, 8a	359	19	20	.81
17	7a, 8a, 9	359	21	20	.82
18	3, 4, 5, 9, 10	359	13	20	4.97
19	6a, 7a	359	19	20	.21
20	6a, 7a, 8a	359	19	20	.30
21	6a, 7a, 8a	359	19	20	.32
22	6b, 7b, 8b	359	19	20	.80
23	6b	359	19	20	.18
	7b	359	21	20	.21

Table 8 (Continued)

Field No.	Data Set	Epoch			rms (Hz)
		Day	Hr.	Min.	
	8b	359	23	20	.22
24	6b, 7b, 8b	359	19	20	.81
25	6b, 7b, 8b	359	19	20	1.52
26	6b, 7b, 8b	359	19	20	.87
27	6b, 7b, 8b	359	19	20	.30
28	6a, 7a, 8a	359	19	20	.81
29	6a, 7a, 8a	359	19	20	.81
30	6b, 7b	359	19	20	.16
31	6b	359	19	20	.19
	7b	359	21	20	.21
	8b	359	23	20	.21

Data set 3: Pass Nos. 302, 303, 305, 306 (rev 3)

Data set 4: Pass Nos. 401, 402, 403, 404, 405, 407 (rev 4)

Data set 5: Pass Nos. 502, 503, 504, 505, 506, 507, 509 (rev 5)

Data set 6a: Pass Nos. 601, 603, 604, 605, 606, 607, 608, 609 (rev 6)

Data set 6b: Pass Nos. 601, 602, 603, 604, 605, 606, 608, 609 (rev 6)

Data set 7a: Pass Nos. 701, 702, 703, 704, 705, 706, 708, 709, 710 (rev 7)

Data set 7b: Pass Nos. 701, 702, 703, 704, 705, 706, 707, 709, 710 (rev 7)

Data set 8a: Pass Nos. 801, 802, 803, 804, 805, 806, 807, 809, 810 (rev 8)

Data set 8b: Pass Nos. 801, 802, 803, 804, 805, 806, 807, 808, 809 (rev 8)

Data set 9: Pass Nos. 901, 902, 903, 904, 905, 906, 907, 908, 909, 910, 911 (rev 9)

Data set 10: Pass Nos. 1001, 1002, 1003, 1004, 1005, 1006, 1007, 1008, 1009 (rev 10)

Table 9

Lunar Potential Models*

			C-Terms		S-Terms
n	m	TRIAX	R2	B	B
2	0	-2.07108	-2.07108	-1.9564	
2	1			- .1279	.1290
2	2	.20716	.20716	.1587	.1014
3	0		.21	- .1299	
3	1		.34	.3493	.0948
3	2			.0076	.0283
3	3			.0284	-.0447
4	0			.1230	
4	1			- .1607	.1099
4	2			.0265	.0012
4	3			.0027	.0148
4	4			.0039	.00005
5	0			- .0365	
6	0			- .0978	
7	0			.2603	
8	0			- .0905	

*Multiply all coefficients by 10^{-4}

Table 10

Residual Bounds and Standard Deviations

Field	Residual Bounds (Cm/Sec)		Standard Deviation (Cm/Sec)
	Negative	Positive	
TRIAX	- 8.7	7.5	
R2	- 6.6	7.6	5.5
3	- 6.7	6.3	3.4
4	- 7.3	5.4	3.1
15	- 3.2	5.1	1.7
27	- 3.7	8.3	2.2
30	-16.4	14.9	9.8

Table 11

Track Error Bounds

Field	Down Track Bounds (km)		Cross Track Bounds (km)		Perpendicular Bounds (km)	
	Negative	Positive	Negative	Positive	Negative	Positive
R2	-6.7	2.0	- 2.4	2.4	-1.9	0.2
3	-2.2	0.7	- 1.2	1.2	-3.4	0.4
4	0.5	0.0	- 0.6	0.6	-0.3	0.0
15	1.3	0.7	- 0.4	0.4	-0.3	0.2
27	-2.3	- 0.1	-13.8	13.8	-3.9	4.8
30	6.4	10.4	- 7.4	6.4	-1.1	1.2

Table 12

Normalized Eccentricity vs. Time Slope

Field	Slope
R2 (Converged (Reference Field))	1.000
TRIAX	0.143
R2	0.841
B	0.701
3	0.650
4	0.994
15	-0.255
27	1.153

Table 13

Converged Elements Using Field-R2

Revolution Number	Apolune ht. (Km)		Perilune ht. (Km)		a (Km)		Ω (Deg)		e		i (Deg)	
	Value	Differences	Value	Differences	Value	Differences	Value	Differences	Value	Differences	Value	Differences
1	310.61	.11	111.76	-.52	1949.28	-.21	-172.05	.02	.051007	.000165	146.36	-.01
2	310.72		111.24		1949.07		-172.03		.051172		146.35	
4	114.02	.23	110.67	-.82	1850.43	-.29	-172.00	.10	.000905	.000284	146.36	.08
5	114.25	.33	109.85	-.68	1850.14	-.17	-171.90	.01	.001189	.000272	146.44	-.05
6	114.58	.38	109.17	-.65	1849.97	-.14	-171.89	.07	.001461	.000280	146.39	.01
7	114.96	.56	108.52	-.50	1849.83	..03	-171.82	.05	.001741	.000285	146.40	.06
8	115.52	.35	108.02	-.62	1849.86	-.13	-171.77	.07	.002026	.000263	146.46	.06
9	115.87	.52	107.40	-.53	1849.73	-.01	-171.70	.00	.002289	.000285	146.52	-.01
10	116.39		106.87		1849.72		-171.70		.002574		146.51	

Table 14

Converged Elements Using Field-3

Revolution Number	Apolune ht. (Km)		Perilune ht. (Km)		a (Km)		Ω(Deg)		e		i(Deg)	
	Value	Differences	Value	Differences	Value	Differences	Value	Differences	Value	Differences	Value	Differences
1	310.71	.05	111.34	-.79	1949.11	-.36	-172.07	.06	.051144	.000070	146.32	.03
2	310.76		110.55		1948.75		-172.01		.051370		146.35	
4	113.56	.29	110.56	-.79	1850.15	-.25	-171.98	.07	.000811	.000293	146.36	.04
5	113.85	.32	109.77	-.65	1849.90	-.17	-171.91	.03	.001104	.000260	146.40	-.02
6	114.17	.31	109.12	-.69	1849.73	-.19	-171.88	.10	.001364	.000273	146.38	.03
7	114.48	.52	108.43	-.51	1849.54	.01	-171.78	.03	.001637	.000277	146.41	.05
8	115.00	.32	107.92	-.64	1849.55	-.16	-171.75	.04	.001914	.000279	146.46	.02
9	115.32	.47	107.28	-.57	1849.39	-.05	-171.71	.02	.002173	.000264	146.98	-.01
10	115.79		106.71		1849.34		-171.69		.002457		146.47	

Table 15

Converged Elements Using Field-15

Revolution Number	Apolune ht. (Km)		Perilune ht. (Km)		a (Km)		Ω(Deg)		e		i(Deg)	
	Value	Differences	Value	Differences	Value	Differences	Value	Differences	Value	Differences	Value	Differences
1	310.75	.08	111.47	-.49	1949.20	-.20	-172.06	.03	.051120	.00015	146.33	.01
2	310.83		110.98		1949.00		-172.03		.051270		146.34	
4	113.71	.51	110.44	-.45	1850.17	.02	-171.98	.04	.000884	.000259	146.36	.03
5	114.22	.37	109.99	-.57	1850.19	-.10	-171.94	.05	.001143	.000255	146.39	.00
6	114.59	.38	109.42	-.61	1850.09	-.11	-171.89	.04	.001398	.000268	146.39	.00
7	114.97	.40	108.81	-.58	1849.98	-.09	-171.85	.04	.001666	.000263	146.39	.03
8	115.37	.31	108.23	-.60	1849.89	-.15	-171.81	.05	.001929	.000249	146.42	.00
9	115.68	.49	107.63	-.57	1849.74	-.04	-171.76	.02	.002178	.000284	146.42	.02
10	116.17		107.06		1849.70		-171.74		.002462		146.44	

Table 16

Converged Elements Using Field-27

Revolution Number	Apolune ht. (Km)		Perilune ht. (Km)		a (Km)		Ω(Deg)		e		i(Deg)	
	Value	Differences	Value	Differences	Value	Differences	Value	Differences	Value	Differences	Value	Differences
1	310.02	.28	110.73	-.17	1948.47	.05	-172.33	.27	.051139	.000115	146.20	.21
2	310.30		110.56		1948.52		-172.05		.051254		146.41	
4	113.04	.58	109.37	-.43	1849.30	.07	-172.13	.07	.000993	.000274	146.42	.02
5	113.62	.48	108.94	-.57	1849.37	-.05	-172.06	.06	.001267	.000284	146.44	.00
6	114.10		108.37		1849.32		-172.00		.001551		146.44	

Table 17

Converged Elements Using Field-30

Revolution Number	Apolune ht. (Km)		Perilune ht. (Km)		a (Km)		Ω(Deg)		e		i(Deg)	
	Value	Differences	Values	Differences	Value	Differences	Value	Differences	Value	Differences	Value	Differences
1	310.38	0.02	110.25	-3.51	1948.40	-1.74	-171.69	.10	.051359	.000949	146.24	.00
2	310.40		106.74		1946.66		-171.58		.052308		146.24	
4	113.49	0.52	109.87	-0.18	1849.77	- .38	-171.82	.02	.000978	.000271	146.27	.05
5	114.01	0.25	109.39	-0.48	1849.39	.16	-171.80	.03	.001249	.000267	146.32	.01
6	114.26	0.22	108.65	-0.74	1849.55	- .30	-171.77	.02	.001516	.000281	146.33	.01
7	114.48	0.34	107.83	-0.82	1849.25	- .19	-171.75	-.01	.001797	.000286	146.34	.04
8	114.82	0.17	107.12	-0.71	1849.06	- .30	-171.76	.00	.002083	.000257	146.38	-.01
9	114.99	0.33	106.34	-0.78	1848.76	- .22	-171.76	.01	.002340	.000293	146.37	.02
10	115.32		105.59		1848.54		-171.75		.002633		146.39	

Table 18

Predicted Elements Using Field-Triax

Time (hr:min)	Apolune (Km)		Perilune (Km)		a (Km)		Ω(Deg)		e		i(Deg)	
	Value	Differences	Value	Differences	Value	Differences	Value	Differences	Value	Differences	Value	Differences
15:20	1851.60	-.04	1849.35	.04	1850.47	-.01	-172.31	.03	.00060747	-.00002195	146.03	.01
17:20	1851.56	-.03	1849.39	-.03	1850.46	-.01	-172.28	.04	.00058552	.00000107	146.04	.01
19:20	1851.53	.03	1849.36	-.05	1850.45	-.02	-172.24	.03	.00058659	.00002189	146.05	.01
21:20	1851.56	.05	1849.31	-.10	1850.43	-.02	-172.21	.04	.00060848	.00003880	146.06	.01
23.20	1851.61	.07	1849.21	-.12	1850.41	-.02	-172.17	.04	.00064728	.00005146	146.07	.01
01:20	1851.68	.08	1849,09	-.14	1850.39	-.03	-172.13	.03	.00069874	.00006043	146.08	.01
03:20	1851.76	.10	1848.95	-.15	1850.36	-.03	-172.10	.04	.00075917	.00006664	146.09	.01
05:20	1851.86		1848.80		1850.33		-172.06		.00082581		146.10	

Table 19

Predicted Elements Using Field-R2

Time (hr:min)	Apolune (Km)		Perilune (Km)		a (Km)		Ω(Deg)		e		i(Deg)	
	Value	Differences	Value	Differences	Value	Differences	Value	Differences	Value	Differences	Value	Differences
15:20	1851.60	0.41	1849.35	0.43	1850.47	-.01	-172.31	.03	.00060741	.00022585	146.03	.01
17:20	1852.01	0.40	1848.92	0.42	1850.46	-.01	-172.28	.04	.00083332	.00022460	146.04	.01
19:20	1852.41	0.40	1848.50	-0.43	1850.45	-.01	-172.24	.03	.00105792	.00022138	146.05	.01
21:20	1852.81	0.38	1848.07	0.58	1850.44	-.02	-172.21	.04	.0012793	.00021770	146.06	.01
23:20	1853.19	0.38	1848.65	-1.41	1850.42	-.02	-172.17	.03	.00149700	.00021400	146.07	.01
01:20	1853.57	0.36	1847.24	-0.42	1850.40	-.02	-172.14	.04	.0017110	.00021040	146.08	.01
03:20	1853.93	0.36	1846.82	-0.40	1850.38	-.02	-172.10	.03	.0019214	.00020720	146.09	.01
05:20	1854.29		1846.42		1850.36		-172.07		.0021286		146.10	

Table 20

Predicted Elements Using Field-3

Time (hr:min)	Apolune (Km)		Perilune (Km)		a (Km)		Ω(Deg)		e		i(Deg)	
	Value	Differences	Value	Differences	Value	Differences	Value	Differences	Value	Differences	Value	Differences
15:20	1851.59	0.24	1849.35	-0.24	1850.47	.00	-172.31	.04	.00060747	.00012776	146.03	.01
17:20	1851.83	0.28	1849.11	-0.30	1850.47	-.01	-172.27	.02	.00073523	.00015850	146.04	.00
19:20	1852.11	0.32	1848.81	-0.33	1850.46	.00	-172.25	.04	.00089373	.00017370	146.04	.01
21:20	1852.43	0.33	1848.48	-0.34	1850.46	-.01	-172.21	.03	.00106743	.00018097	146.05	.00
23:20	1852.76	0.34	1848.14	-0.35	1850.45	-.01	-172.18	.04	.0012484	.00018410	146.05	.01
01:20	1853.10	0.33	1847.79	-0.34	1850.44	.00	-172.14	.03	.0014325	.00018500	146.06	.00
03:20	1853.43	0.34	1847.45	-0.35	1850.44	-.01	-172.11	.03	.0016175	.00018450	146.06	.01
05:20	1853.77		1847.10		1850.43		-172.08		.0018020		146.07	

Table 21

Predicted Elements Using Field-4

Time (hr:min)	Apolune (Km)		Perilune (Km)		a (Km)		Ω(Deg)		e		i(Deg)	
	Value	Differences	Value	Differences	Value	Differences	Value	Differences	Value	Differences	Value	Differences
15:20	1851.60	0.42	1849.35	-0.47	1850.47	-.03	-172.31	.05	.00060747	.00024087	146.03	.03
17:20	1852.02	0.41	1848.88	-0.49	1850.44	-.03	-172.26	.06	.00084834	.00024543	146.06	.01
19:20	1852.43	0.41	1848.39	-0.50	1850.41	-.05	-172.20	.05	.00109377	.00024443	146.07	.03
21:20	1852.84	0.39	1847.89	-0.51	1850.36	-.06	-172.15	.05	.0013382	.00024270	146.10	.02
23:20	1853.23	0.38	1847.38	-0.51	1850.30	-.07	-172.10	.05	.0015809	.00024150	146.12	.02
01:20	1853.61	0.36	1846.87	-0.53	1850.23	-.09	-172.05	.05	.0018224	.00024130	146.14	.02
03:20	1853.97	0.37	1846.34	-0.53	1850.16	-.07	-172.00	.06	.0020637	.00024230	146.16	.02
05:20	1854.34		1845.81		1850.07		-171.94		.0023060		146.18	

Table 22

Predicted Elements Using Field-15

Time (hr:min)	Apolune (Km)		Perilune (Km)		a (Km)		Ω(Deg)		e		i(Deg)	
	Value	Differences	Value	Differences	Value	Differences	Value	Differences	Value	Differences	Value	Differences
15:20	1851.59	-.24	1849.35	.24	1850.47	.00	-172.31	.04	.00060747	-.00012934	146.03	.01
17:20	1851.35	-.21	1849.59	.21	1850.47	.00	-172.27	.03	.00047813	-.00011630	146.04	.00
19:20	1851.14	-.16	1849.80	.15	1850.47	.00	-172.24	.03	.00036183	-.00008361	146.04	.01
21:20	1850.98	-.03	1849.95	.03	1850.47	-.01	-172.21	.04	.00027822	-.00001450	146.05	.00
23:20	1850.95	-.24	1849.98	-.02	1850.46	-.13	-172.17	.00	.00026372	-.00006315	146.05	.01
01:20	1850.71	.57	1849.96	-.32	1850.33	.13	-172.17	.07	.00020057	.00024320	146.06	.00
03:20	1851.28	.25	1849.64	-.26	1850.46	.00	-172.10	.03	.00044377	.00013531	146.06	.01
05:20	1851.53		1849.38		1850.46		-172.07		.00057908		146.07	

Table 23

Predicted Elements Using Field-B

Time (hr:min)	Apolune (Km)		Perilune (Km)		a (Km)		Ω(Deg)		e		i(Deg)	
	Value	Differences	Value	Differences	Value	Differences	Value	Differences	Value	Differences	Value	Differences
15:20	1851.59	0.32	1849.34	-0.34	1850.47	-.01	-172.31	.02	.00060747	-.00017911	146.03	.00
17:20	1851.91	0.30	1849.00	-0.35	1850.46	-.03	-172.29	.03	.00078658	-.00017635	146.03	.00
19:20	1852.21	0.28	1848.65	-0.38	1850.43	-.06	-172.26	.02	.00096293	-.00017743	146.03	-.01
21:20	1852.49	0.27	1848.27	-0.40	1850.37	-.06	-172.24	.03	.00114036	-.00018164	146.02	.00
23:20	1852.76	0.27	1847.87	-0.42	1850.31	-.07	-172.21	.03	.0013220	-.00027490	146.02	.00
01:20	1853.03	0.28	1847.45	-0.44	1850.24	-.08	-172.18	.02	.0015969	-.00010700	146.02	.00
03:20	1853.31	0.29	1847.01	-0.45	1850.16	-.08	-172.16	.03	.0017039	-.00020010	146.02	-.01
05:20	1853.60		1846.56		1850.08		-172.13		.001904		146.01	

Table 24

Predicted Elements Using Field 27

Time (hr:min)	Apolune (Km)		Perilune (Km)		a (km)		Ω(Deg)		e		i(Deg)	
	Value	Differences	Value	Differences	Value	Differences	Value	Differences	Value	Differences	Value	Differences
15:20	1851.59	0.63	1849.35	-0.55	1850.47	.04	-172.31	.41	.00060747	.00031713	146.03	0.39
17:20	1852.22	0.62	1848.80	-0.56	1850.51	.03	-171.90	.40	.00092460	.00031850	146.42	0.38
19:20	1852.84	0.61	1848.24	-0.54	1850.54	.03	-171.50	.40	.0012431	.00031040	146.80	0.39
21:20	1853.45	0.58	1847.70	-0.53	1850.57	.03	-171.10	.40	.0015535	.00029900	147.19	0.40
23:20	1854.03	0.55	1847.17	-0.50	1850.60	.02	-170.70	.29	.0018525	.00028620	147:59	0.40
01:20	1854.58	0.52	1846.67	-0.50	1850.62	.01	-170.31	.28	.0021387	.00027300	147.99	0.40
03:20	1855.10	0.50	1846.17	-0.47	1850.63	.01	-169,93	.22	.0024117	.00025970	148.39	0.40
05:20	1855.60		1845.70		1850.64		-169.55		.0026714		148.79	

Table 25

Predicted Elements (1 Revolution) Using Field-R2

Revolution Number	Apolune ht. (Km)		Perilune ht (Km)		a (Km)		Ω(Deg)		e		i(Deg)	
	Value	Differences	Value	Differences	Value	Differences	Value	Differences	Value	Differences	Value	Differences
1 to 2	310.73		111.35		1949.13		-172.02		.051143		146.36	
4 to 5	114.44	.24	110.22	-.84	1850.43	-.31	-172.00	.14	.001140	.000292	146.36	.09
5 to 6	114.68	.33	109.38	-.68	1850.12	-.17	-171.86	.01	.001432	.000275	146.45	-.05
6 to 7	115.01	.39	108.70	-.76	1849.95	-.14	-171.85	.07	.001707	.000281	146.40	.01
7 to 8	115.40	.45	108.04	-.58	1849.81	.02	-171.78	.04	.001988	.000286	146.41	.06
8 to 9	115.95	.36	107.54	-.63	1849.83	-.09	-171.74	.07	.002274	.000334	146.47	.06
9 to 10	116.31		106.91		1849.74		-171.67		.002608		146.53	

Table 26

Predicted Elements (1 Revolution) Using Field-3

Revolution Number	Apolune ht. (Km)		Perilune ht. (Km)		a (Km)		Ω(Deg)		e		i(Deg)	
	Value	Differences	Value	Differences	Value	Differences	Value	Differences	Value	Differences	Value	Differences
1 to 2	310.52		111.24		1948.97		-172.04		.051123		146.34	
4 to 5	114.04	.28	110.03	-.81	1850.12	-.26	-171.95	.07	.001085	.000293	146.38	.04
5 to 6	114.32	.31	109.22	-.67	1849.86	-.18	-171.88	.03	.001378	.000265	146.42	-.03
6 to 7	114.63	.32	108.55	-.71	1849.68	-.19	-171.85	.09	.001643	.000278	146.39	.03
7 to 8	114.95	.53	107.84	-.52	1849.49	.00	-171.76	.04	.001921	.000384	146.42	.06
8 to 9	115.48	.32	107.32	-.66	1849.49	-.17	-171.72	.04	.002205	.000265	146.48	.01
9 to 10	115.80		106.66		1849.32		-171.68		.002470		146.49	

Table 27

Predicted Elements (1 Revolution) Using Field-15

Revolution Number	Apolune ht. (Km)		Perilune ht. (Km)		a (Km)		Ω(Deg)		e		i(Deg)	
	Value	Differences	Value	Differences	Value	Differences	Value	Differences	Value	Differences	Value	Differences
1 to 2	310.67		111.23		1949.04		-172.03		.051154		146.34	
4 to 5	114.15	.50	109.99	-.48	1850.16	.01	-171.94	.06	.001122	.000267	146.37	.03
5 to 6	114.65	.37	109.51	-.60	1850.17	-.11	-171.88	.02	.001389	.000261	146.40	.00
6 to 7	115.02	.38	108.91	-.64	1850.06	-.14	-171.86	.04	.001650	.000276	146.40	.01
7 to 8	115.40	.40	108.27	-.60	1849.92	-.10	-171.82	.05	.001926	.000274	146.41	.02
8 to 9	115.80	.33	107.67	-.64	1849.82	-.15	-171.77	.04	.002200	.000260	146.43	.01
9 to 10	116.13		107.03		1849.67		-171.73		.002460		146.44	

Table 28

Predicted Elements (1 Revolution) Using Field-27

Revolution Number	Apolune ht. (Km)		Periline ht. (Km)		a (Km)		Ω (Deg)		e		i (Deg)	
	Value	Differences	Value	Differences	Value	Differences	Value	Differences	Value	Differences	Value	Differences
1 to 2	310.07		110.74		1948.50		-171.87		.051151		146.56	
4 to 5	113.62	.38	108.87	-.45	1849.33	.07	-171.72	.05	.001285	.000278	146.81	.02
5 to 6	114.00		108.42		1849.40		-171.67		.001563		146.83	

Table 29

Predicted Elements (1 Revolution) Using Field-30

Revolution Number	Apolune ht. (Km)		Perilune ht. (Km)		a (Km)		Ω(Deg)		e		i (Deg)	
	Value	Differences	Value	Differences	Value	Differences	Value	Differences	Value	Differences	Value	Differences
1 to 2	309.37		107.60		1946.58		-171.93		.051928		146.15	
4 to 5	113.81	.49	109.27	-.56	1849.23	.37	-171.93	.00	.001227	.000286	146.15	-.05
5 to 6	114.30	.17	108.71	-.85	1849.60	-.29	-171.93	.02	.001513	.000292	146.10	.01
6 to 7	114.47	.38	107.86	-.95	1849.31	-.34	-171.91	.03	.001815	.000332	146.11	.01
7 to 8	114.85	.41	106.91	-.83	1848.97	-.21	-171.88	-.01	.002147	.000336	146.12	.03
8 to 9	115.26	.31	106.08	-.94	1848.76	-.31	-171.89	.00	.002483	.000338	146.15	.00
9 to 10	115.57		105.14		1848.45		-171.89		.002821		146.15	

Table 30

Track Error Bounds

Field	Orbits	Down Track (Km)		Cross Track (Km)		Perpendicular (Km)	
		Low	High	Low	High	Low	High
R2	678 to 9	-5.20	-3.78	-48.8	43.5	-2.6	.8
R2	1 to 2	-2.58	-2.15	- 0.8	0.7	-1.9	.09
R2	4 to 5	-6.75	-5.70	- 2.4	2.4	- .45	- .06
R2	5 to 6	-4.95	-3.25	- 1.6	1.5	- .86	- .08
R2	6 to 7	-3.28	-2.40	- 0.6	0.5	- .2	- .03
R2	7 to 8	-2.53	-2.30	- 1.4	1.5	-1.3	0.2
R2	8 to 9	-3.55	-2.85	- 1.9	1.9	- .14	- .07
R2	9 to 10	-2.50	-1.98	- 1.0	0.9	- .14	.11
3	1 to 2	-2.20	- .55	- .6	.6	- .84	.4
3	4 to 5	-1.67	-2.15	- .9	.9	-3.4	.02
3	5 to 6	- .20	.15	- 1.2	1.1	- .21	- .01
3	6 to 7	.15	.70	- 1.2	1.2	- .20	- .04
3	8 to 9	.33	.58	- .4	.2	- .18	.01
4	4 to 5	.46	0.0	- .6	.6	- .3	0.0
15	1 to 2	-1.30	.67	- .2	.2	- .26	.18
15	4 to 5	- .75	- .55	- .4	.4	- .02	.08
15	6 to 7	-1.20	-1.03	- .3	.2	- .13	.01
15	8 to 9	-1.00	- .80	- .3	.2	- .13	0.0
27	678 to 9	2.84	3.28	-37.2	37.1	.02	4.6
27	1 to 2	2.3	-1.35	- 6.5	6.1	-3.9	4.8
27	4 to 5	- .23	- .08	-13.6	13.6	- .01	.14
27	5 to 6	- .70	- .65	-13.8	13.8	- .01	.04
30	1 to 2	6.45	10.45	- 7.45	6.4	-1.07	1.23
30	5 to 6	.05	1.90	- 5.1	5.1	- .37	.48
30	8 to 9	- .95	- .05	- 4.4	4.4	- .28	.24

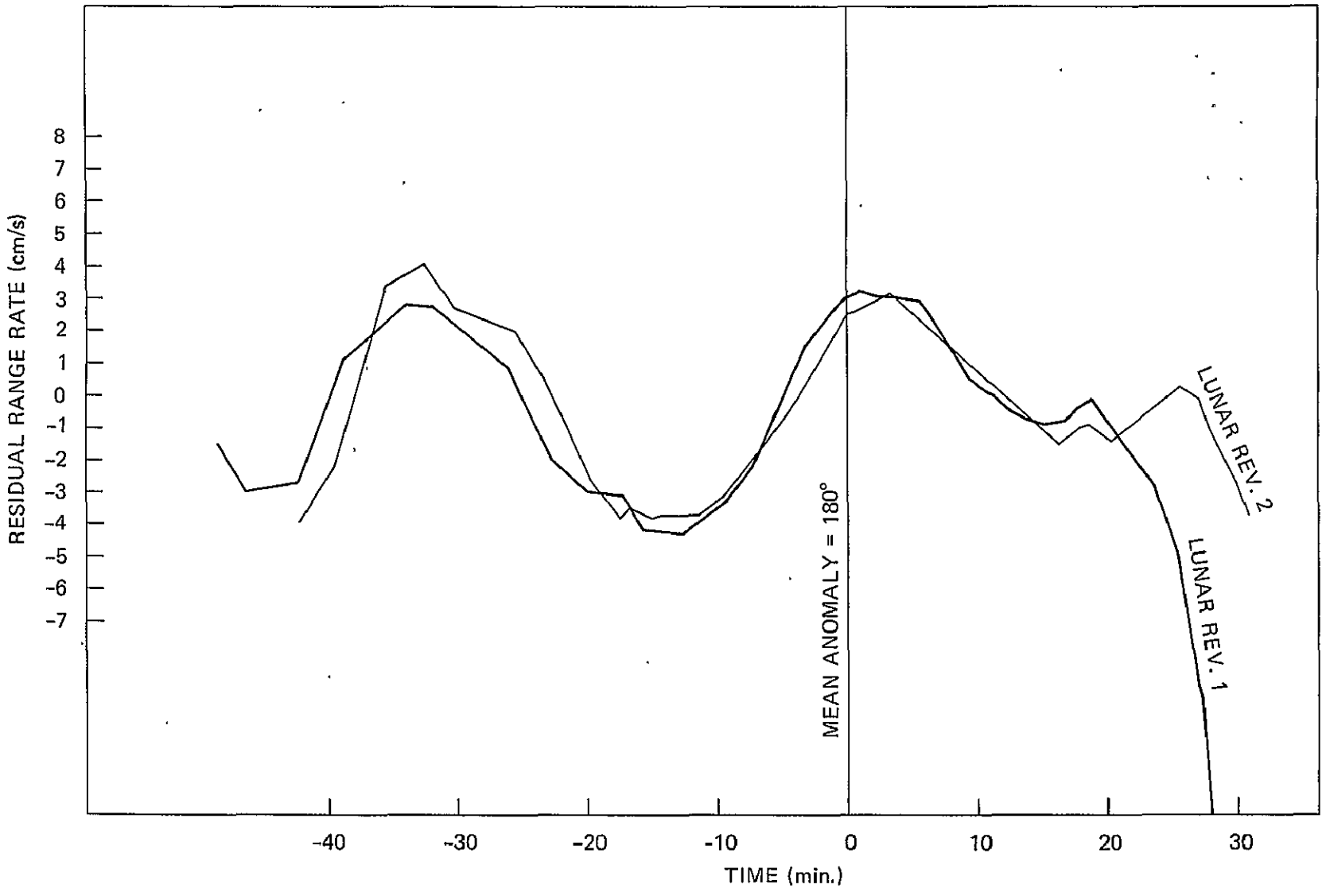

Figure 1. Apollo 8 Range Rate Mean Residuals

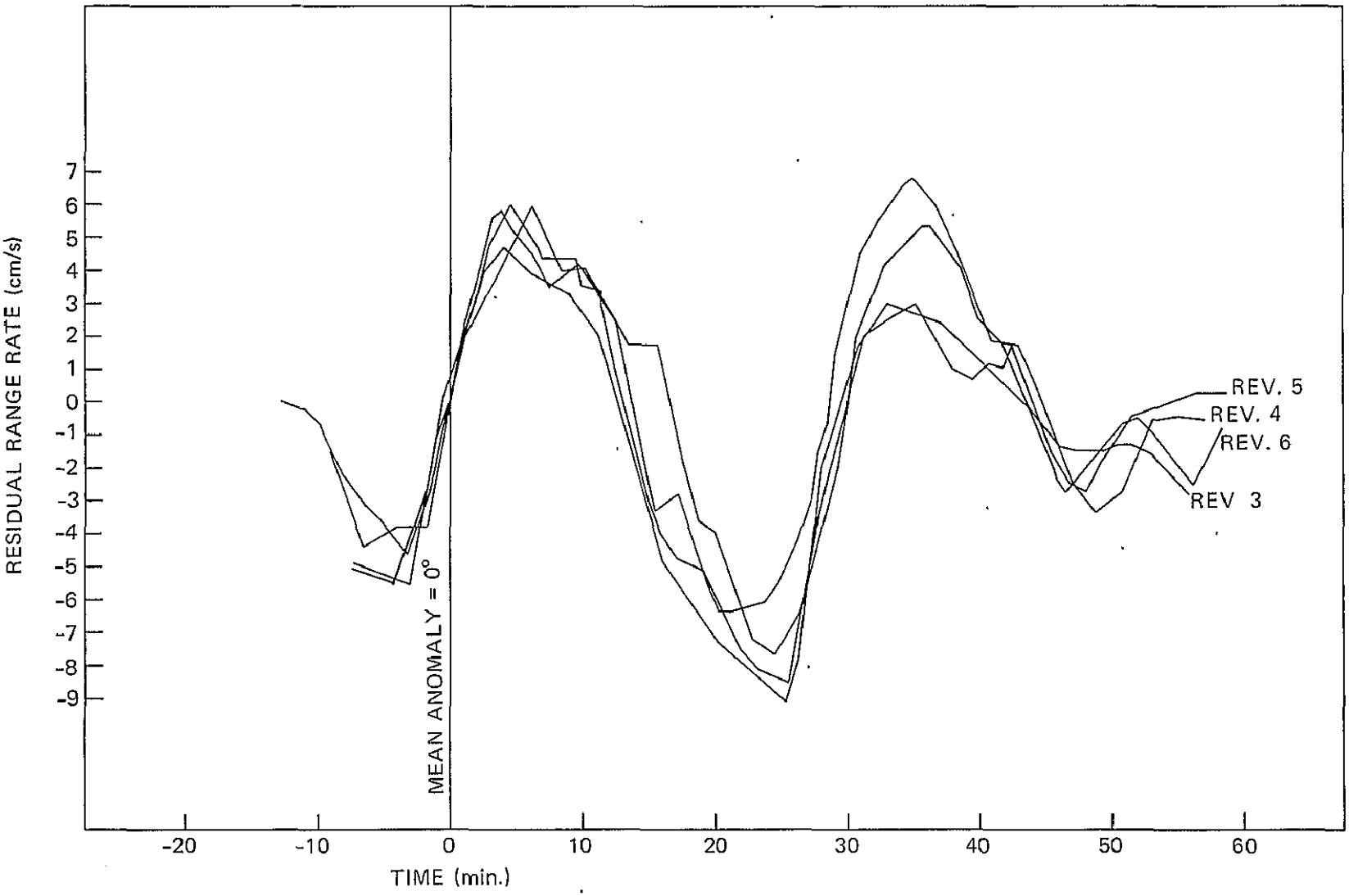

Figure 2. Apollo 8 Range Rate Mean Residuals

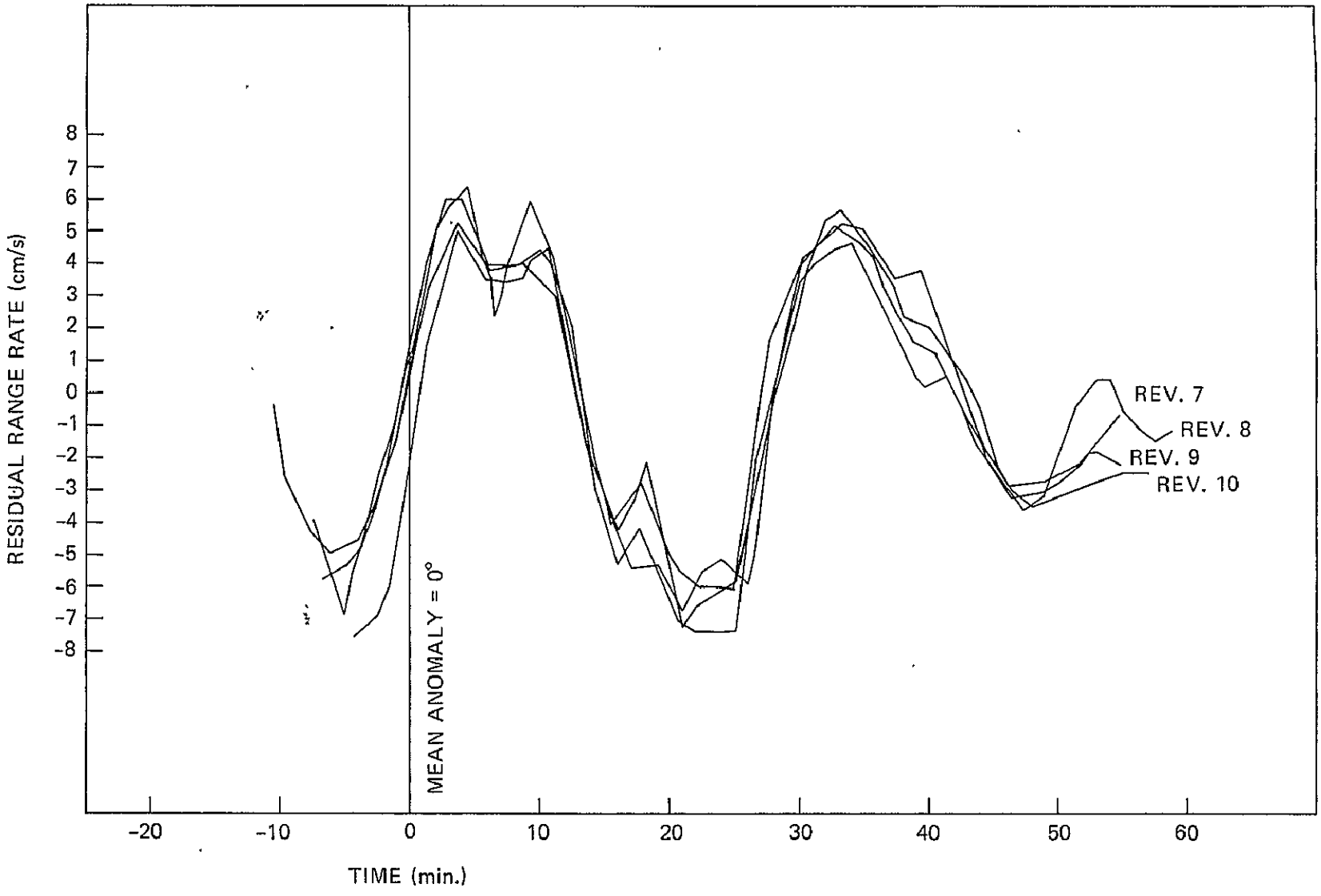

Figure 3. Range Rate Mean Residuals

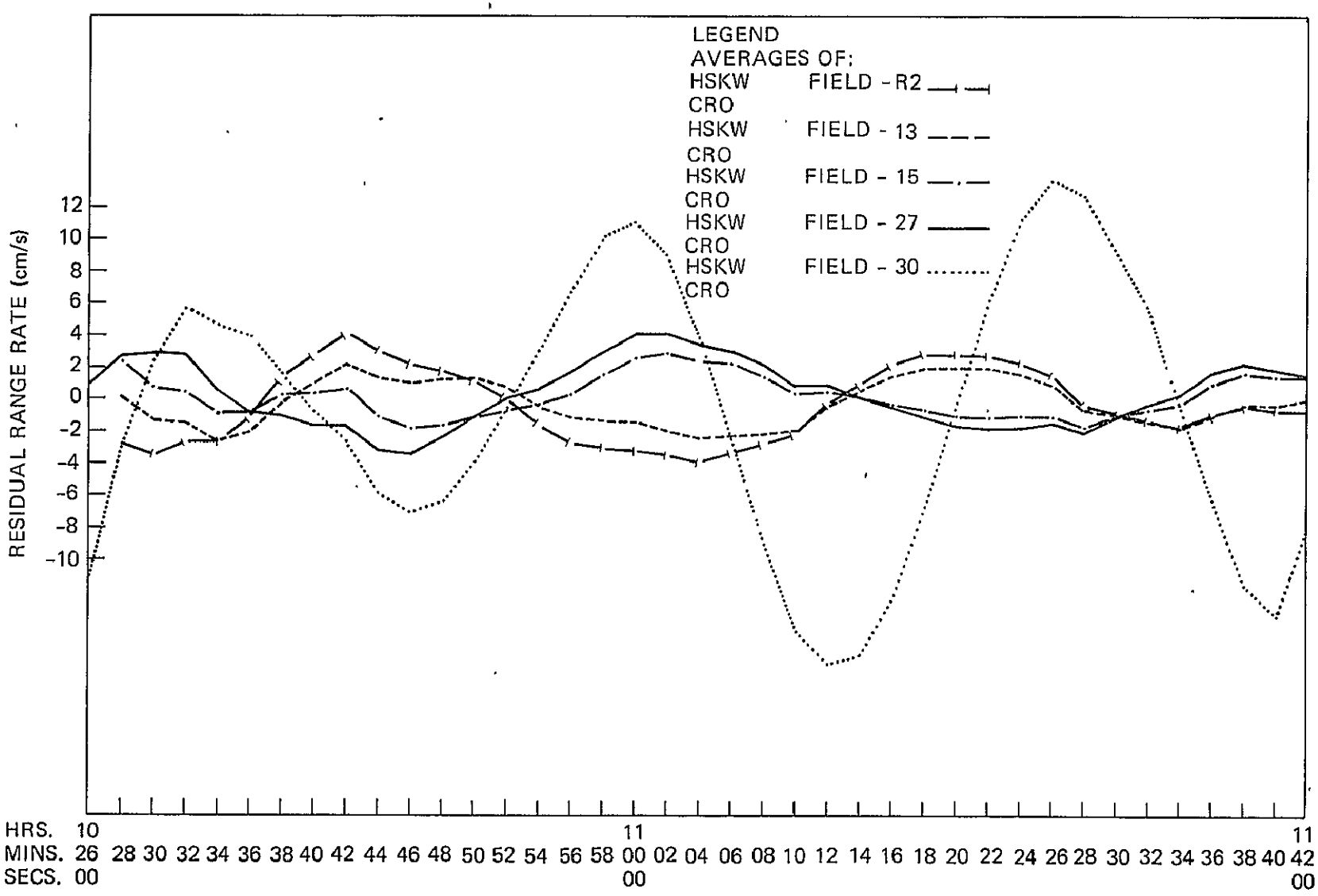

Figure 4. Apollo 8 Range Rate Residuals (Lunar Orbit 1)

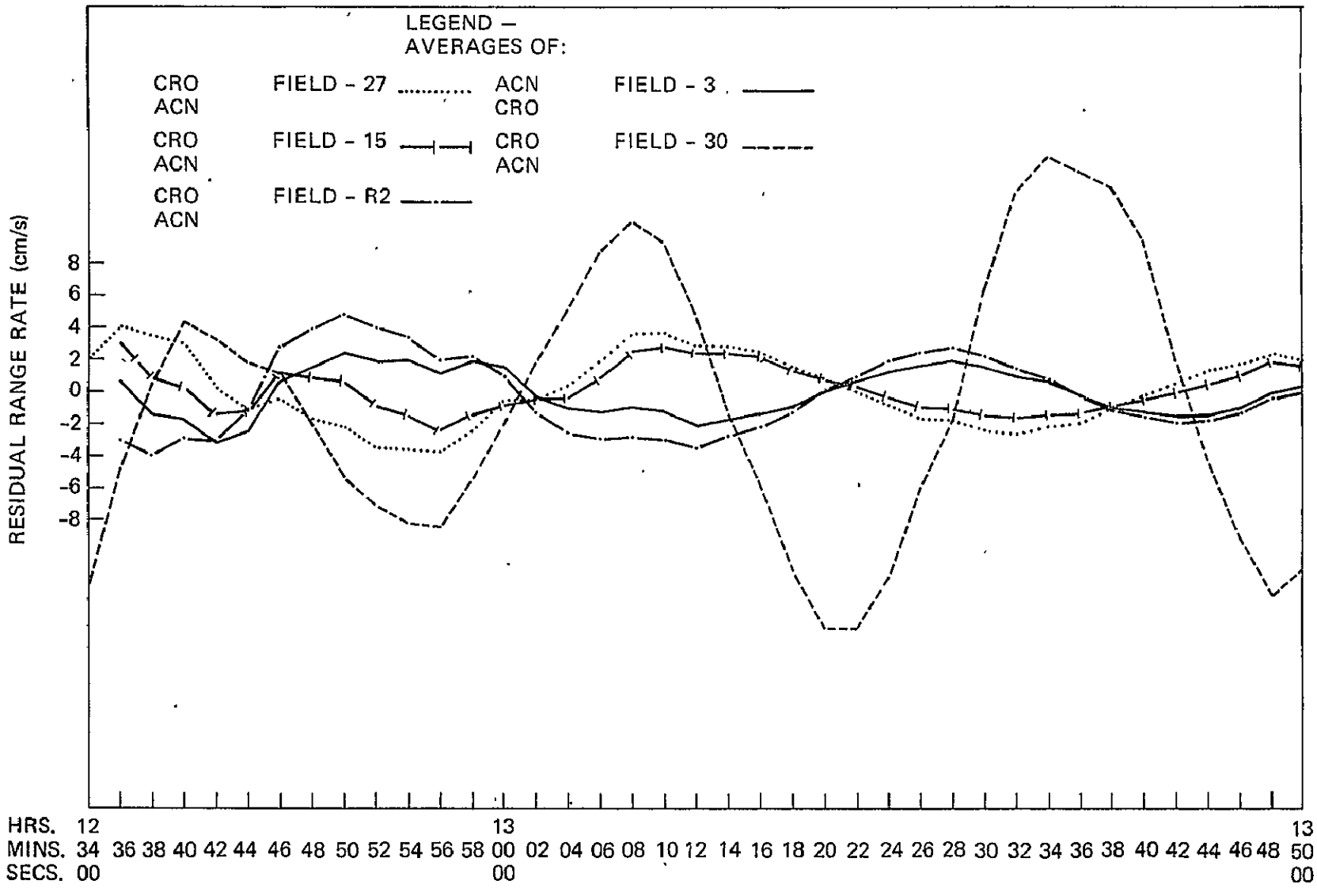

Figure 5. Apollo 8 Range Rate Residuals (Lunar Orbit 2)

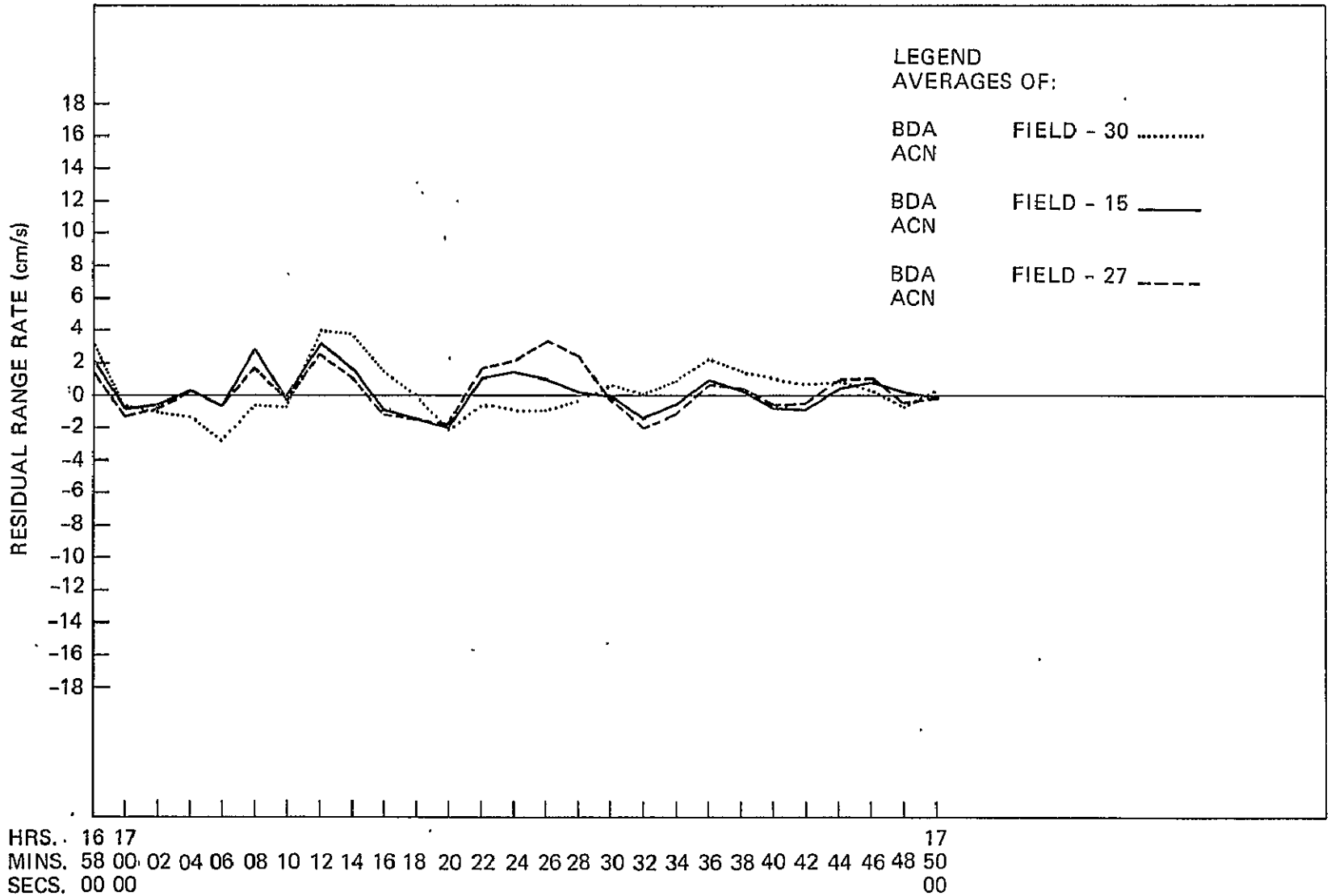

Figure 6. Apollo 8 Range Rate Residuals (Lunar Orbit 4)

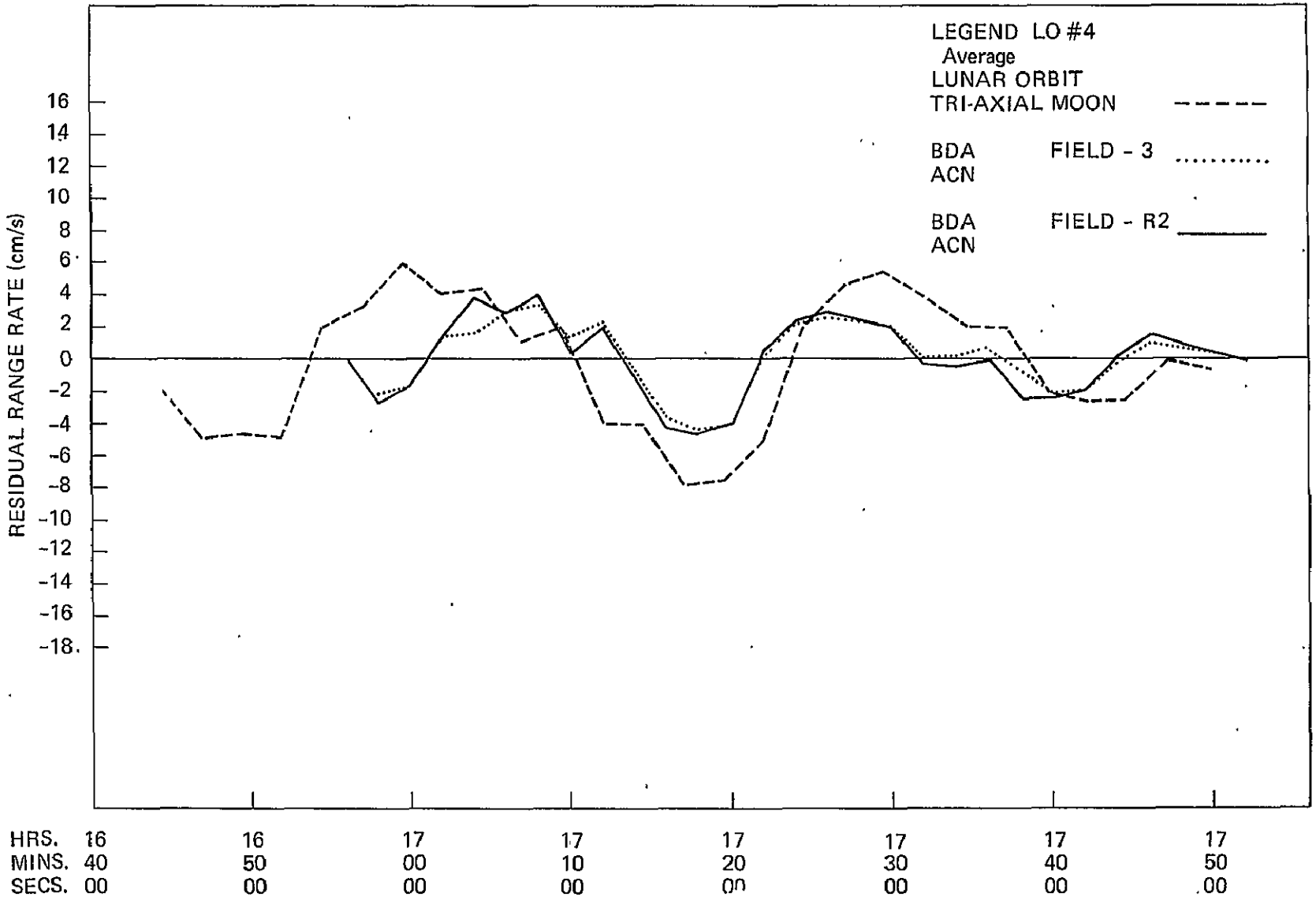

Figure 7. Apollo 8 Range Rate Residuals (Lunar Orbit 4)

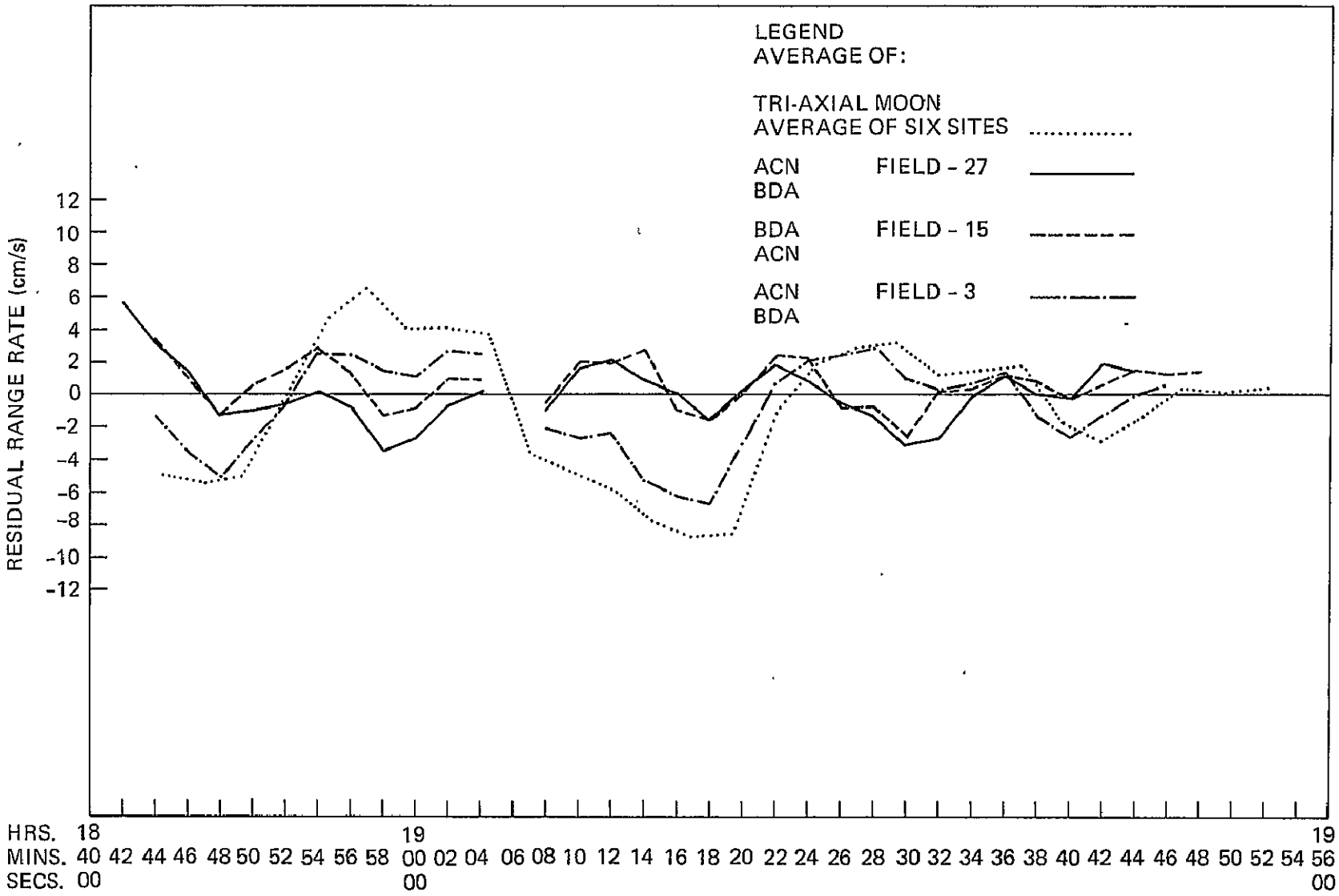

Figure 8. Apollo 8 Range Rate Residuals (Lunar Orbit 5)

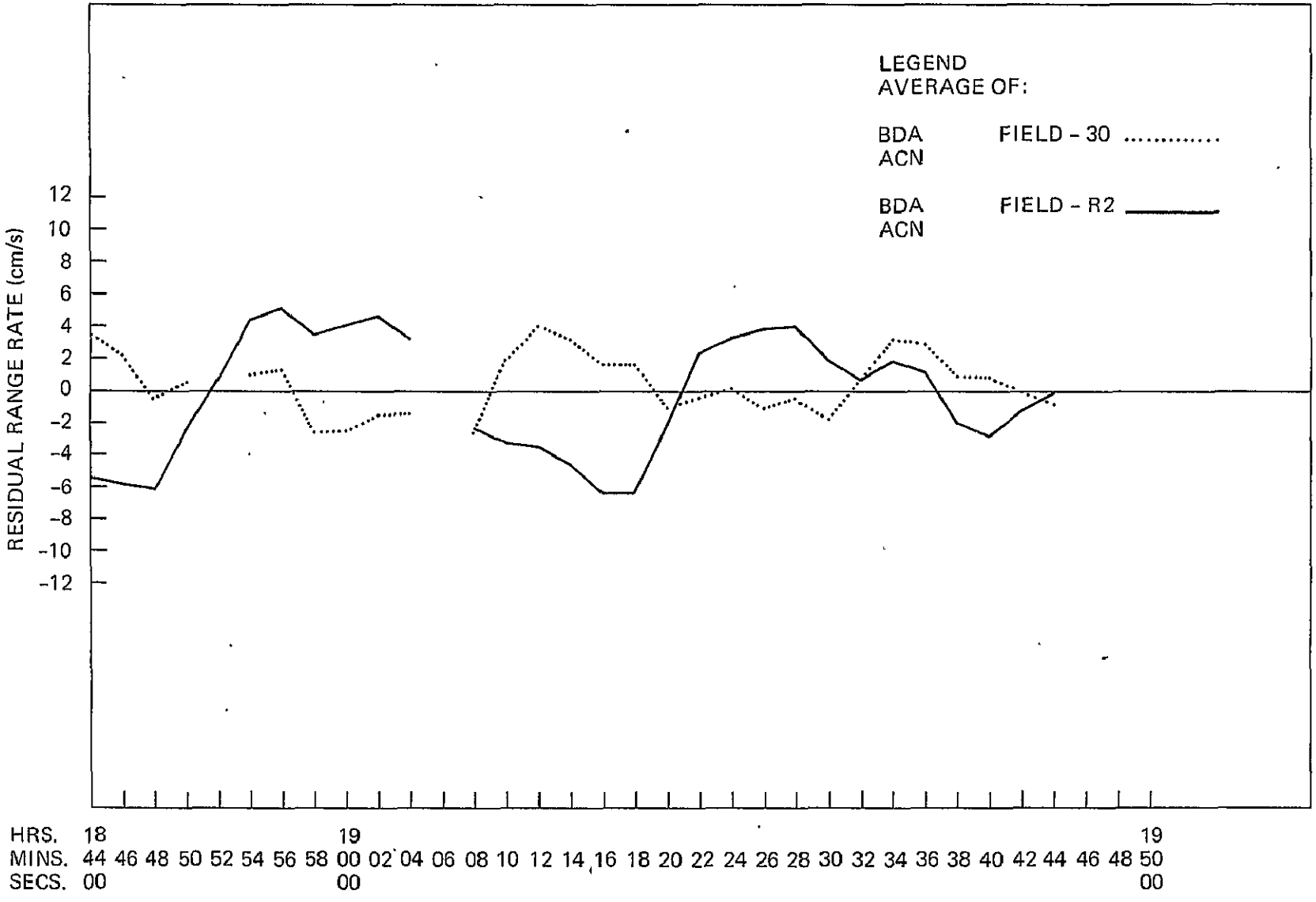

Figure 9. Apollo 8 Range Rate Residuals (Lunar Orbit 5)

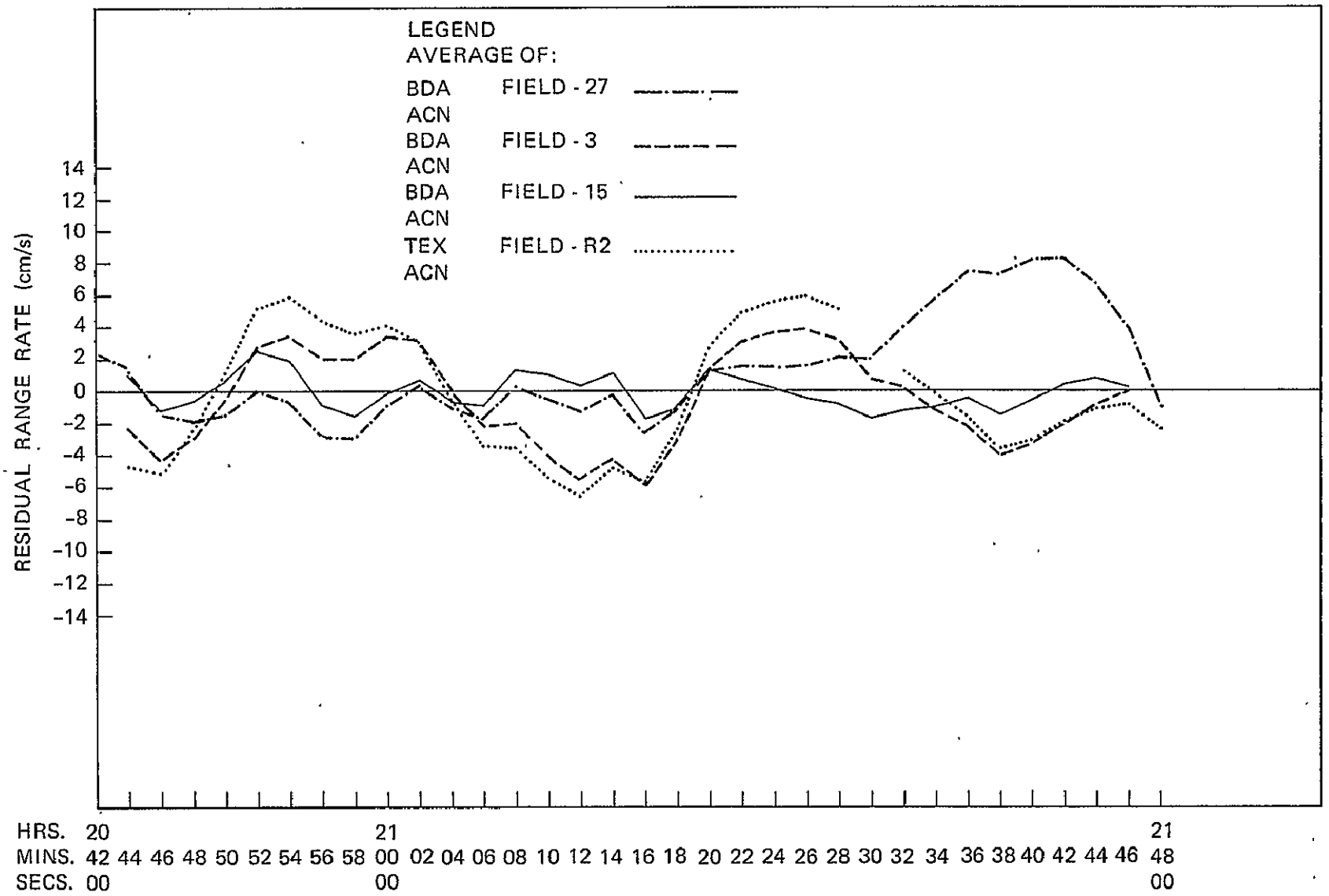

Figure 10. Apollo 8 Range Rate Residuals (Lunar Orbit 6)

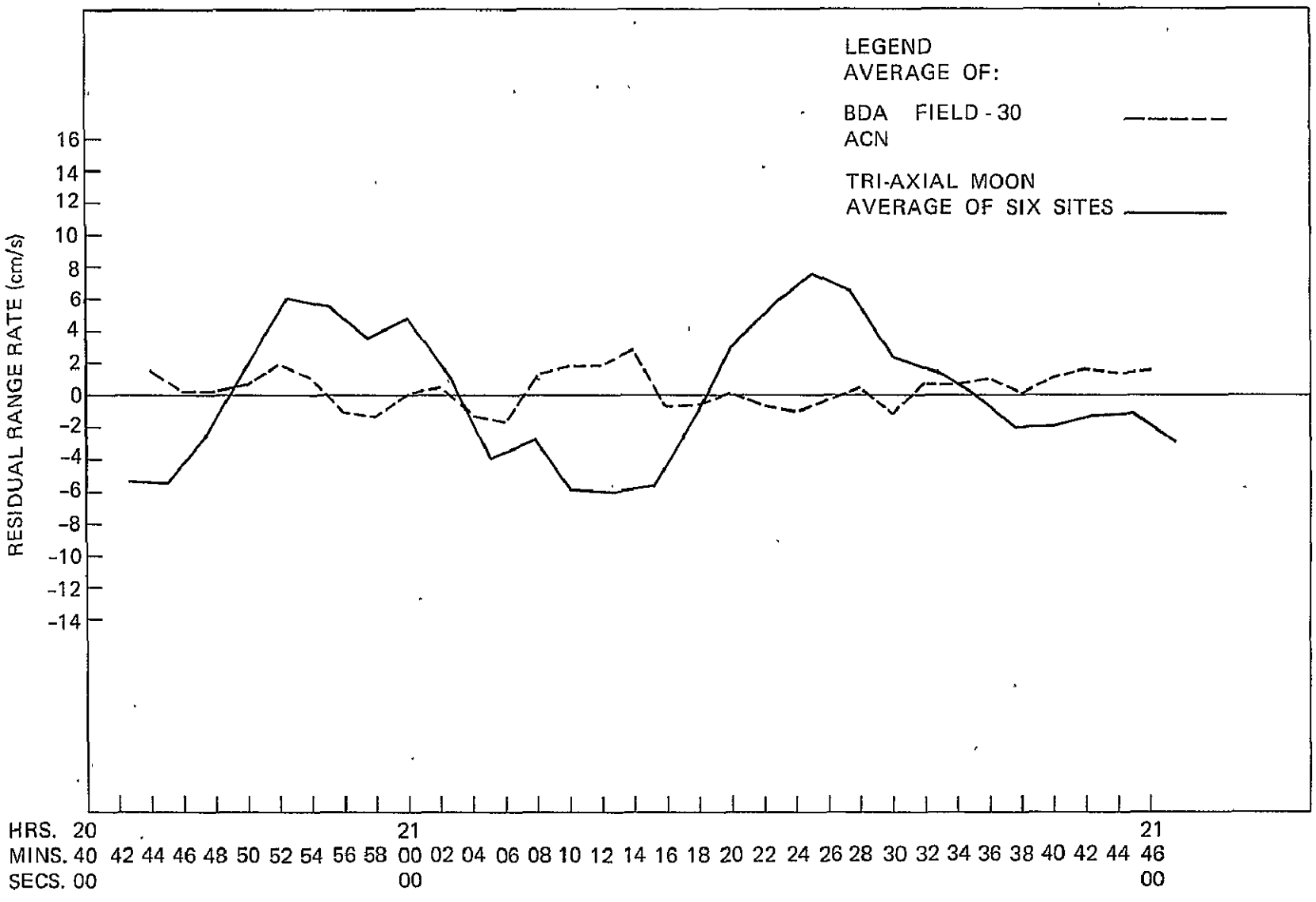

Figure 11. Apollo 8 Range Rate Residuals (Lunar Orbit 6)

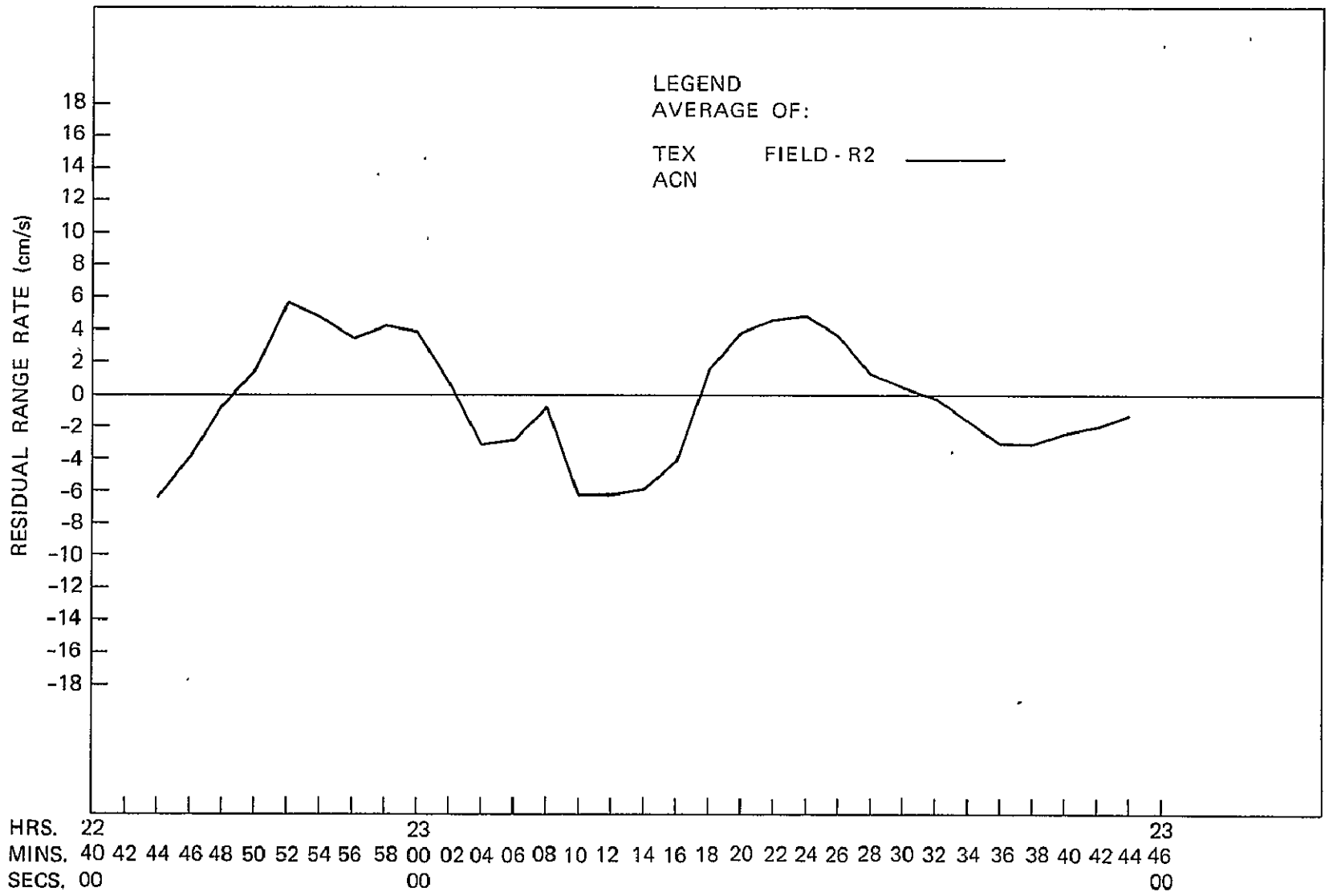

Figure 12. Apollo 8 Range Rate Residuals (Lunar Orbit 7)

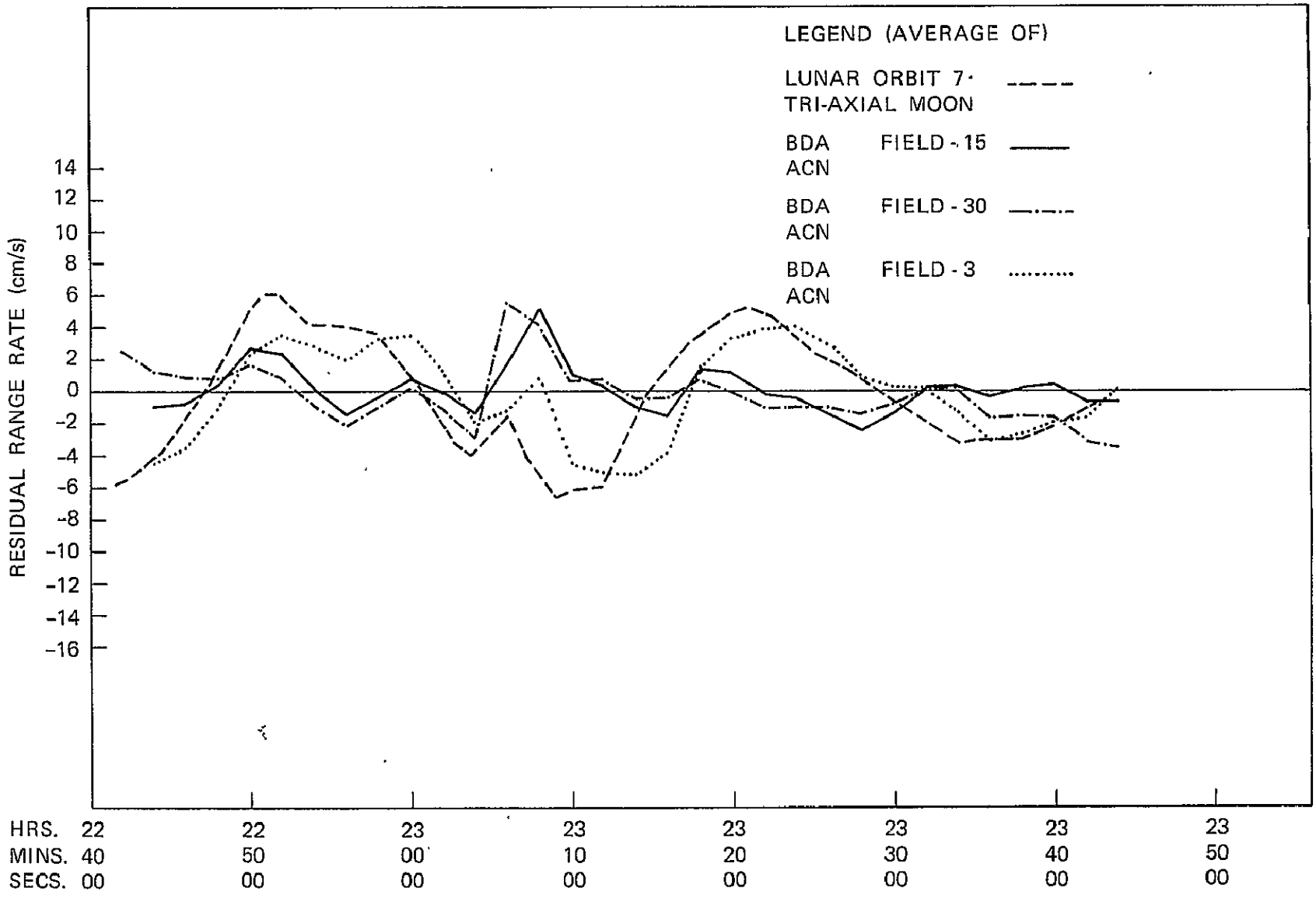

Figure 13. Apollo 8 Range Rate Residuals (Lunar Orbit 7)

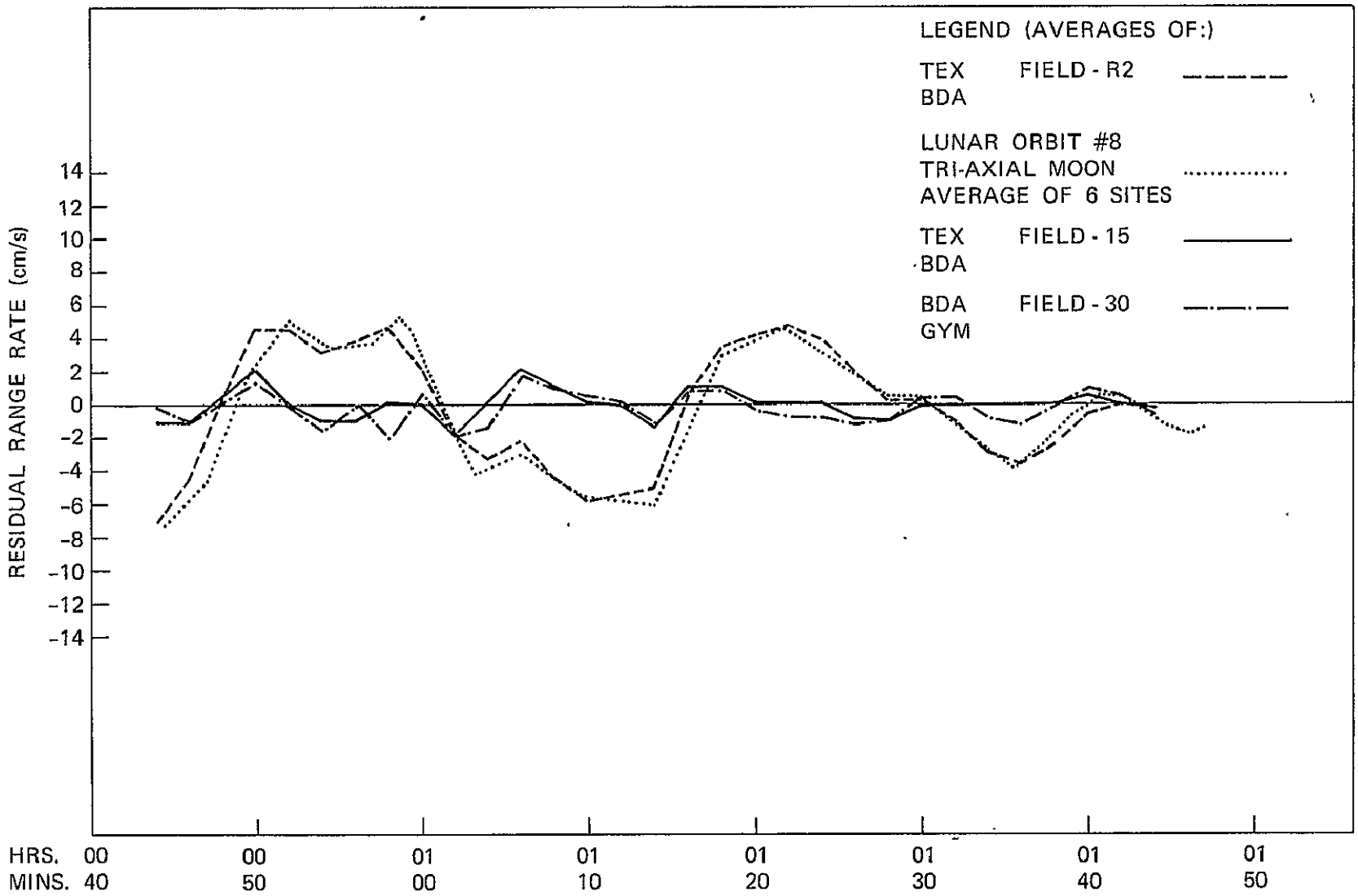

Figure 14. Apollo 8 Range Rate Residuals (Lunar Orbit 8)

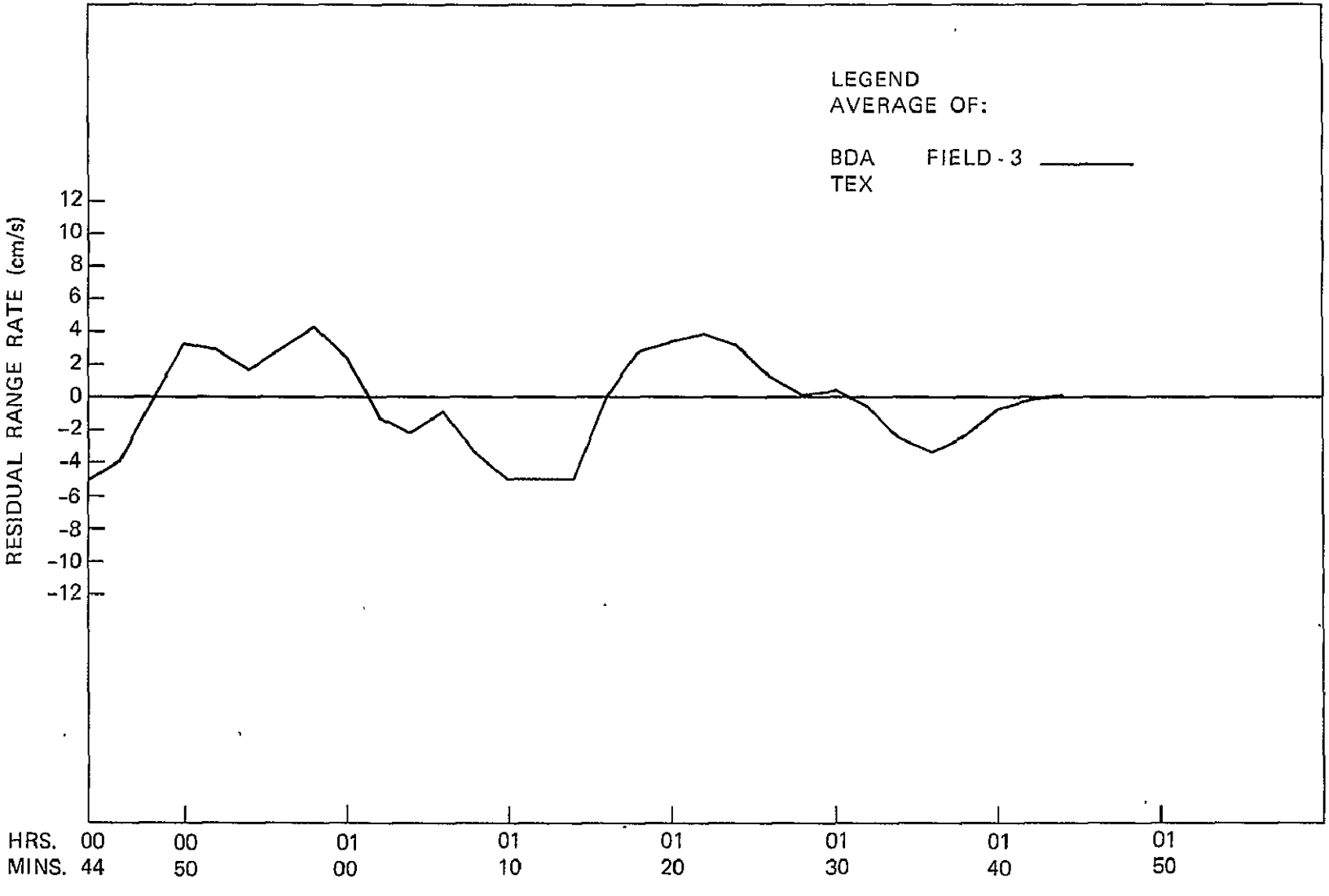

Figure 15. Apollo 8 Range Rate Residuals (Lunar Orbit 8)

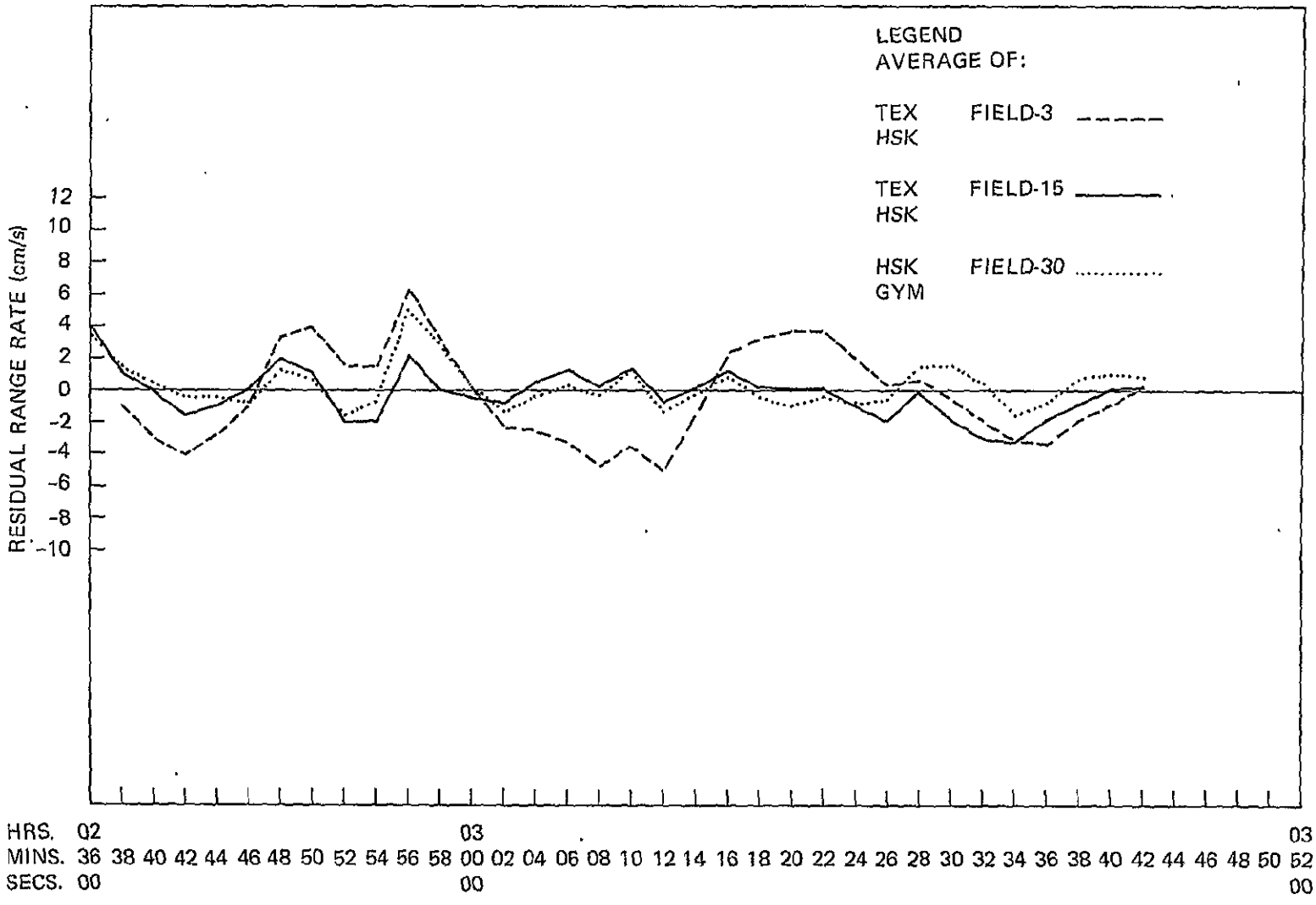

Figure 16. Apollo 8 Range Rate Residuals (Lunar Orbit 9)

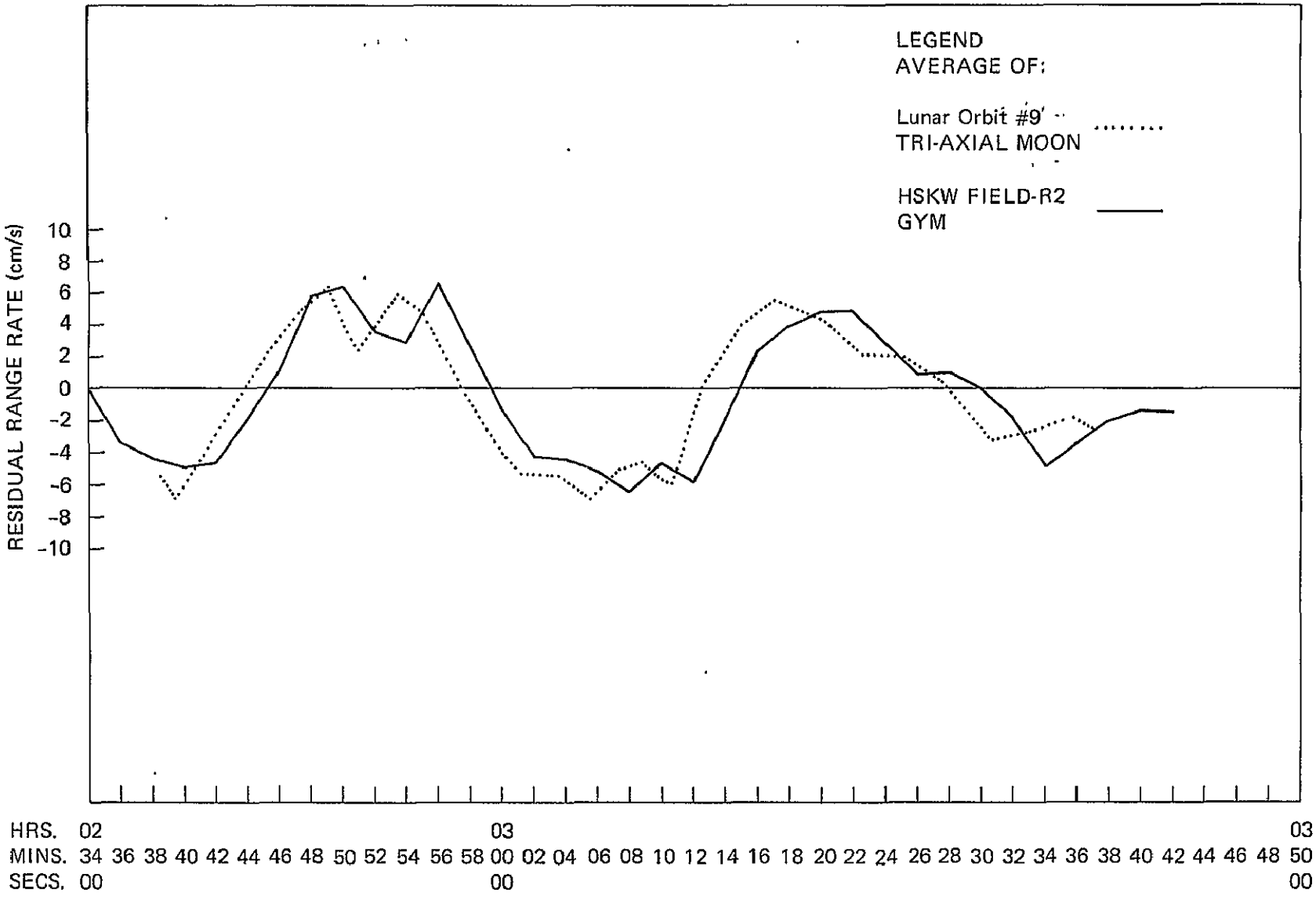

Figure 17. Apollo 8 Range Rate Residuals (Lunar Orbit 9)

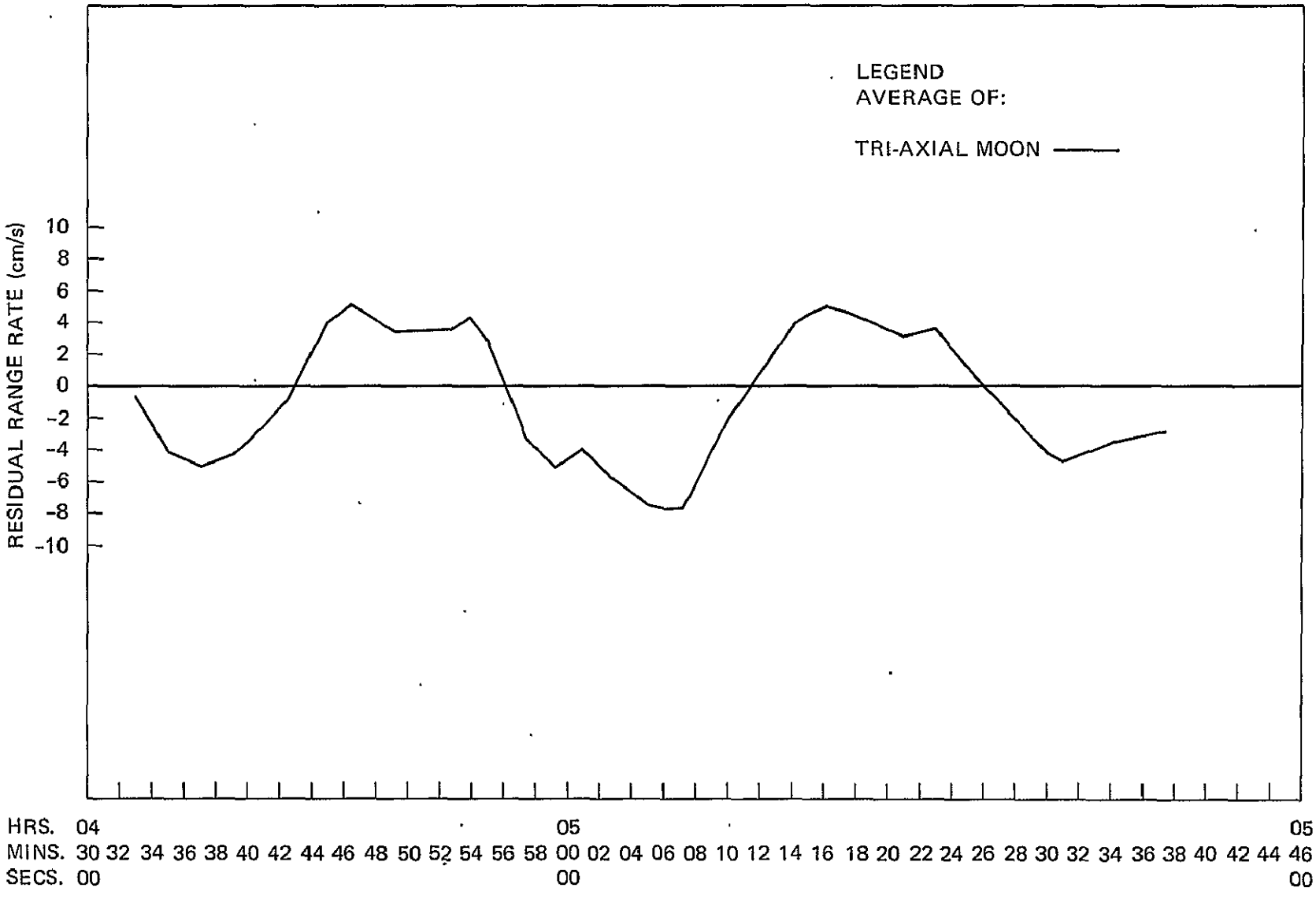

Figure 18. Apollo 8 Range Rate Residuals (Lunar Orbit 10)

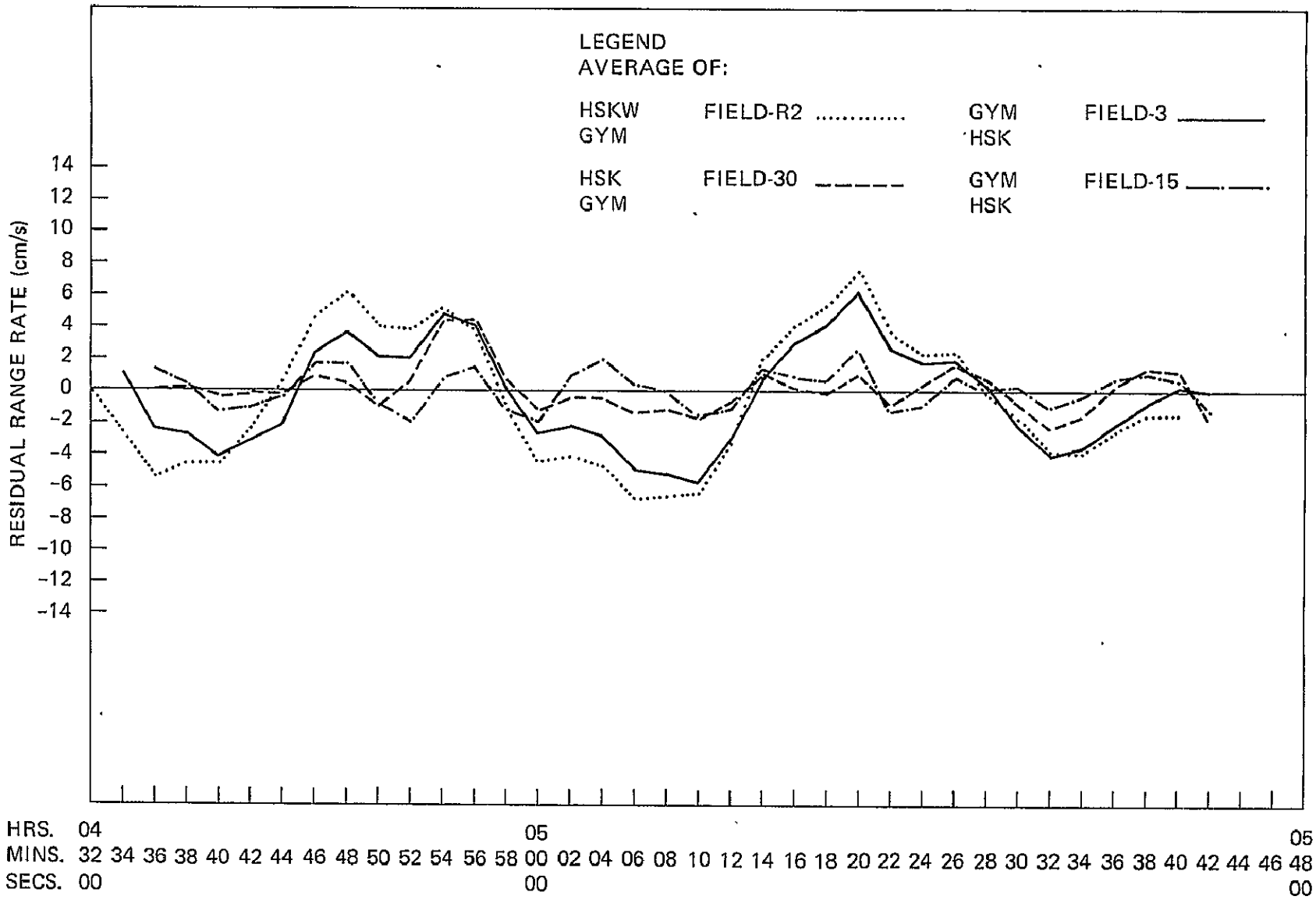

Figure 19. Apollo 8 Range Rate Residuals (Lunar Orbit 10)

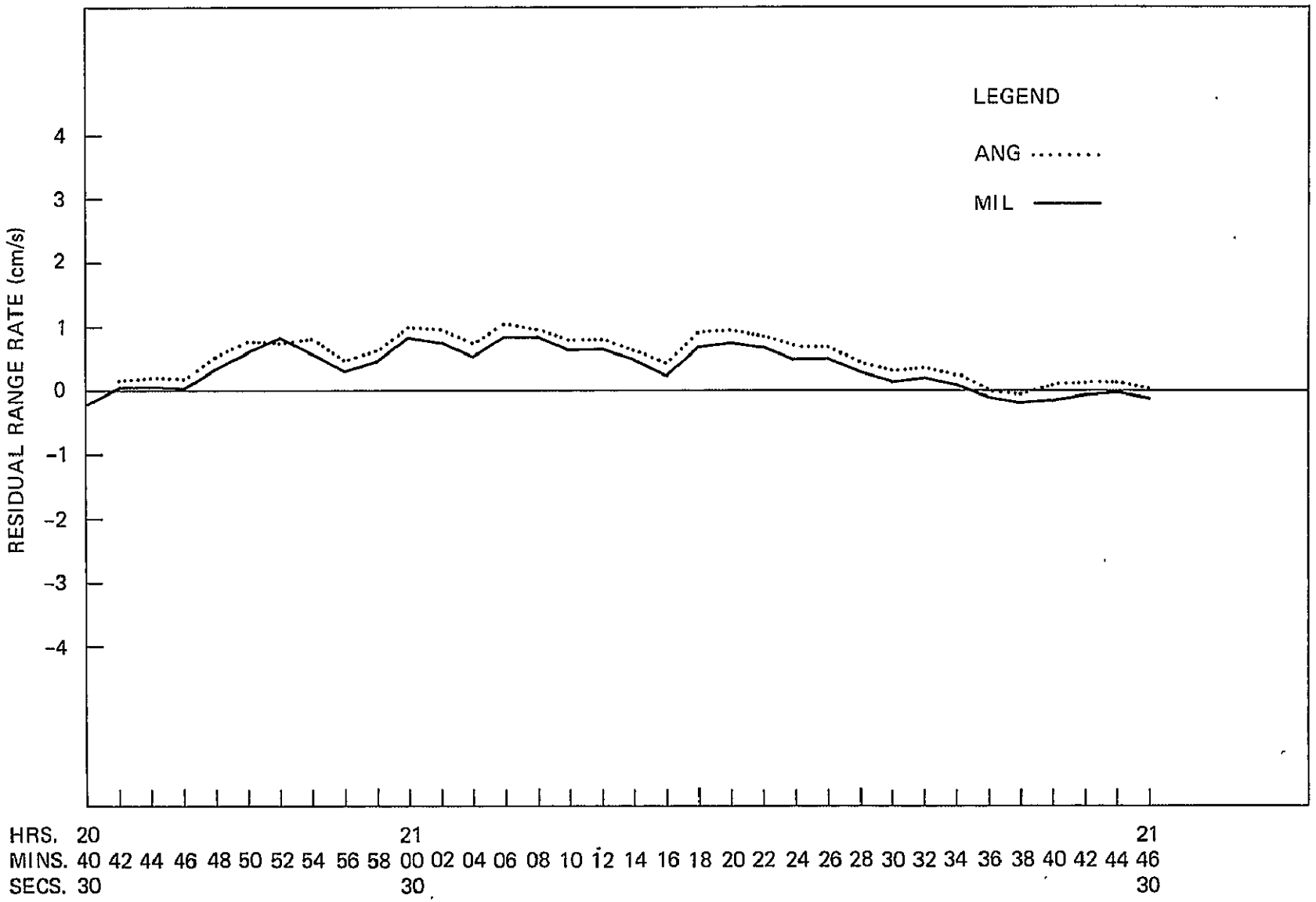

Figure 20. Apollo 8 Range Rate Residuals (Field 26, Lunar Orbit 6)

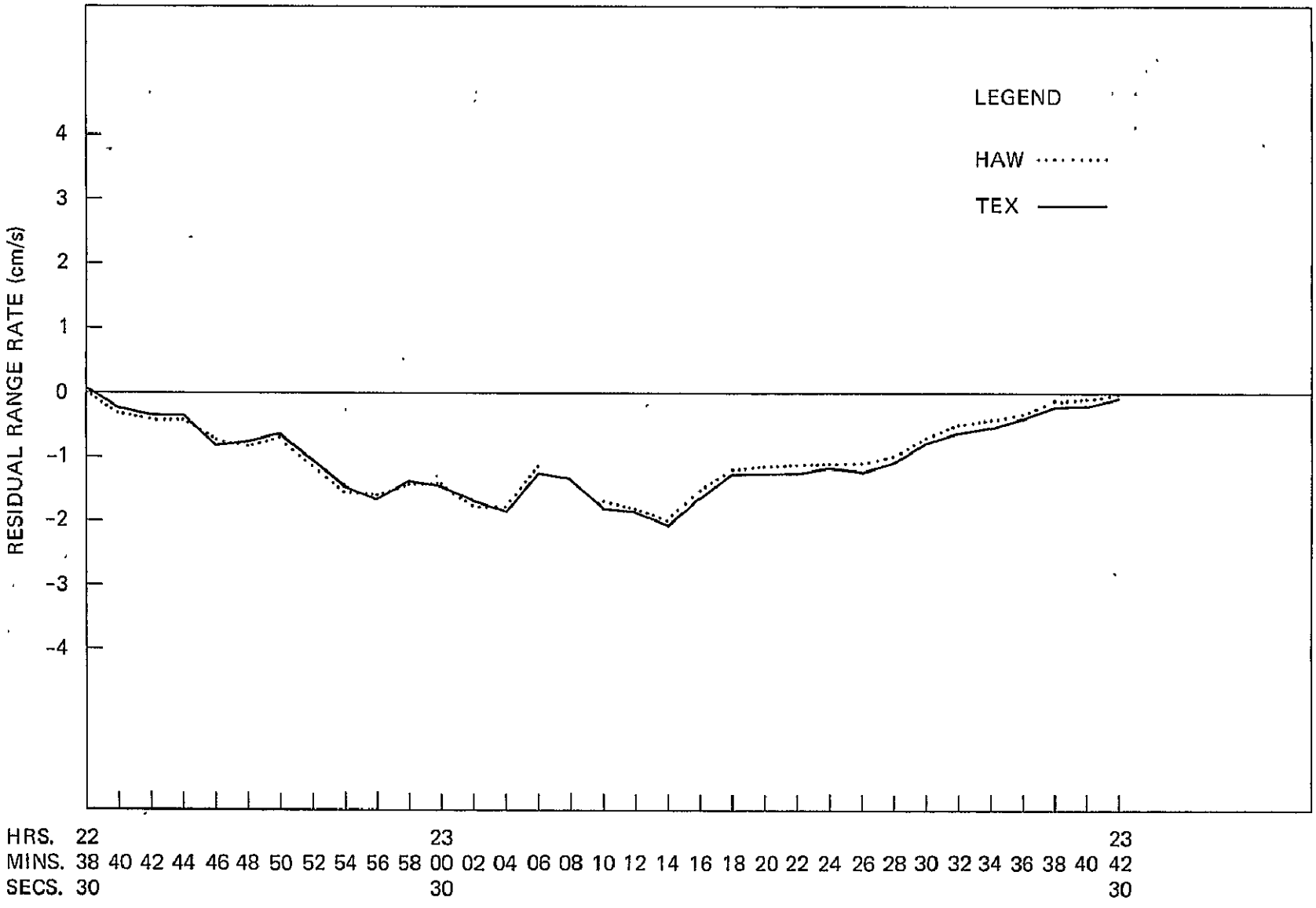

Figure 21. Apollo 8 Range Rate Residuals (Field 26, Lunar Orbit 7)

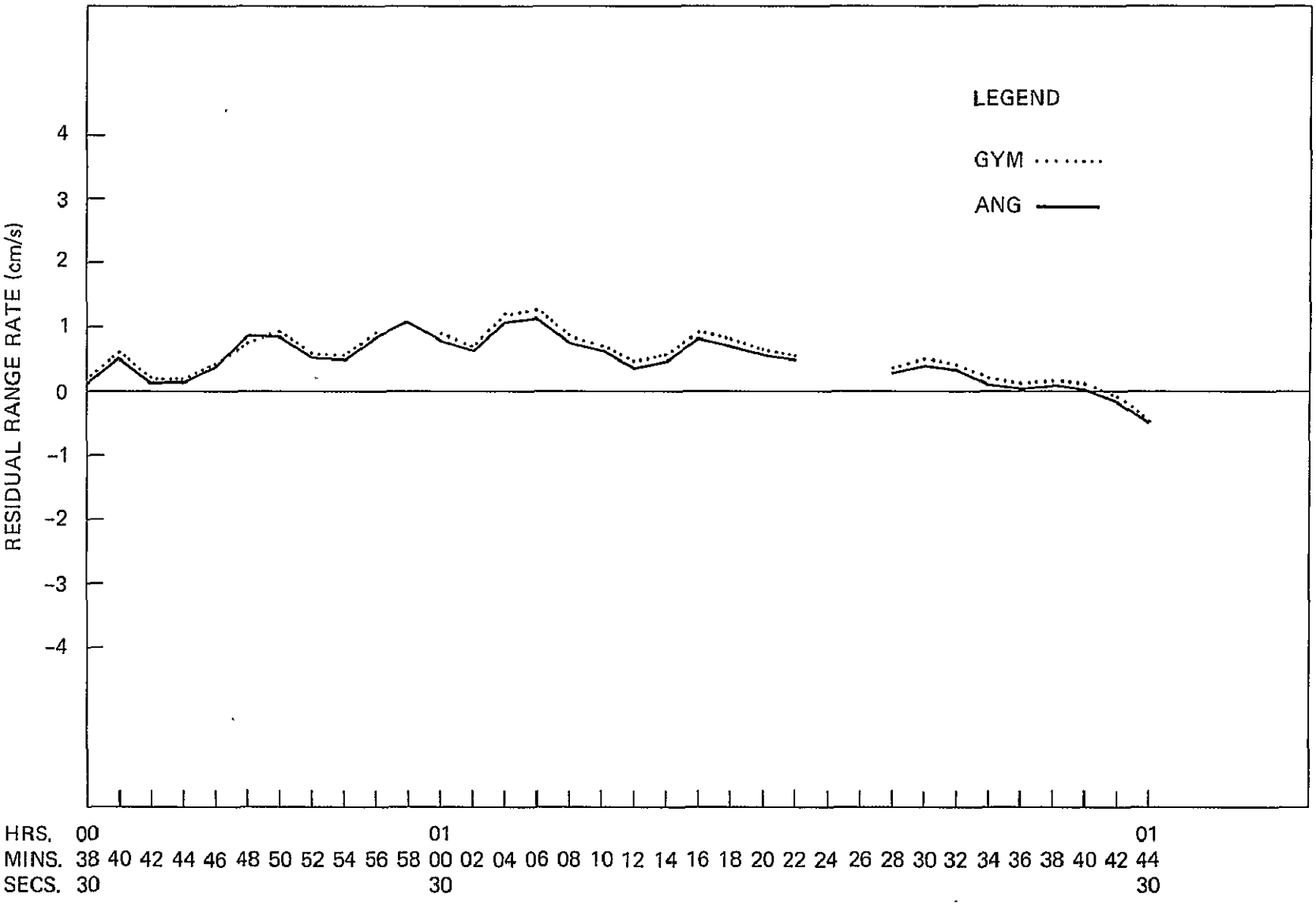

Figure 22. Apollo 8 Range Rate Residuals (Field 26, Lunar Orbit 8)

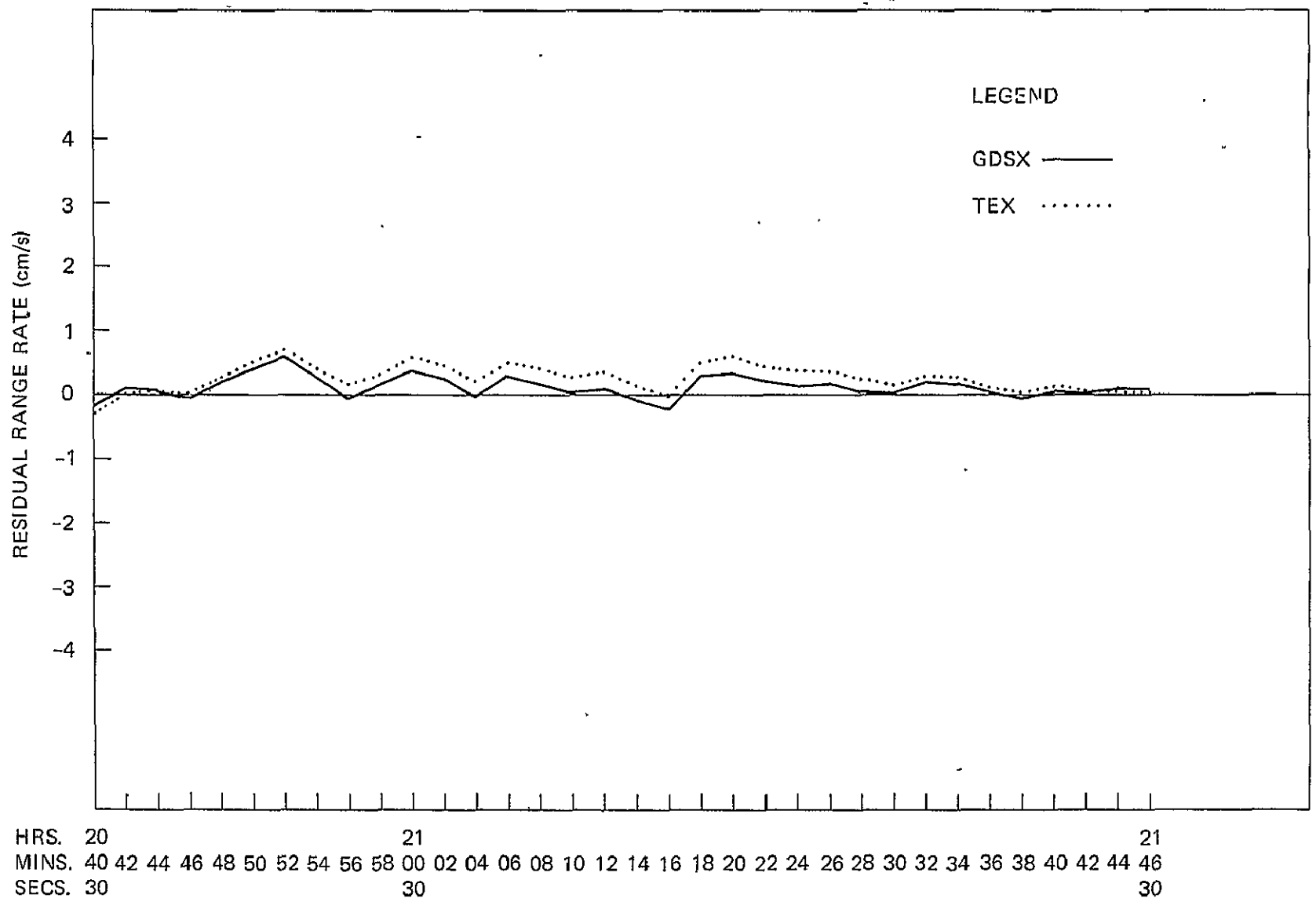

Figure 23. Apollo 8 Range Rate Residuals (Field 27, Lunar Orbit 6)

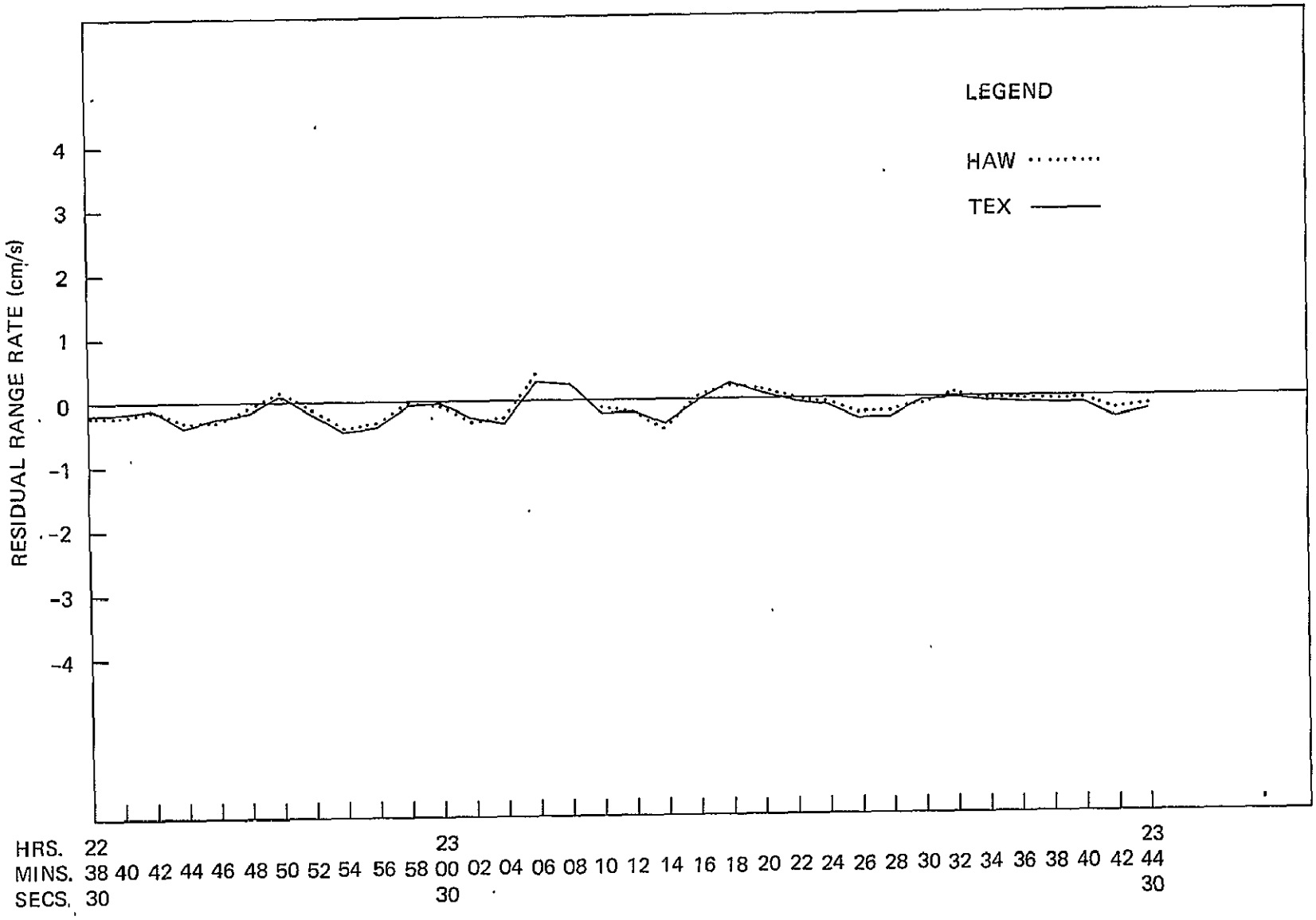

Figure 24. Apollo 8 Range Rate Residuals (Field 27, Lunar Orbit 7)

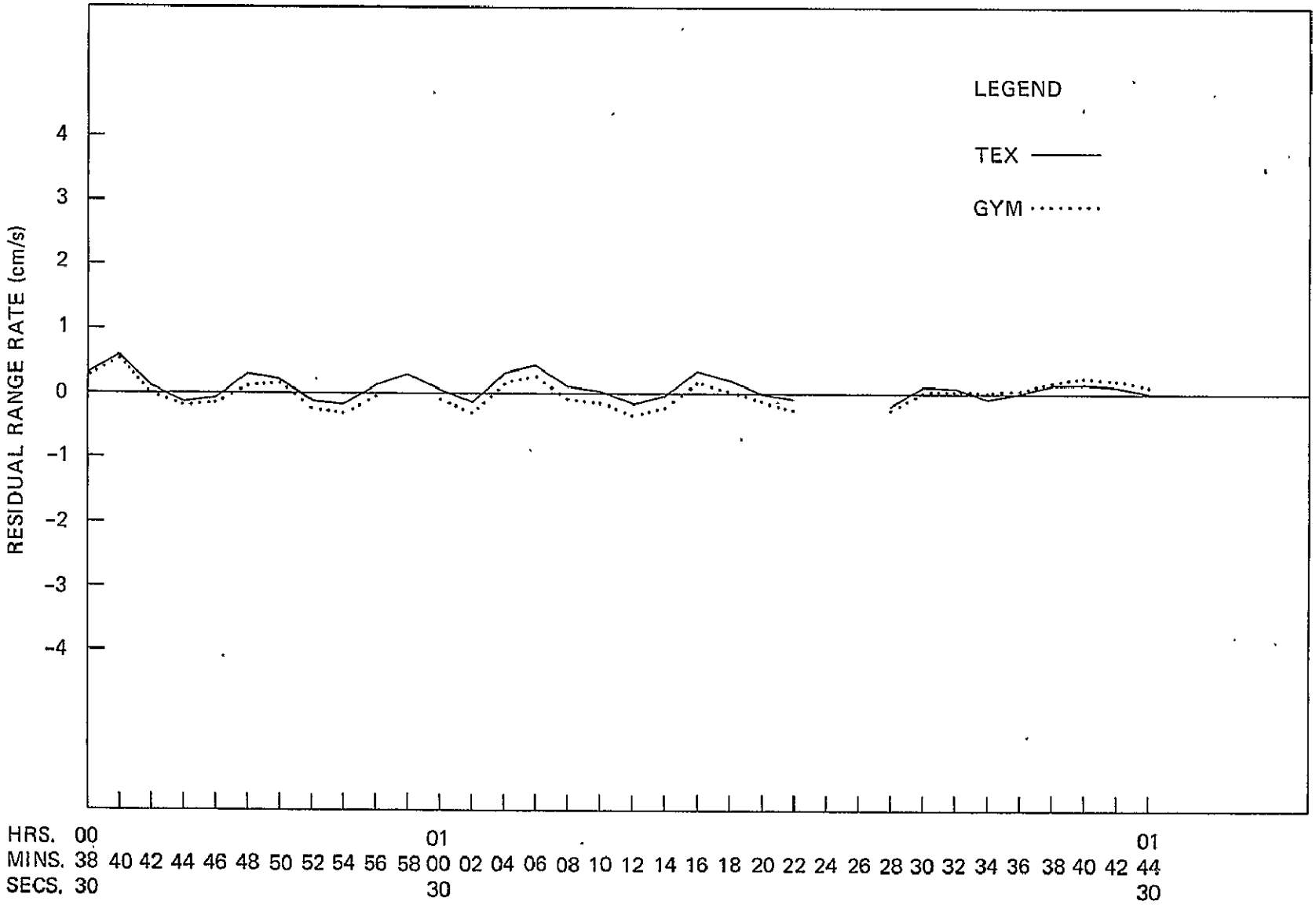

Figure 25. Apollo 8 Range Rate Residuals (Field 27, Lunar Orbit 8)

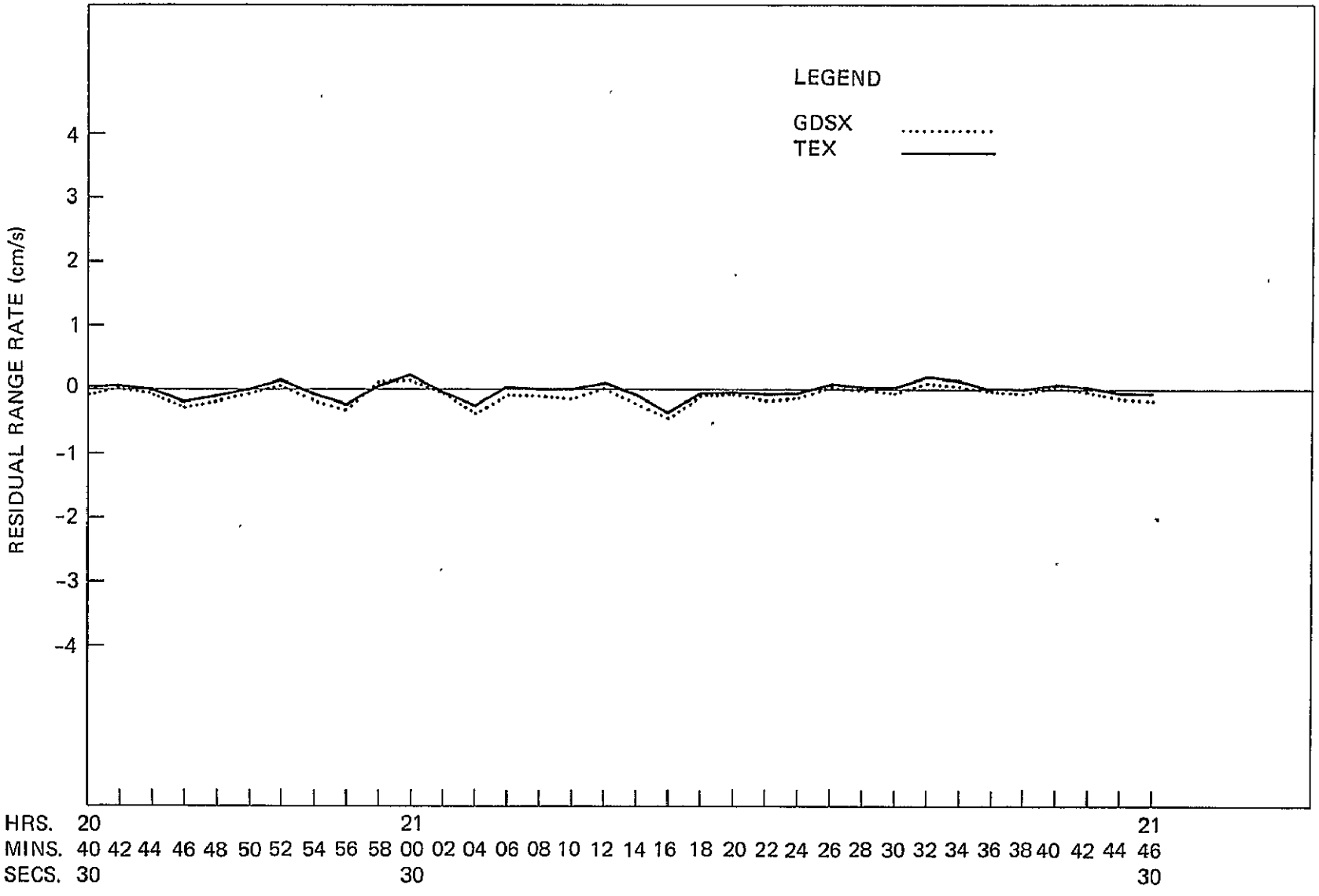

Figure 26. Apollo 8 Range Rate Residuals (Field 30, Lunar Orbit 6)

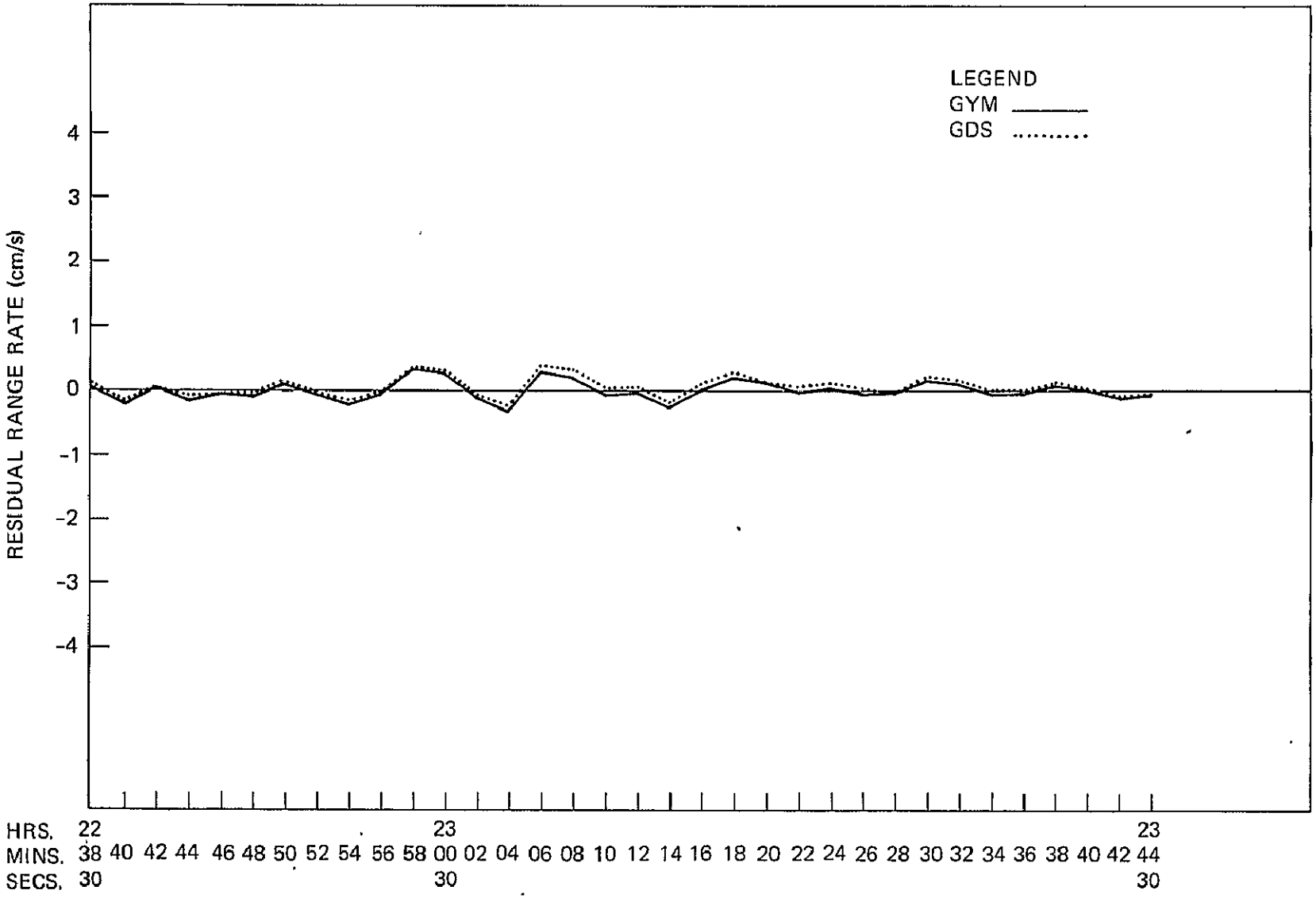

Figure 27. Apollo 8 Range Rate Residuals (Field 30, Lunar Orbit 7)

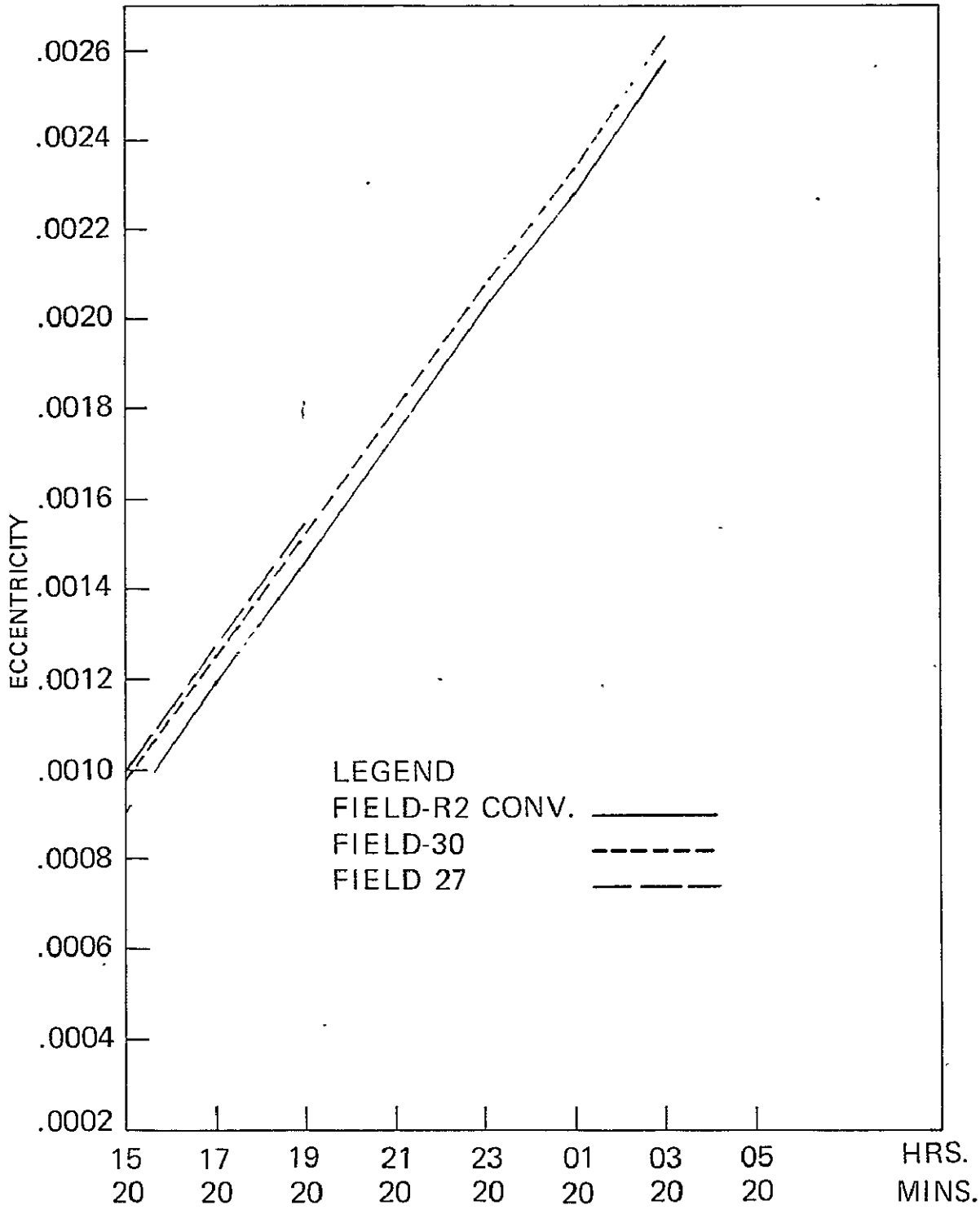

Figure 28. Eccentricity (Converged)

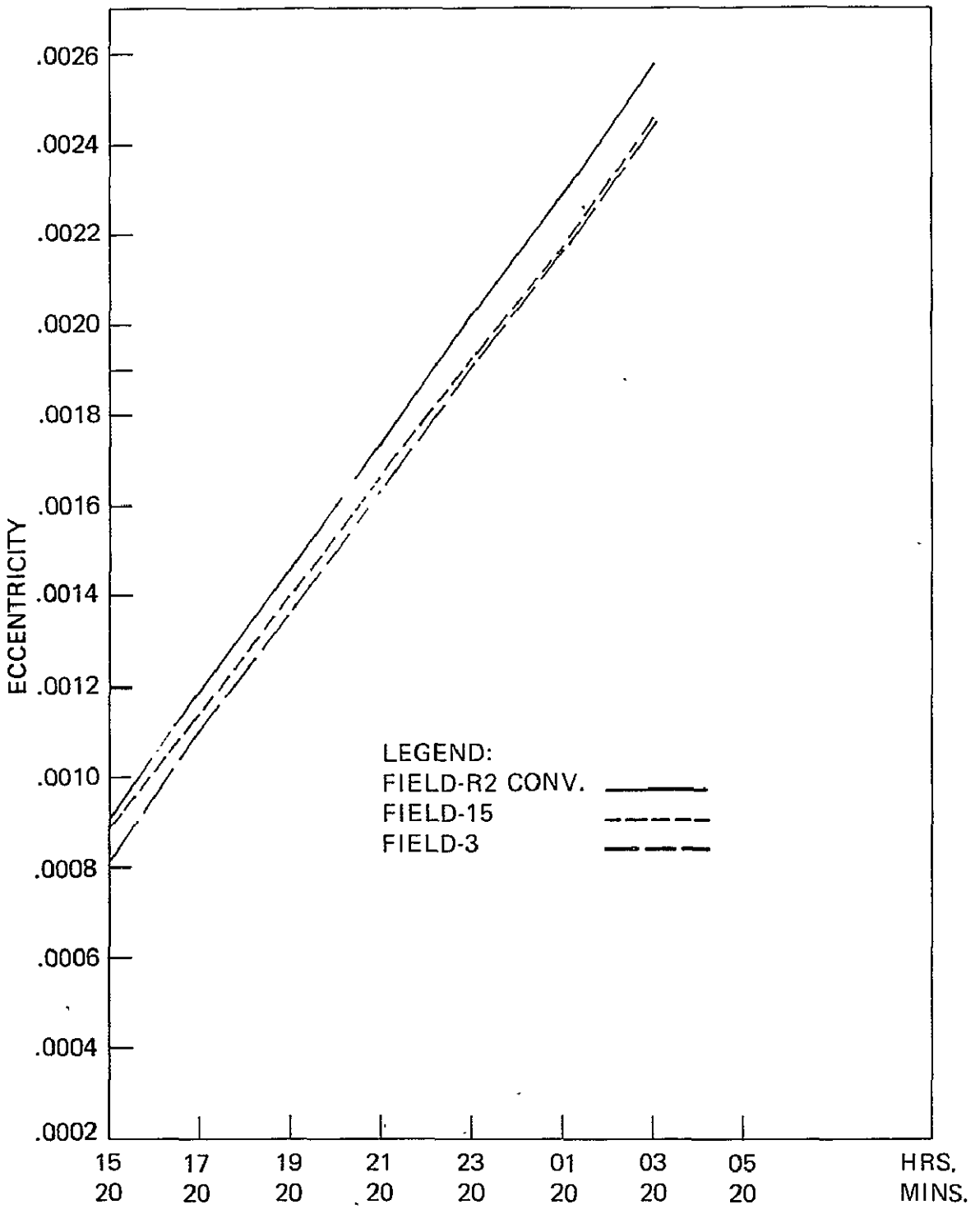

Figure 29. Eccentricity (Converged)

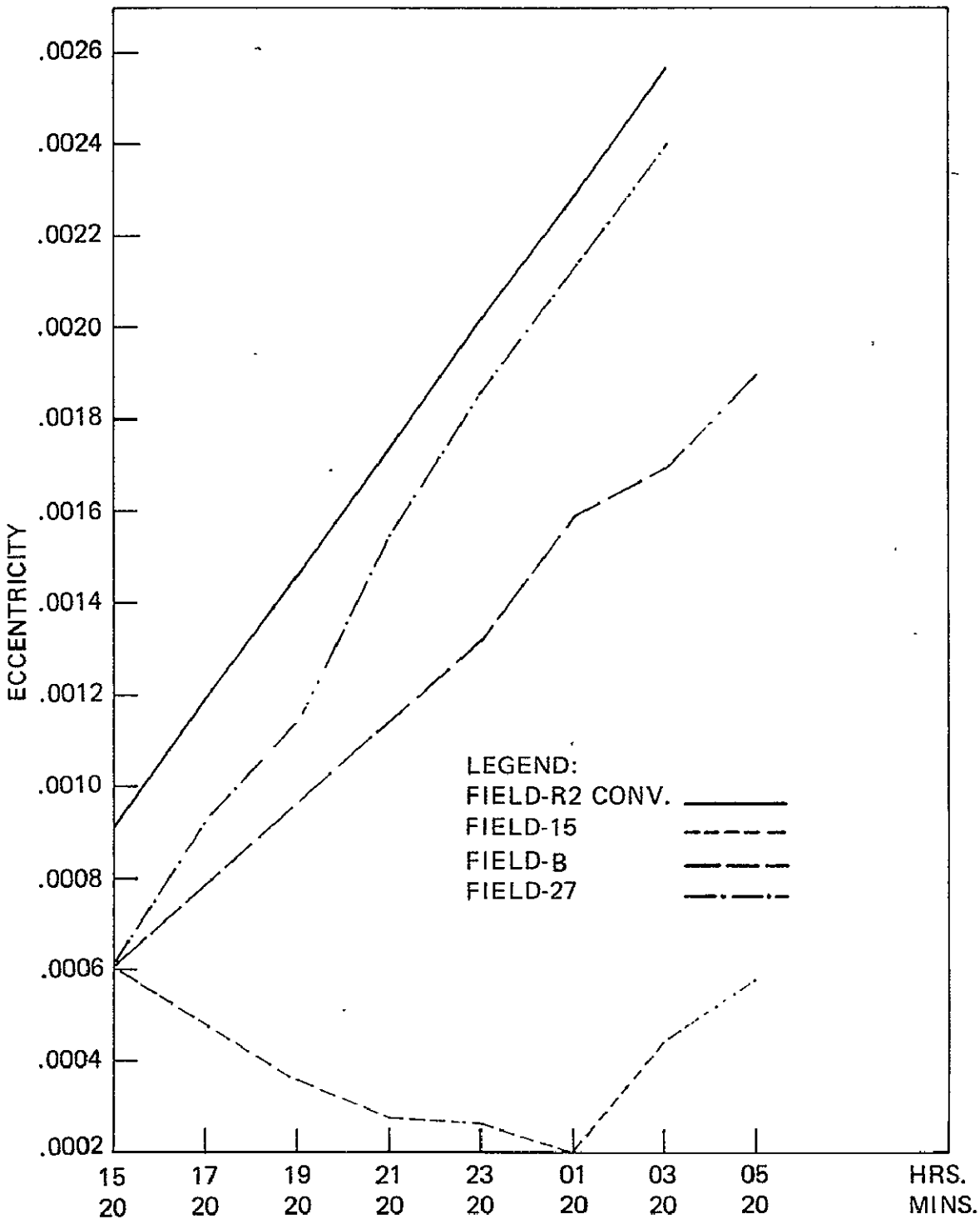

Figure 30. Eccentricity (Predicted)

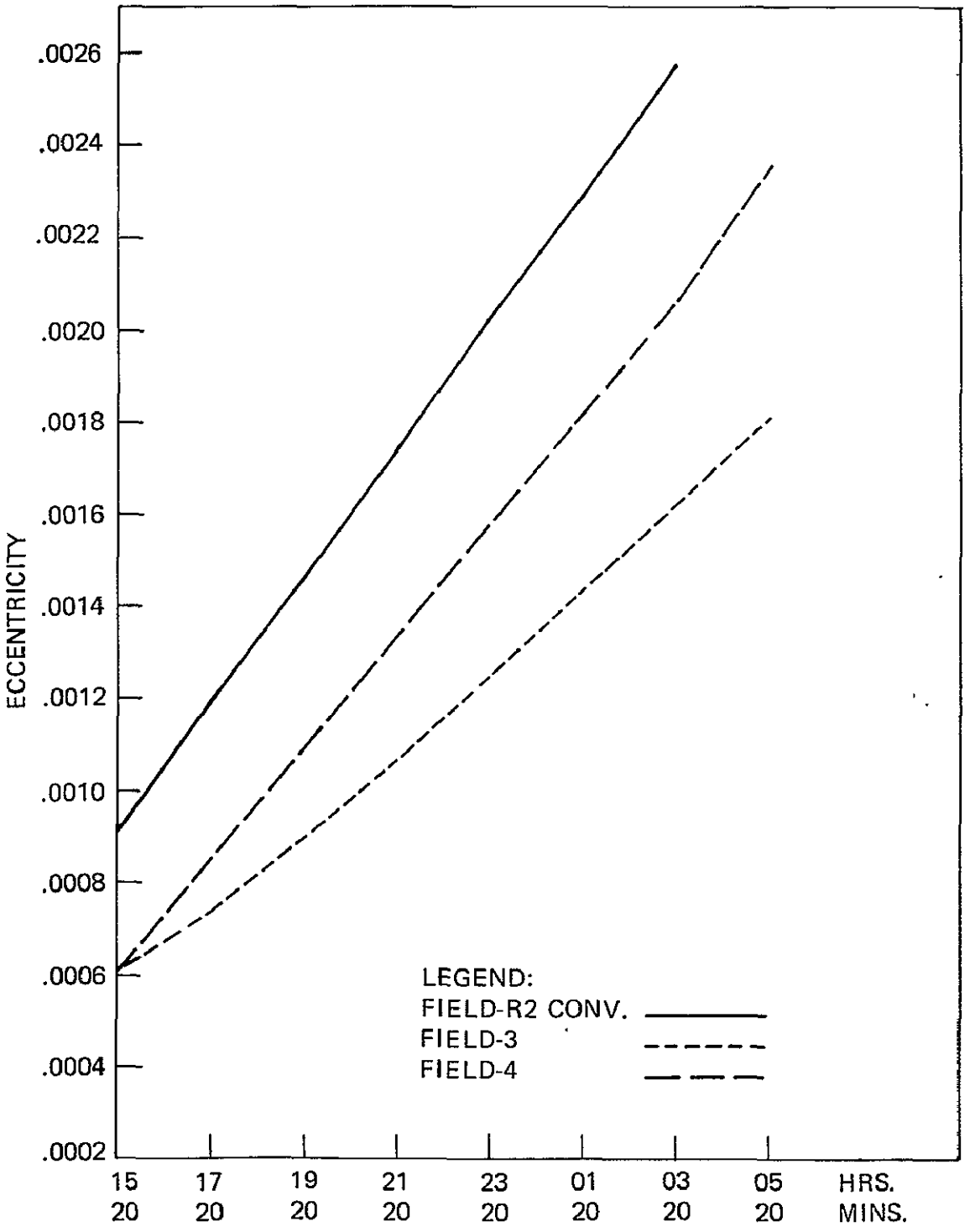

Figure 31. Eccentricity (Predicted)

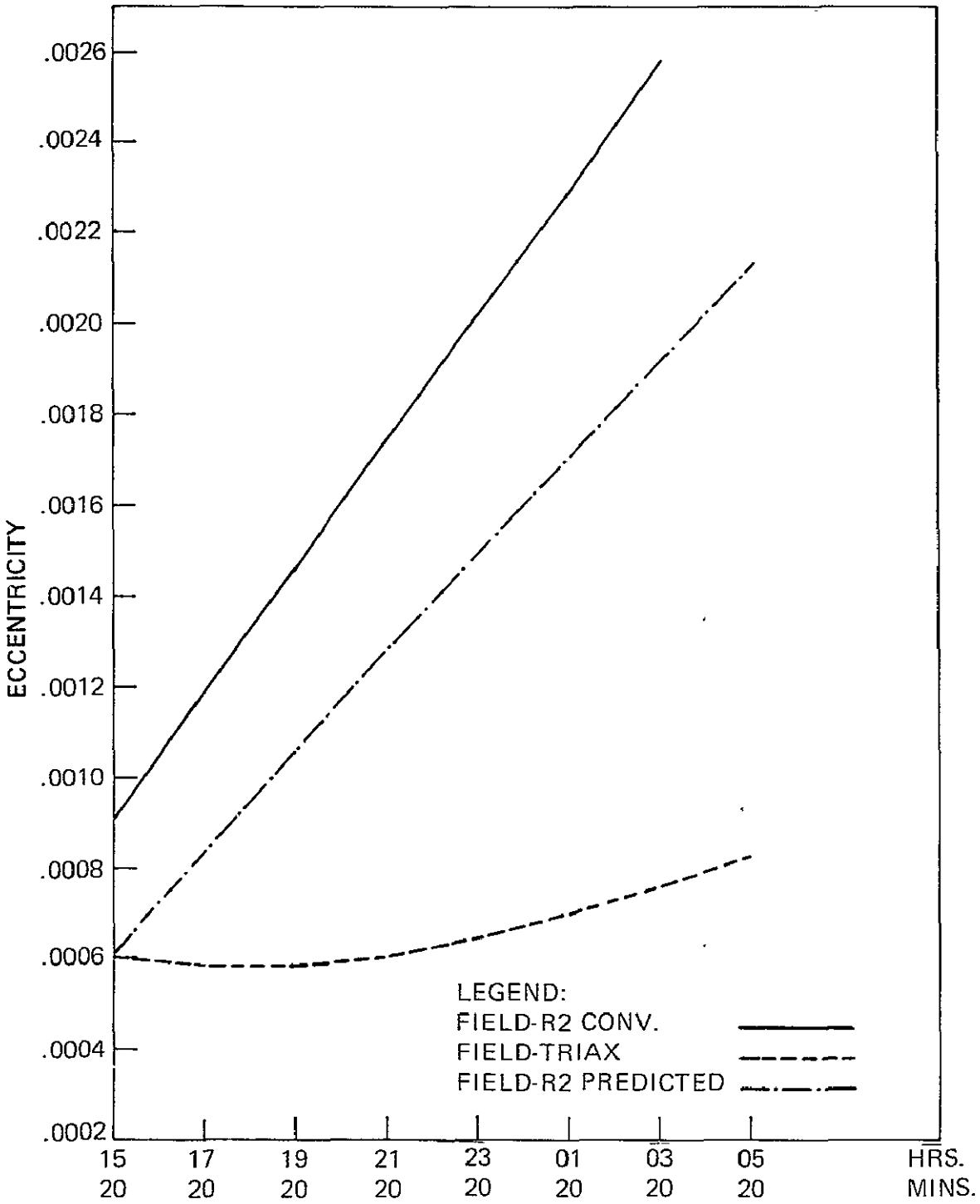

Figure 32. Eccentricity (Predicted)

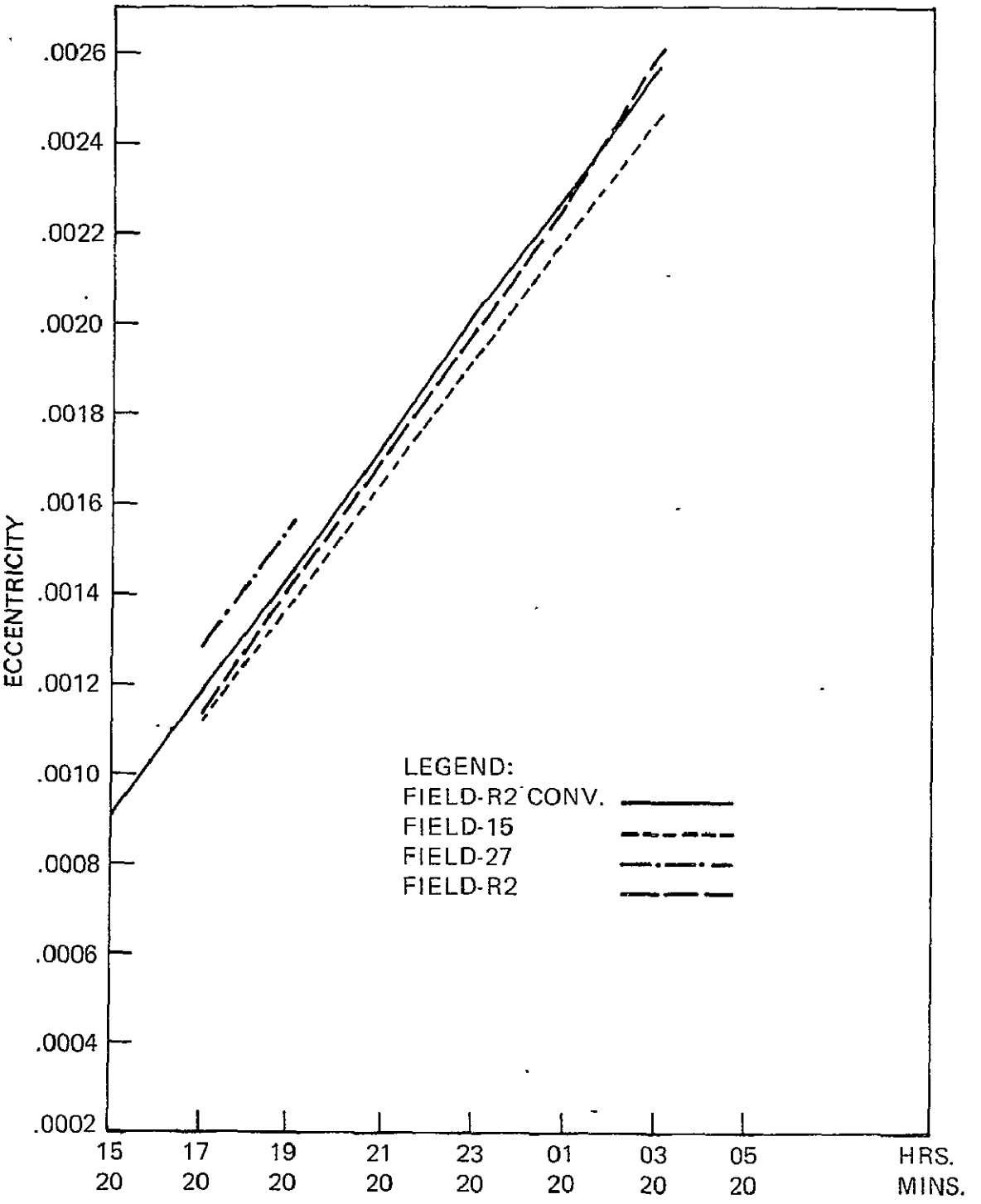

Figure 33. Eccentricity (Predicted)

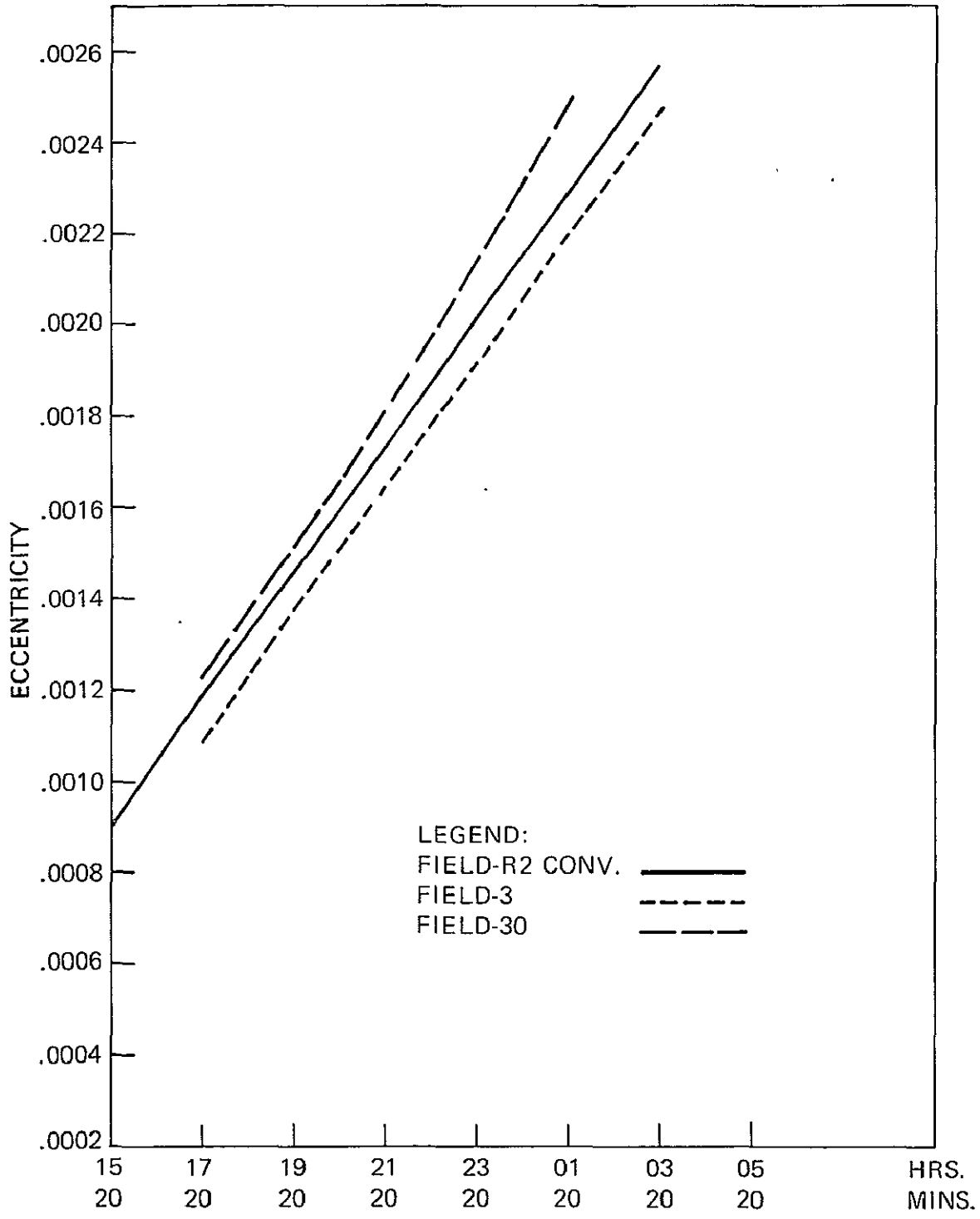

Figure 34. Eccentricity (Predicted)

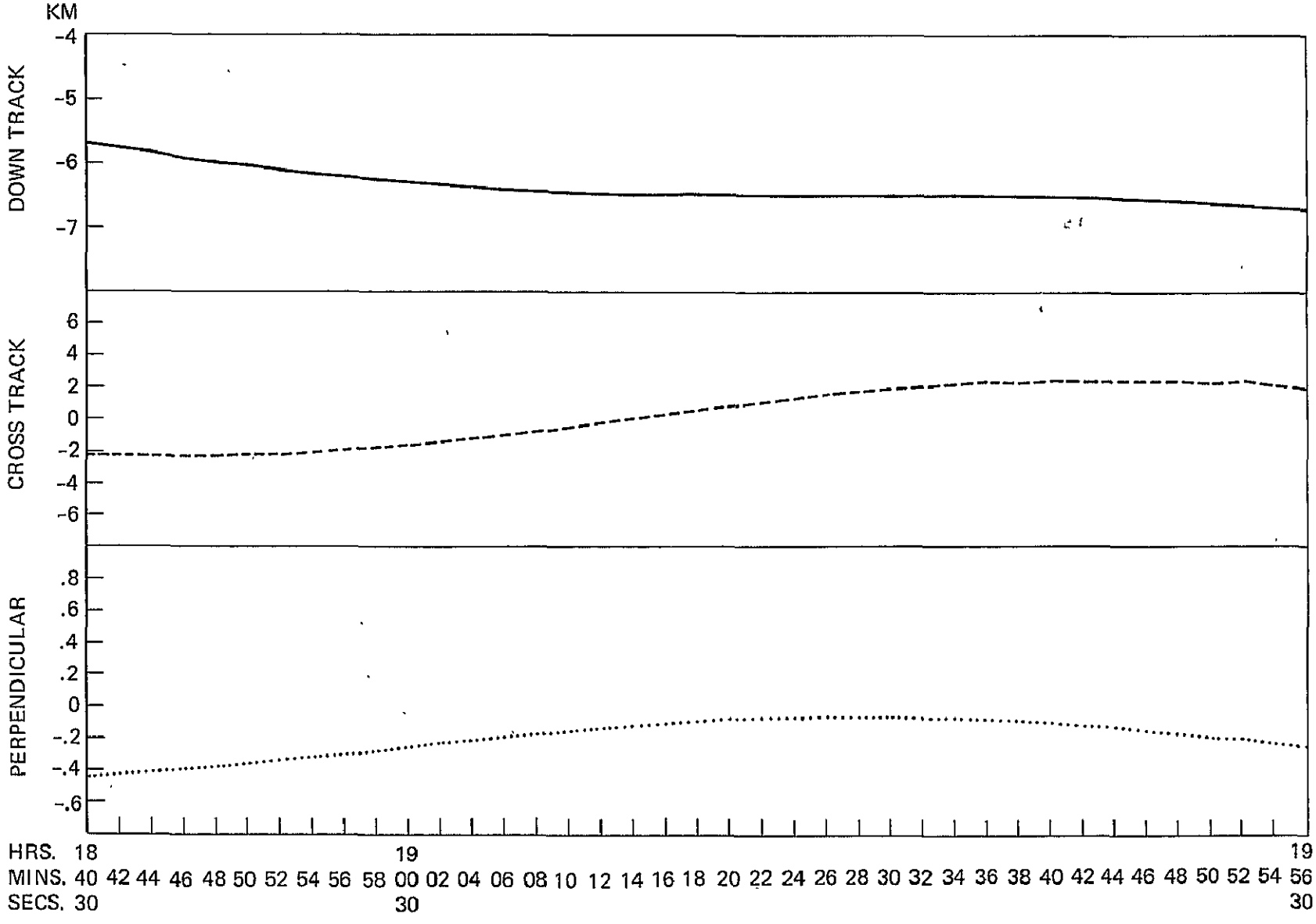

Figure 35. Apollo 8 Track Errors (R2 Field, Lunar Orbit 5)

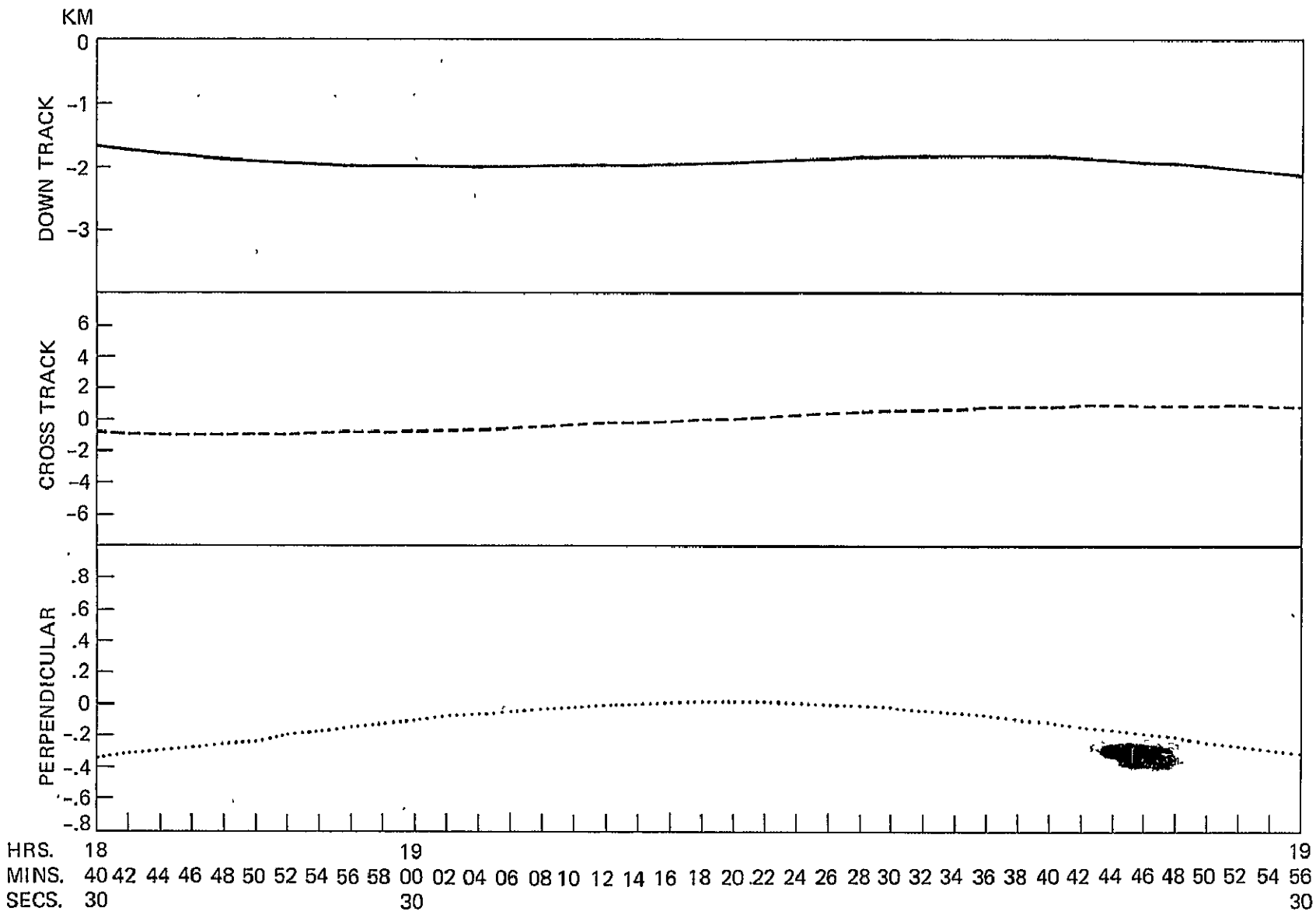

Figure 36. Apollo 8 Track Errors (Field 3, Lunar Orbit 5)

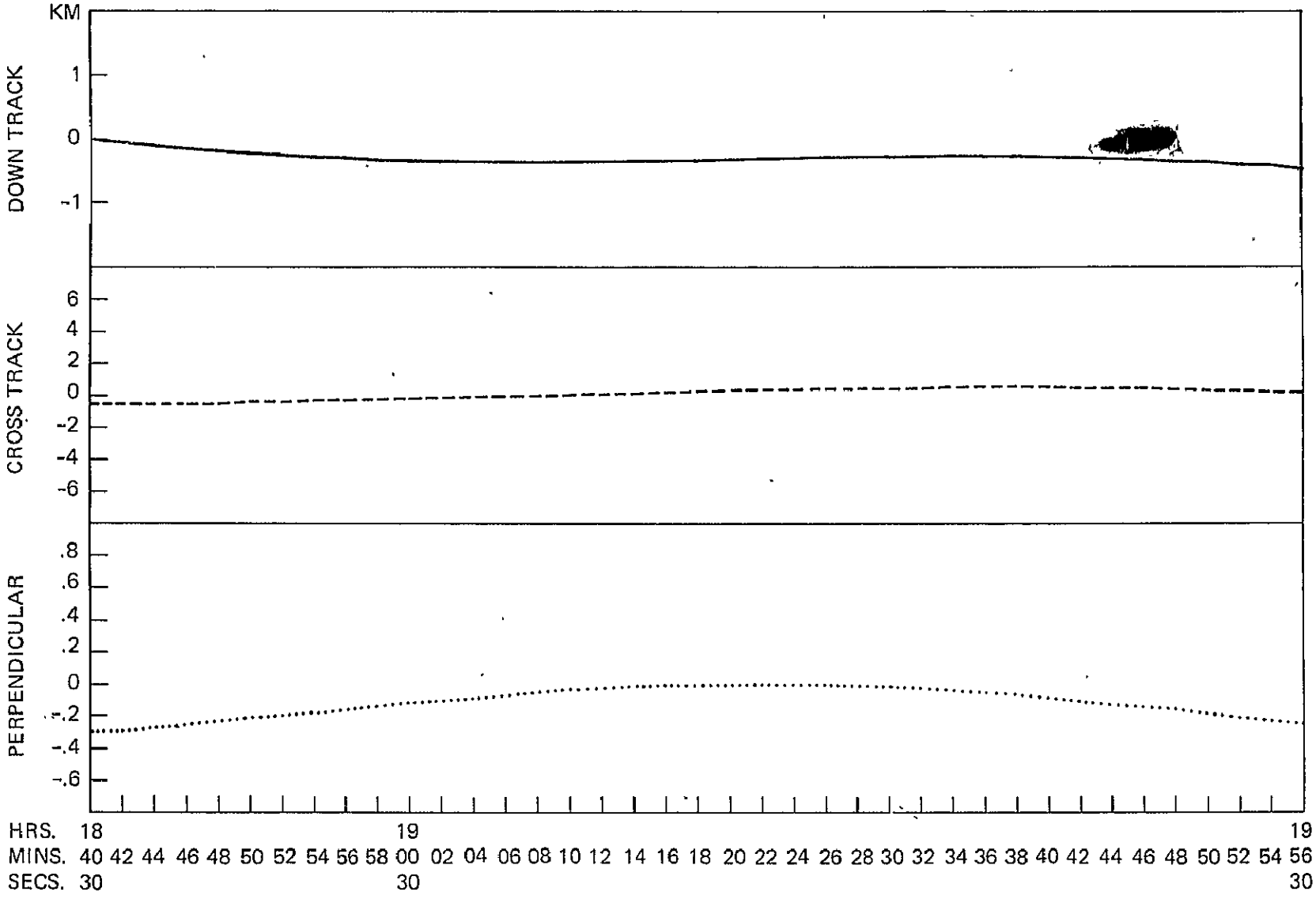

Figure 37. Apollo 8 Track Errors (Field 4, Lunar Orbit 5)

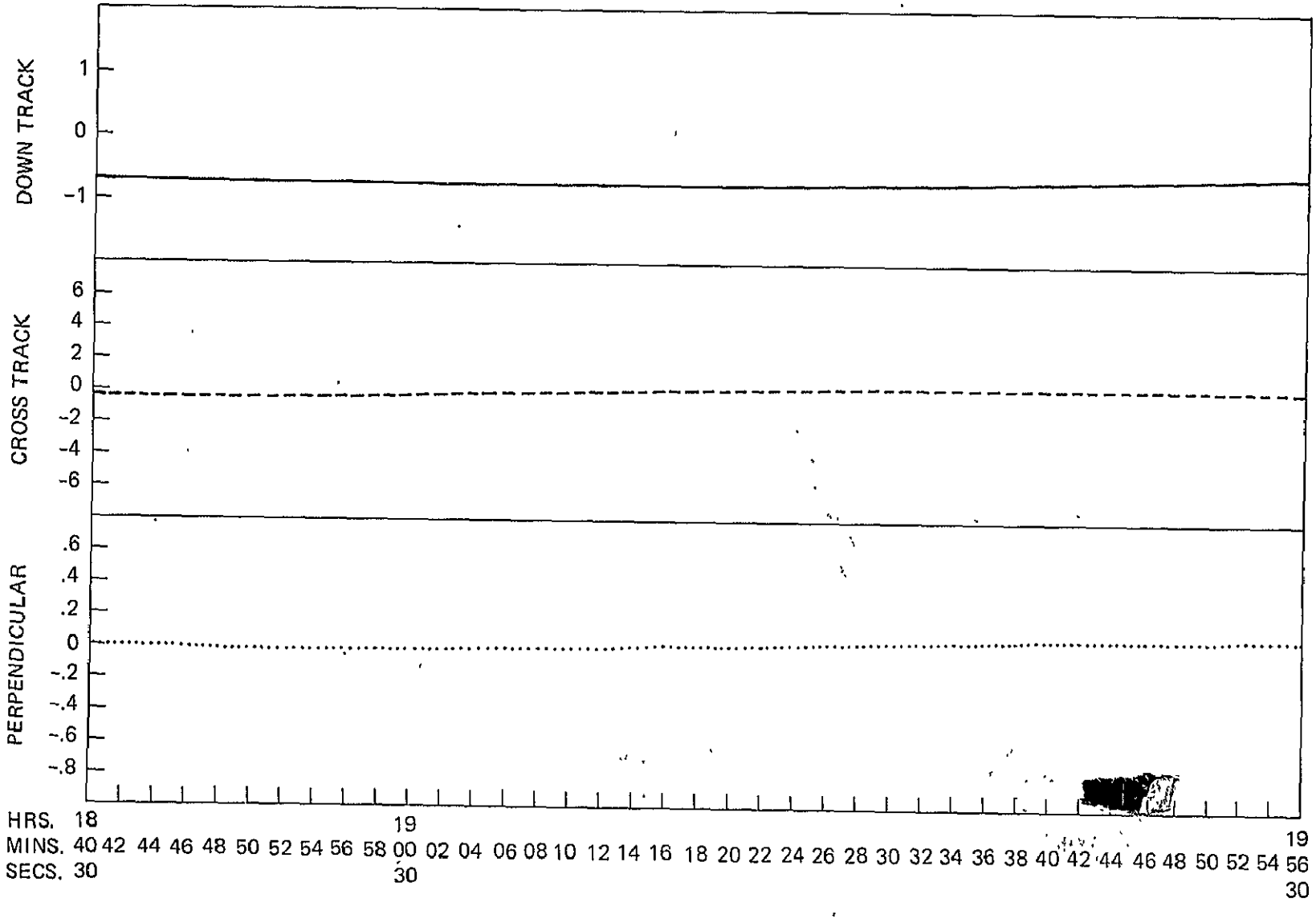

Figure 38. Apollo 8 Track Errors (Field 15, Lunar Orbit 5)

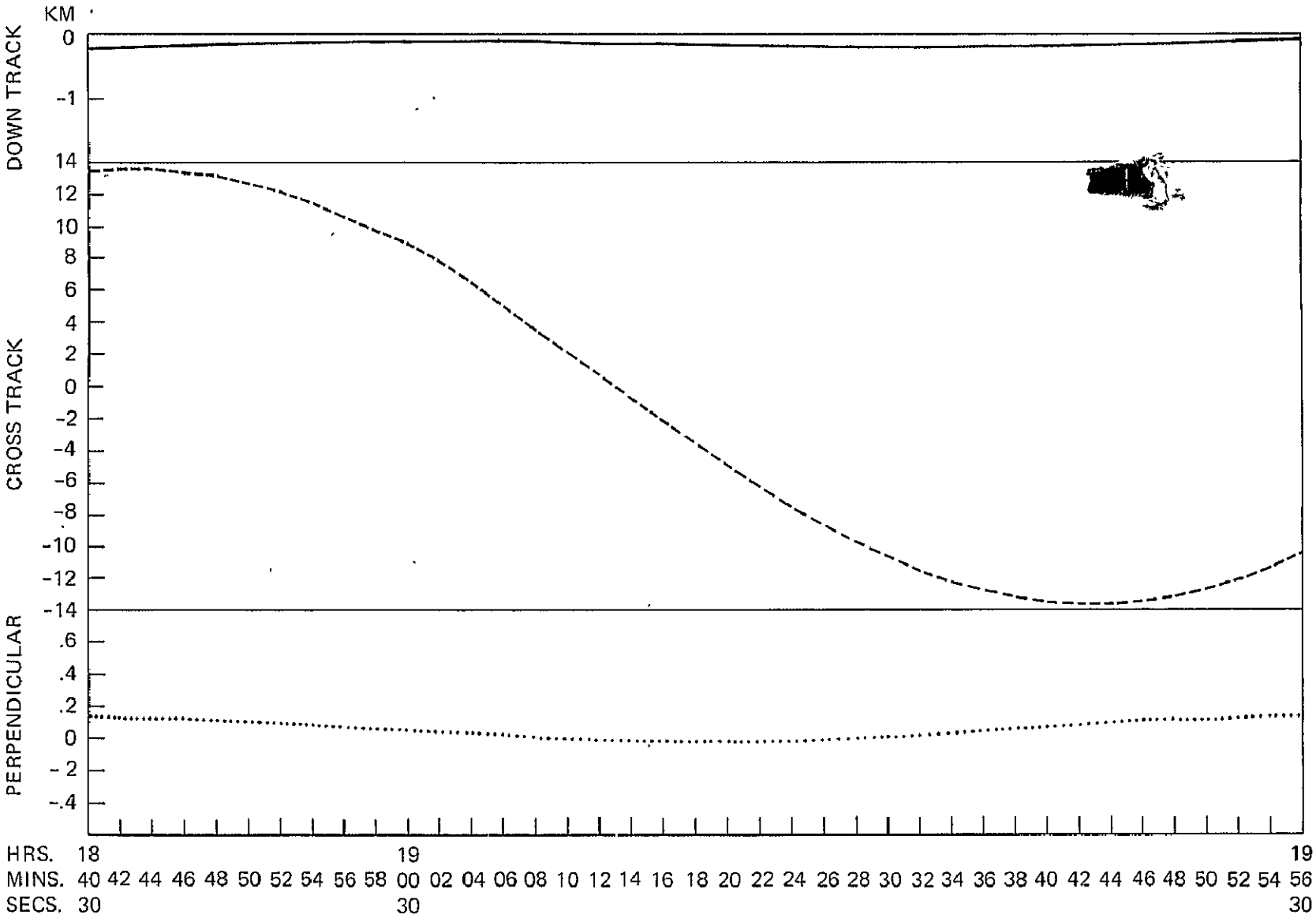

Figure 39. Apollo 8 Track Errors (Field 27, Lunar Orbit 5)